A siRNA SCREEN TO IDENTIFY MOLECULAR DETERMINANTS OF TUMOUR RADIOSENSITIVITY

A thesis submitted for the degree of Doctor of Philosophy at the University of Oxford

Geoff Higgins

Green Templeton College

Michaelmas Term, 2010

A siRNA SCREEN TO IDENTIFY MOLECULAR DETERMINANTS OF TUMOUR RADIOSENSITIVITY

Geoff Higgins

Gray Institute for Radiation Oncology and Biology

and

Green Templeton College

A thesis submitted for the degree of Doctor of Philosophy at the University of Oxford, Michaelmas Term, 2010

Abstract

A siRNA Screen To Identify Molecular Determinants Of Tumour Radiosensitivity

Geoff Higgins, Green Templeton College

Submitted for the degree of D.Phil., at the University of Oxford, Michaelmas Term 2010

The effectiveness of radiotherapy treatment could be significantly improved if tumour cells could be rendered more sensitive to ionising radiation without altering the sensitivity of normal tissues. However, many of the key mechanisms that determine intrinsic tumour radiosensitivity are largely unknown. This thesis is concerned with the identification of novel determinants of tumour radiosensitivity. A siRNA screen of 200 genes involved in DNA damage repair was conducted using γH2AX foci post-irradiation as a marker of cell damage. This screen identified POLQ as a potential tumour-specific contributor to radioresistance. Subsequent investigations demonstrated that POLQ knockdown resulted in radiosensitisation of a panel of tumour cell lines, whilst having little or no effect on normal tissue cell lines.

It was subsequently shown that POLQ depletion rendered tumour cells significantly more sensitive to several classes of cytotoxic agents. Following exposure to etoposide, it was found that tumour cells depleted of POLQ had reduced RAD51 foci formation, suggesting that POLQ is involved in homologous recombination. A homologous recombination assay was used to confirm that POLQ depletion does indeed result in reduced homologous recombination efficiency.

These findings led to the investigation of the clinical significance of tumour overexpression of *POLQ*. The clinical outcomes of patients with early breast cancer were correlated with tumour expression levels of *POLQ*. It was found that *POLQ* overexpression was correlated with ER negative disease and high tumour grade, both of which are associated with poor clinical outcomes. *POLQ* overexpression was associated with extremely poor relapse free survival rates, independently of any other clinical or pathological feature. The mechanism that causes this adverse outcome may in part arise from resistance to adjuvant chemotherapy and radiotherapy treatment. These findings, combined with the limited normal tissue expression of POLQ, make it an appealing target for possible clinical exploitation.

Acknowledgements

I am extremely grateful to my supervisor and mentor Professor Gillies McKenna for enabling me to undertake a D.Phil in his group. I am hugely appreciative of all the encouragement and guidance that he has given me over the last three years, and for his ongoing support.

I am particularly indebted to Remko Prevo who has been a constant source of help and advice. I have been very fortunate to have worked with him. I would also like to thank former colleagues Eric Bernhard and Michio Yoshimura. I am also privileged to have worked in collaboration with several other groups and am thankful for the help I received from Francesca Buffa, Cecilia Lundin, Ian Hickson, Ruth Muschel, Thomas Helleday and Adrian Harris.

My research was largely funded by Cancer Research UK and the Royal College of Radiologists, and I acknowledge their generous support.

Finally I would like to thank my parents for their continual encouragement, my wife Ruth for her endless support, and our daughters Sophie and Emma, who make my time at home so hugely enjoyable.

Table of Contents

List of Figures and Tables

List of Abbreviations

53BP1	p53 binding protein 1
5-FU	5-Fluorouracil
AFM	antibiotic-free medium
AP	apurinic/apyrimidinic site
APEX2	apurinic/apyrimidinic endonuclease 2
ATM	ataxia telangiectasia mutated
BCA	bicinchoninic acid
BCR	B cell receptor
BER	base excision repair
bp	base pair
BSA	bovine serum albumin
CCNE2	cyclin E
chaos1	chromosome aberration occurring spontaneously
CI	confidence interval
CMF	cyclophosphamide, methotrexate, and 5-fluorouracil
Ct	cycle threshold
DAPI	4',6-diamidino-2-phenylindole
DMEM	Dulbecco's modified Eagle’s Medium
DMSO	dimethyl sulphoxide
DNA	deoxyribonucleic acid
DNA-PKcs	DNA-dependent protein kinase catalytic subunit
dRP	deoxyribose phosphate
DSB	DNA double strand break
DSBR	DNA double strand break repair
dsRNA	Double strand RNA

DTT	dithiothreitol
ECL	enhanced chemiluminescence
EGFR	epidermal growth factor receptor
ER	oestrogen receptor
FACS	fluorescence activated cell sorting
FBS	fetal bovine serum
GAPDH	glyceraldehyde-3-phosphate dehydrogenase
GCMRA	Guanine Cytosine robust multi-array average
GFP	green fluorescent protein
GGI	Gene expression Grade Index
GO	Gene Ontology
H2AX	histone 2A family member X
HBO	hyperbaric oxygen
HJ	Holliday junction
HR	homologous recombination
HR	hazard ratio
HRP	horseradish peroxidase
HTS	High-throughput screen
IR	Ionising radiation
KEGG	Kyoto Encyclopaedia of Genes and Genomes
LET	linear energy transfer
LN	lymph node
LQ	linear quadratic
MCD	mitotic cell death
MMEJ	microhomology-mediated end joining
MN	micronuclei
mRNA	messenger RNA

NER	nucleotide excision repair
NHEJ	non-homologous end-joining
NT	non-targeting
NTCP	normal-tissue complication probability
PBS	phosphate buffered solution
PCR	polymerase chain reaction
PFA	paraformaldehyde
PLD	potentially lethal damage
POLB	DNA polymerase beta
POLH	DNA polymerase eta
POLQ	DNA polymerase theta
qRT-PCR	quantitative reverse-transcription PCR
RFS	relapse free survival
RIPA	radio immunoprecipitation assay lysis buffer
RISC	RNA-Induced Silencing Complex
RNA	ribonucleic acid
RNAi	RNA interference
RPA	replication protein A
SDS-PAGE	sodium dodecyl sulphate polyacrylamide gel electrophoresis
SER	sensitisation enhancement ratio
SF_2	surviving fraction at 2Gy
SFM	serum-free medium
siRNA	small interfering RNA
SLD	sublethal damage
SMH	somatic hypermutation
SNP	single nucleotide polymorphism
STEEP	Standardised Definitions for Efficacy End Points

TBS	tris-buffered saline
TCP	tumour control probability
TLS	translesion synthesis
UTR	untranslated region
XAB2	XPA binding protein 2

Chapter 1

INTRODUCTION

1.1 Overview of Radiotherapy

Radiotherapy is a cancer treatment that involves delivering ionising radiation (IR) to tumour cells, typically in the form of megavoltage X-rays. Radiotherapy is routinely used in a variety of different clinical scenarios to treat many different tumour sites. It is often used with curative intent, either on its own, as is often the case with patients with non-small cell lung cancer (1), or in combination with other treatments such as chemotherapy (2), or biological therapy (3, 4). Following surgical excision of the primary tumour, radiotherapy is also used as an adjuvant therapy to reduce the risk of the patient developing local recurrence. This is the standard practice in the management of diseases such as breast cancer (5). As well as playing an important role in the management of patients with potentially curable cancer, radiotherapy plays a vital role in the palliation of patients with incurable disease. For example, it is an effective means of providing symptomatic improvement in the symptoms caused by bone (6) and brain metastases (7).

1.2 Ionisation Events

IR induces cell damage predominantly through its effects on DNA. The ionising effects on DNA can be said to be either direct or indirect. Direct radiation damage results from ionisation of the DNA without the involvement of any intermediate steps, and is the predominant process by which high linear energy transfer forms of radiation such as neutrons and α particles exert their effects (8). Megavoltage X-rays predominantly cause their effects as a result of indirect ionisation of DNA. This means that they do not produce chemical and biological damage by themselves, but when they are absorbed in the material through which they pass, their energy is transferred to produce fast-moving charged particles that in turn are able to produce damage (8). At the energies used by most clinical linear accelerators, the Compton

process dominates (9). In this process, the megavoltage photon interacts with a ‘free’ electron of the absorbing material. Some of the photon energy is transferred to the electron in the form of kinetic energy. The scattered photon travels further into the absorbing material with slightly reduced energy interacting with more ‘free’ electrons. The net result is the production of a large number of fast electrons, which can ionise other atoms in the irradiated material, as shown in Figure 1.1 below.

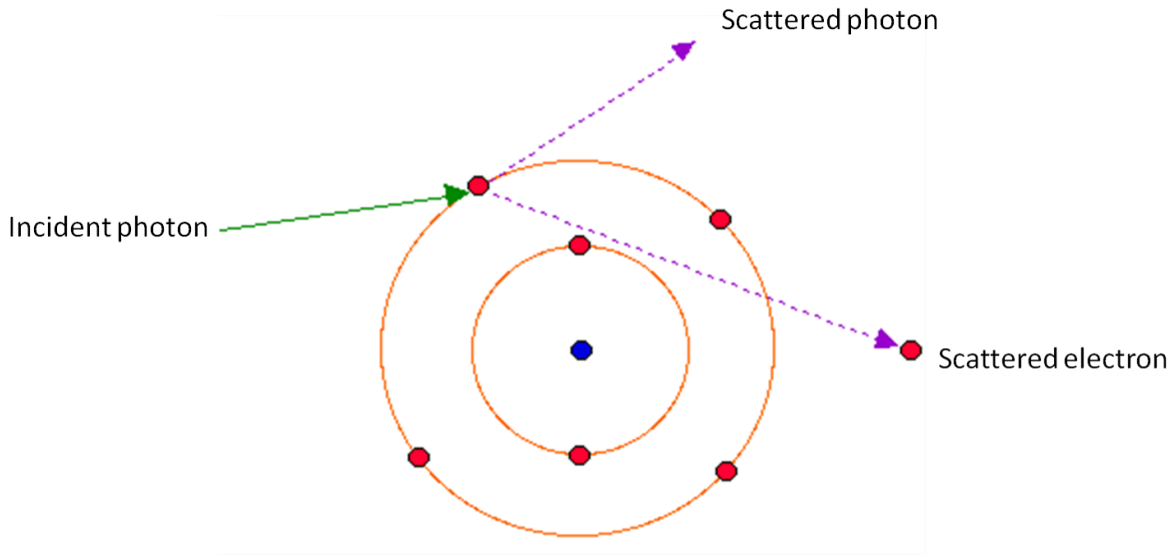

Figure 1.1. The Compton Effect. An incident X-ray photon interacts with a ‘free’, outer electron to which it transfers some of its energy. The scattered photon and electron travel deeper into the irradiated material, both of which can cause further ionisation.

Free radical reactions

These initial ionisation events trigger a series of chemical processes. It is useful to consider the radiochemistry of water following ionisation, since it comprises such a large proportion of cells. Following exposure to IR the water becomes ionised as shown below.

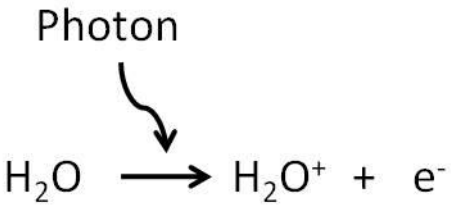

H_2O^+ is an ion radical and rapidly interacts with another water molecule to form the highly reactive hydroxyl radical (OH•).

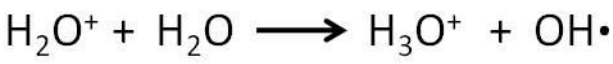

Free radicals formed following X-ray exposure can interact with DNA causing damage to the DNA molecule. This indirect action can be thought of as comprising physical, chemical and biological phases, which take place over very different time-scales. The physical process of ionisation occurs within 10^{-9} seconds following irradiation, whilst the formation of free radicals and subsequent free radical reactions are completed within approximately one millisecond of radiation exposure (9). The subsequent 'biological phase' includes all subsequent processes; from initial attempts at DNA repair, through to the development of late effects.

1.3 Radiation induced DNA damage

For several years, it has been recognised that IR induces multiple cellular lesions including, DNA-protein crosslinks, base alterations, base detachments, and DNA single and double strand breaks (10). However, DNA double strand breaks (DSBs) are the principle cytotoxic lesions induced by IR. The evidence supporting this arises from work correlating the number of DSBs produced by IR with the degree of cytotoxcity (10). For example the use of high linear energy transfer (LET) radiation causes more cell killing compared with low LET radiation. High LET radiation

increases the number of unrepaired DSBs, but does not increase the number of single strand breaks or base alterations compared to low LET radiation (11). Additionally, irradiating cells under hyperthermic conditions causes increased cytotoxicity due to an increase in unrepaired DSB formation but does not cause an alteration in other types of DNA damage (12). Therefore the formation of DSBs is central to the cell killing associated with IR exposure, and has resulted in complex mechanisms capable of repairing DSBs.

1.4 DNA double-strand break repair

DSBs are generated when the two complementary stands of the DNA double helix are broken simultaneously, at sites that are sufficiently close to one another that base-pairing and chromatin structure are insufficient to keep the two DNA ends juxtaposed. As a consequence, the two DNA ends generated by a DSB are liable to become physically dissociated from one another, making ensuing repair difficult to perform and providing the opportunity for inappropriate recombination with other sites in the genome.

The critical importance of being able to repair DSBs has resulted in the evolution of two distinct DNA repair processes; non-homologous end-joining (NHEJ), and homologous recombination (HR).

Non-homologous end-joining

NHEJ provides a mechanism for the repair of DSBs throughout the cell cycle, but is of particular importance during G0-, G1- and early S-phase of mitotic cells. The components of NHEJ are summarised below in Figure 1.2.

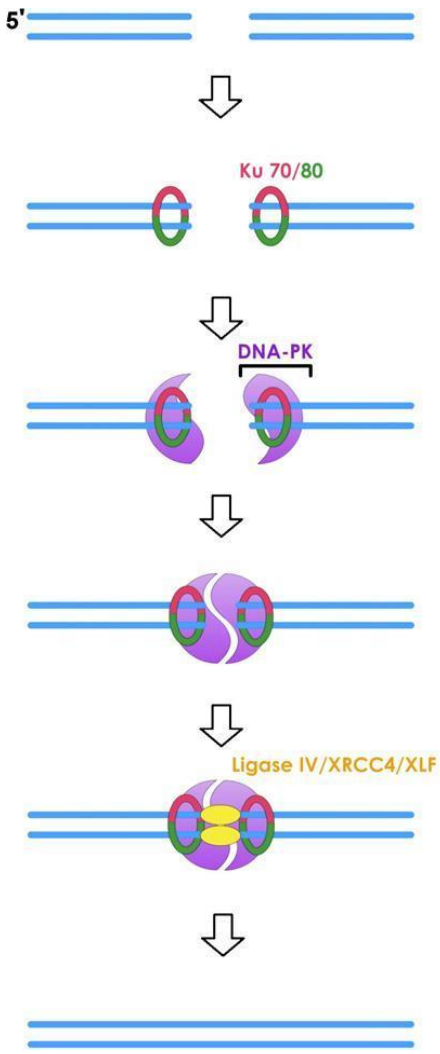

Figure 1.2. Summary of the key steps required for non-homologous end joining. DNA ends are first bound by the Ku70/80 heterodimer, which then attracts DNA-PKcs to form the DNA-PK complex. DNA-PK then attracts the ligase IV complex (comprised of ligase IV, XRCC4 and XLF), which together seal the DNA ends. Summary of NHEJ adapted from (13).

NHEJ is initiated by the binding of a complex composed of Ku70 and Ku 80 (Ku) to both ends of the broken DNA molecule. The Ku-DNA complex recruits DNA-dependent protein kinase catalytic subunit (DNA-PKcs), a 460kDa protein of the phosphoinositide 3-kinase-like family of protein kinases (PIKKs) (14). Ku then moves inward on the DNA, allowing DNA-PKcs to contact DNA (15). The association of DNA-PKcs with both DNA and Ku leads to activation of the serine/threonine kinase

activity of DNA-PKcs (16). Inward translocation of Ku also allows two DNA-PKcs molecules to interact across the DSB, forming a molecular ‘bridge’ between the two DNA ends (17).

Since DSBs can occur with a variety of different ends, a number of processing enzymes are often required to repair breaks. Ends must be transformed to 5’-phosphorylated ligatable ends in order for repair to be completed. One key end-processing enzyme in mammalian NHEJ is Artemis, a member of the metallo-*β*-lactamase family of enzymes, which may be recruited to DSBs through its ability to interact with DNA-PKcs (18). Artemis possesses both DNA-PKcs-independent 5’- to 3’ exonuclease activity, and DNA-PKcs-dependent endonuclease activity towards DNA-containing ds–ssDNA transitions and DNA hairpins, each of which might be important for processing of DNA termini during NHEJ (18). Inactivation of Artemis results in radiation sensitivity; however, cells lacking Artemis do not have major defects in DSB repair, suggesting that only a subset of DNA lesions are repaired in an Artemis-dependent manner *in vivo* (19). Processing of complex lesions may lead to the creation of DNA gaps that must be filled in by DNA polymerases to enable break repair (20).

NHEJ is completed by ligation of the DNA ends. This is mediated primarily by XRCC4, XLF and DNA ligase IV. Although XRCC4 has no known enzymatic activity, it acts as a scaffold interacting with both Ku and DNA and stimulates DNA ligase IV to ligate the processed ends, repairing the break (21). XLF has structural similarities to XRCC4 and it has been shown that siRNA mediated downregulation of XLF in human cell lines leads to radiosensitivity and impaired NHEJ (22).

Although NHEJ is an efficient pathway, it is often imprecise, because the DNA ends are modified before joining, leading to deletions or insertions at the break site.

Homologous recombination

HR is the second DSB repair pathway, and uses homologous DNA from a sister chromatid as a template to perform error-free repair of DNA DSBs. The need for a sister chromatid means that HR occurs only in G2 and S phases of the cell cycle. HR is proposed to occur in several discrete stages as illustrated in Figure 1.3 below.

The MRN complex (MRE11-RAD50-NBS1) is involved in the initial process of recognising the DSB. MRN complexes tether the DNA ends, and activate the catalytic function of the ATM protein kinase through direct interaction of ATM and NBS1 (23, 24). ATM phosphorylates numerous substrates in the DNA damage response, including histone H2AX, which is an early chromatin marker of DSB formation (25). BLM helicase, which is a member of the RecQ family, stimulates human exonuclease 1 (hExo1) to process the DNA ends by 5’ to 3’ degradation to create 3’ single-stranded DNA (ssDNA) tails (26). Replication protein A (RPA) then rapidly binds to the single strand DNA (27). A mediator complex that includes BRCA1, BRCA2 and PALB2 then loads RAD51 onto the RPA coated ssDNA (28-32). The RAD51-ssDNA complex searches a second DNA molecule for homology, and then moves into the homologous DNA duplex in a process called ‘strand invasion’ that is mediated by RAD54B (33).

Strand invasion into a homologous sequence forms a D-loop intermediate. After strand invasion, a DNA polymerase extends the end of the invading 3' strand by synthesising new DNA, changing the D-loop to a cross-shaped structure known as a Holliday junction (HJ). It is currently unclear which polymerases mediate D-loop

extension *in vivo*, but POLH (DNA polymerase eta) can perform this function *in vitro* (34). Two separate models; named the synthesis-dependent strand annealing (SDSA) pathway, and the double strand break repair (DSBR) pathway (or double Holliday Junction pathway) have been proposed to describe the remaining steps (35, 36). The DSBR model proposes that the second 3' overhang strand also anneals to the homologous template and forms a second HJ. Recent evidence has implicated RAD52 (37, 38) in this process of 'second-end capture'. Once the second Holliday junction has been formed, and DNA synthesis has been completed, the Holliday junctions are resolved. The MUS81-EME1 complex has been shown to cleave HJs with the formation of crossover products (39, 40). However, there are several complications that arise when using this model to explain the mechanisms of mitotic DSB repair. Importantly, when resolution products are analysed following introduction of a site-specific double-strand break, crossover products are rarely observed (41). Although it has been shown that the product of the Bloom's syndrome gene, BLM, in complex with topoisomerase IIIα can dissolve HJs to form non-crossover products (42), and that a novel resolvase, GEN1 dissolves HJs by a symmetrical cleavage and would therefore also be expected to give rise to crossovers and non-crossovers with equal efficiency (43), the SDSA model is thought to be the predominant mechanism by which homology directed repair handles two-ended DSBs.

The SDSA model is initially the same as the DSBR in that the 3' end of the ssDNA invades the homologous template forming a D-loop. DNA synthesis then occurs beyond the original break site to restore the missing sequence information. The next step in this pathway is to release the newly synthesised end. This requires the Holliday Junction to be slid towards the 3' end; a procedure called 'branch migration'

that involves the RAD54 protein (44). The newly synthesised DNA strand is then displaced and anneals with the other DSB end. Break repair is completed by DNA synthesis and ligation with only non-crossover products formed.

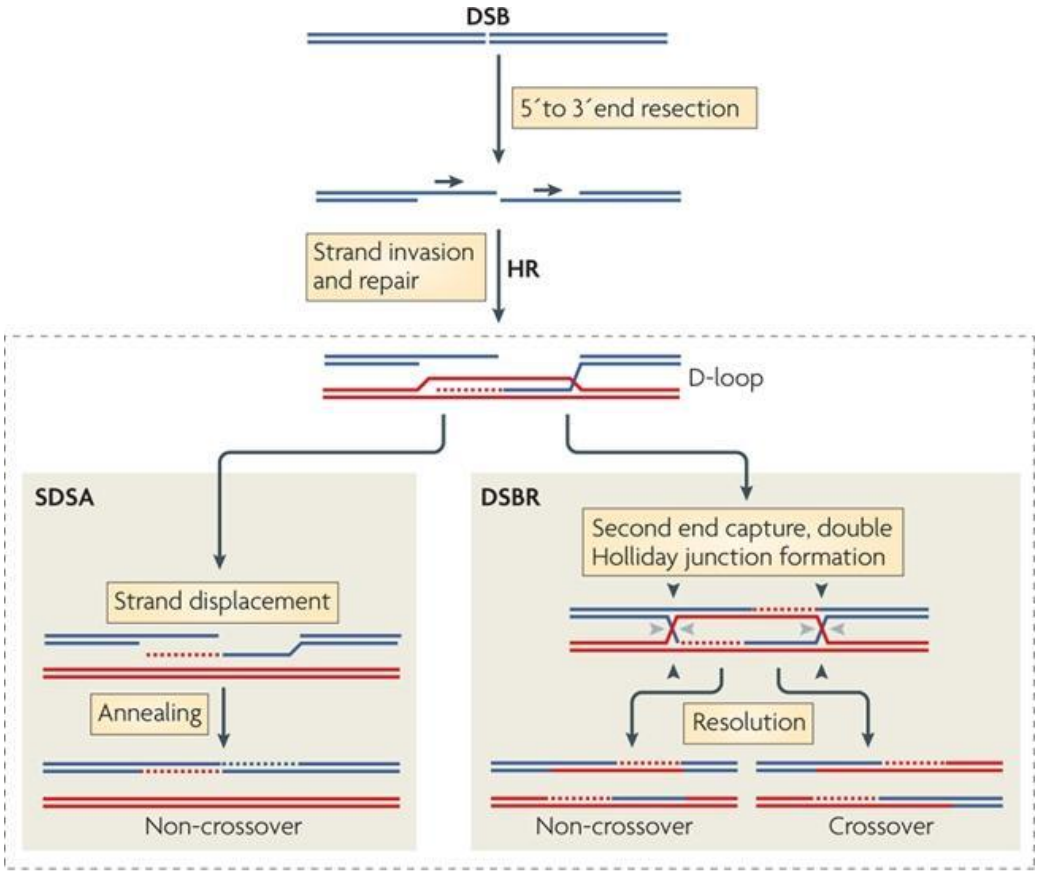

Figure 1.3. Pathways of homologous recombination. HR is initiated by end resection, which produces a 3′ single-stranded end that can invade a homologous template to initiate repair. Alternative HR pathways can ensue from the displacement loop (D-loop) intermediate: SDSA and DSBR. In SDSA, the newly synthesised strand is displaced to anneal to the other DNA end, resulting in a non-crossover outcome with no change to the template DNA. In DSBR, the second DNA end is 'captured' to form a double Holliday junction, which in principle can result in a non-crossover (cleavage at grey arrowheads on both sides) or a crossover (cleavage at black arrowheads on one side and grey arrowheads on the other) outcome. Adapted from (45)

The complex processes of DSB repair reflect the critical importance of being able to repair these potentially lethal lesions. Failure to adequately repair DSBs can result in

cell death. Many oncological treatments such as chemotherapy cause cancer cell death by inducing apoptosis (46). Although IR is recognised as inducing apoptosis in seminomas and lymphomas (47), this is not representative of most cancers. In general IR causes cell death by inducing mitotic cell death (MCD) (48-50). This process is characterised by tumour cells remaining metabolically active post IR until, upon entering mitosis, they undergo mitotic catastrophe. An important feature of this phenomenon is that cells which have been fatally damaged by IR can undergo several rounds of mitosis before they, and their progeny die (48-50). Cell death of normal tissues exposed to IR is the basis for the development of most side effects associated with radiotherapy.

1.5 Side effects associated with radiotherapy

Radiotherapy is a vital tool in the management of cancer patients. However, whenever radiotherapy is given with curative intent there is a risk of causing serious damage to normal tissues. Accordingly, the maximum radiation dose that can safely be delivered to patients is limited by the dose tolerances of surrounding normal tissues (51). Delivering an excessive dose of radiotherapy can result in unacceptable side effects to the patient. The side effects associated with radiotherapy can be broadly stratified into early and late effects.

Early effects

Early effects were traditionally defined as occurring within 3 months from the conclusion of treatment (9). They typically affect rapidly renewing tissues such as the skin, gastrointestinal tract and haemotopoietic system which often have a hierarchical cell lineage, composed of stem cells and their differentiating offspring. Early effects are thought to arise from depletion of regenerative stem cells, and the

severity of reaction depends upon the ability of these cells to repopulate. Examples of early effects of radiotherapy are listed by anatomical site in Table 1.1

Organ	Symptom/Sign
Skin	Erythema, dry desquamation, moist desquamation, ulceration
Mucous membranes	Mucositis, ulceration
Oesophagus	Oesophagitis
Lung	Pneumonitis, cough
Bowel	Diarrhoea, nausea, vomiting
Bladder	Frequency, urgency, dysuria, haematuria
Rectum	Proctitis, bleeding, tenesmus
Haematopoietic	Lymphopaenia, thrombocytopaenia, anaemia

Table 1.1. Examples of acute effects occurring in normal tissues. Adapted from (52).

Late effects

Arguably the more serious side effects of radiotherapy are caused by late effects. These are classically thought of as arising more than 3 months after the completion of treatment and effect slowly proliferating tissues such as the lung, heart, and central nervous system (9). Attempts have previously been made to quantify the radiation doses that can be tolerated by specific organs in order to guide clinicians as to the maximum doses that may be delivered to specific organs (51, 53). In 1991, Emami et al published a landmark article in which the tolerance dose of normal tissues was exhaustively reviewed (51). In that article the 5% risk of complication within 5 years (TD5/5) and 50% risk of complication within 5 years (TD50/5) were reported as a function of volume of normal tissue irradiated (1/3, 2/3, or entire volume). These tolerance doses were based on a comprehensive literature review

as well as expert opinion. A simplified summary of these tolerances is given in Table 1.2.

Organ	Emami TD5/5	Emami TD 50/5	Endpoints
Brainstem	1/3: 60Gy 2/3 53Gy 3/3 50Gy	1/3: - 2/3: - 3/3: 65Gy	Necrosis Infarction
Spinal Cord	5 cm: 50Gy	5cm: 70Gy	Myelitis Necrosis
Oesophagus	1/3: 60Gy 2/3: 58Gy 3/3: 55Gy	1/3: 72Gy 2/3: 70Gy 3/3: 68Gy	Clinical stricture/ perforation
Parotid	1/3: - 2/3: 32Gy 3/3: 32Gy	1/3: - 2/3: 46Gy 3/3: 46Gy	Xerostomia

Table 1.2. Summary of the dose tolerances of critical normal tissues. The 5% risk of complication within 5 years (TD5/5) and 50% risk of complication within 5 years (TD50/5) are partly dependent upon the volume of the organ that is irradiated.

1.6 The four Rs of radiotherapy

Multiple factors influence the response of normal tissues and tumours to fractionated radiotherapy. These factors were summarised by Withers in 1975 as ‘The four R’s of radiotherapy’ (54). In this paper, Withers described four features that influence outcome: Repair, Reassortment, Repopulation and Reoxygenation.

Repair

Repair refers to the processes by which DNA damage is restored following fractionation. The damage caused by radiation exposure has previously been classified as either 1) ‘lethal damage’ which is unrepairable and inevitably results in cell death; 2) ‘potentially lethal damage’ which reflects the aspect of radiation damage that can be repaired if the environmental conditions are changed; and 3) ‘sublethal damage’ which is repairable unless further damage is caused by prompt reirradiation.

The post-irradiation environmental conditions can alter the proportion of cells capable of surviving a given dose of radiation because of the repair of ‘potentially lethal damage’ (PLD). If the post-irradiation conditions are optimal for PLD repair; cells which would normally die following exposure to a given dose of radiation may survive if the environmental conditions are ideal. PLD repair was initially studied in confluent cells that were non-growing due to density inhibition. Following radiation, cells were subcultured, and their colony-forming ability assessed. It was shown that cell survival was significantly increased if cells were left in non-growing conditions for 6 or 12 hours after irradiation before subculturing for colony forming assay (55). In this experiment it has been suggested that the non-growing conditions allow extra time for the damage to be repaired prior to cells undergoing mitosis. This work, along with parallel *in vivo* work, showed that PLD can be repaired if the environmental conditions allow, although the clinical significance of this phenomenon is less clear.

The observation that a given dose of radiation is less effective if split into two fractions several hours apart reflects the ability of cells to recover from exposure to ‘sublethal damage’ (SLD) (56). The ability of cells to recover from sublethal damage contributes to the sparing effect of fractionating external beam radiotherapy

treatment. SLD is also of clinical importance in the context of brachytherapy. Cells exposed to a given dose of radiation are more sensitive to high dose rate exposure over a short duration, than to low dose rate exposure over a long duration. This is in part due to the prolonged exposure allowing greater repair to occur (57).

Reassortment

The concept of ‘reassortment’ refers to the observation that radiosensitivity alters significantly through the different phases of the cell cycle, and that cells surviving a given fraction of radiotherapy may be in a resistant phase of the cell cycle, but may have progressed to a more sensitive phase of the cell cycle during the next fraction. The original data showing that radiosensitivity changes throughout the cell cycle was published in the 1960’s by Sinclair *et al* (58, 59). Chinese hamster cells were synchronised at five different points in the cell cycle. Cell survival was then assessed following exposure to radiation (Fig. 1.4). Cells in mitosis and G2 are the most radiosensitive and those in S phase the most radioresistant. It is likely that the reason why cells in S phase are more radioresistant, relates to the presence of an accessible sister template, increasing the opportunity for DSBs to be repaired by HR.

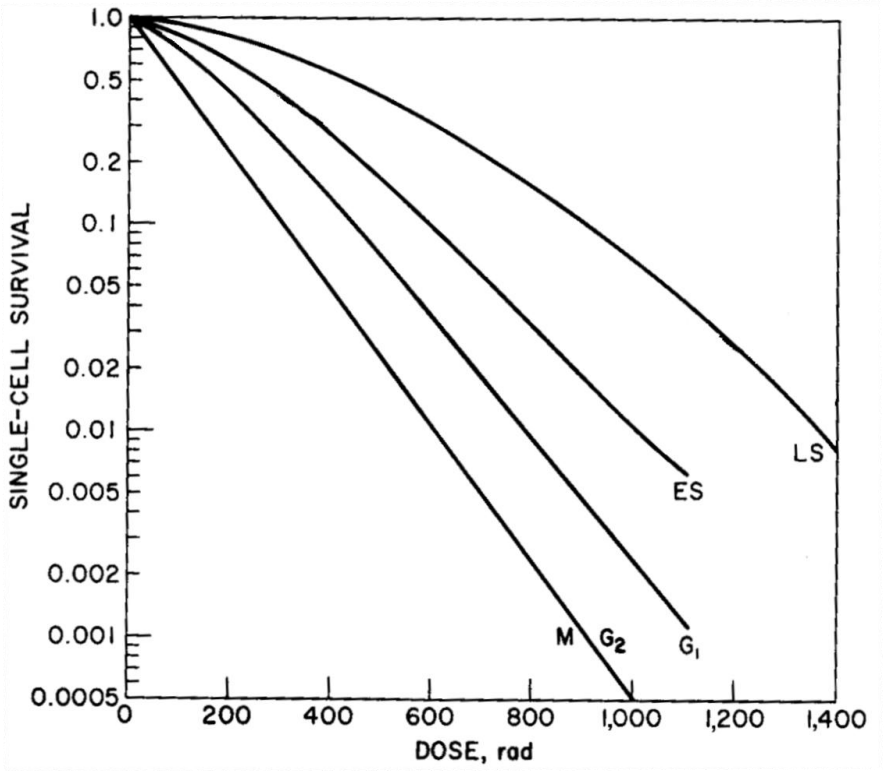

Figure 1.4. Chinese hamster cells irradiated at different points in the cell cycle show altered radiosensitivity. Cells in late S phase (LS) are the most radioresistant and those in M and G2 the most radiosensitive. Early S phase (ES) and G1 are associated with intermediate sensitivity. Adapted from (58).

An advantage of delivering radiotherapy in multiple, discrete fractions, is that tumour cells which survive a given fraction are more likely to be in a resistant phase of the cell cycle, but may have progressed to a more sensitive phase of the cell cycle during the next fraction of treatment. Previous attempts have been made to synchronise tumour cells using cytotoxic drugs prior to delivering radiotherapy. The aim of this approach was to irradiate tumour cells whilst in a sensitive phase of the cell cycle (60). The limited success associated with this technique may be due to the heterogenous cell cycle kinetics within tumours resulting in rapid loss of induced cell synchrony.

Repopulation

Delivering radiotherapy in several separate fractions enables cells that have survived irradiation to divide and 'repopulate'. Prolonging treatment enables normal tissues to repopulate and therefore reduces early reactions. However excessive prolongation results in tumour cell proliferation that can result in treatment failure. Tumour cells surviving irradiation can divide more quickly resulting in 'accelerated repopulation' (61). In head and neck cancers, it has previously been shown that the rate of tumour cell repopulation significantly increases after approximately four weeks from the start of radiotherapy treatment (61). It has been estimated that in order to adequately compensate for this increased repopulation, an additional 0.6 Gy should be delivered each day (61). Radiotherapy dose and fractionation schedules have therefore tried to find the optimal balance between causing excessive toxicity and improving local control rates. 'Accelerated radiotherapy' involves shortening the overall treatment time by delivering more than one fraction of radiotherapy a day. Clinical trials investigating this have typically found that accelerated treatment causes an improvement in local control, but at the cost of increased acute toxicity (62). Other modified fractionation trials have looked at the possible benefits of 'continuous hyperfractionated accelerated radiotherapy' (CHART) in which patients are treated with a strongly accelerated fractionation regimen using a reduced total dose. The use of CHART in NSCLC has been shown to be associated with an increase in acute mucositis (1, 63). However the toxicity associated with CHART was not considered excessive and was satisfactorily offset by the large improvements seen in local control and overall survival rates (1, 63). Consequently it was concluded that CHART treatment improved the therapeutic ratio of radiotherapy and it therefore became an established treatment option for NSCLC patients in the UK. It is likely that the

improvements seen with CHART radiotherapy occur because the treatment is completed before tumour cell accelerated population is established.

Reoxygenation

It is possible that 'reoxygenation' is the most important of the 'Four R's of radiotherapy'. Over fifty years ago it was recognised that the response of cells to IR is strongly dependent upon oxygen (64-66). As shown in Figure 1.5, cells are much more sensitive to X-rays in the presence of oxygen than in its absence. Most cells typical show an oxygen enhancement ratio of 2.5-3.0.

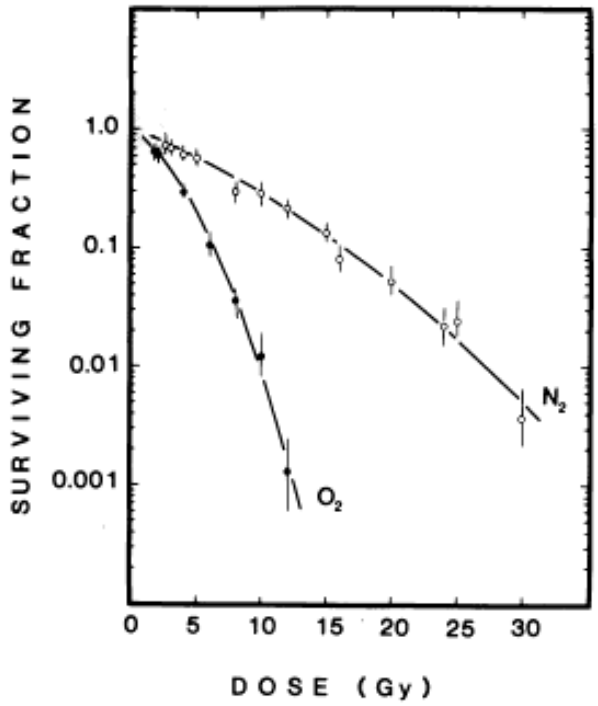

Figure 1.5. Illustration of increased cell radiosensitivity when irradiated under aerobic (O_2) conditions compared with irradiation under hypoxic conditions (N_2). Chinese hamster ovary cells were grown under exponential conditions prior to irradiation with 250 kV x-rays. Figure adapted from (66).

The ‘oxygen fixation hypothesis’ was devised in the 1950’s and attempted to describe the mechanism by which the presence of oxygen increases cell radiosensitivity (67). As described previously, most of the damage caused by ionising radiation results from the indirect damage caused by the formation of free radicals which interact with DNA. The DNA radicals (R•) can be restored through reactions with free radical scavengers such as sulphydryl containing compounds (68, 69). However in the presence of molecular oxygen, the damage can be ‘fixed’ by the DNA radical reacting with O_2 to form RO_2• which is less amenable to restoration by scavenger groups (70). An illustration of the differences between the direct and indirect damage caused by X-rays is shown in Figure 1.6 below.

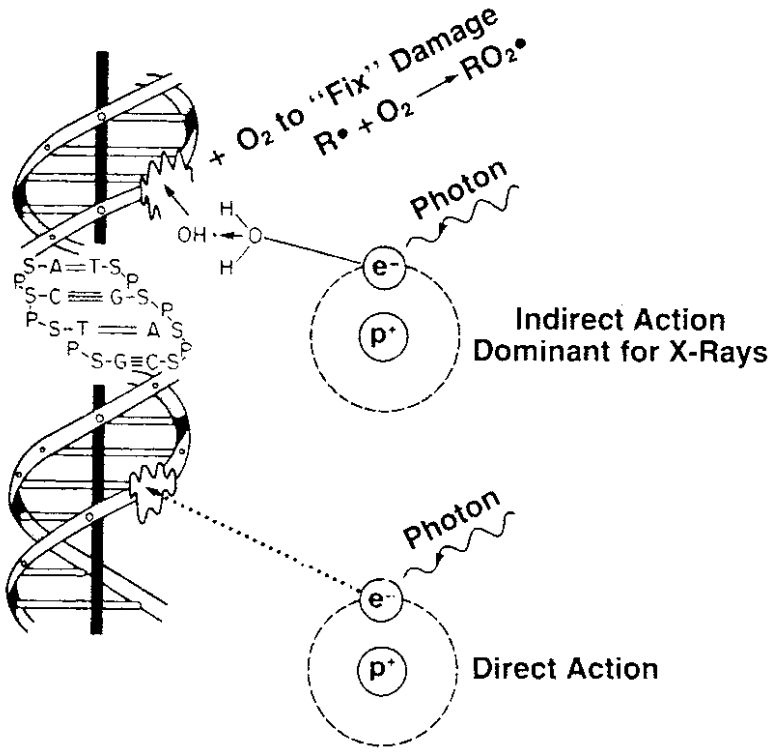

Figure 1.6 Direct and indirect DNA damage. The majority of DNA damage caused by X-rays is due to ionisation of water resulting in free radical damage to DNA which can be ‘fixed’ in the presence of oxygen. A small proportion of the DNA damage occurs due to direct ionisation of the DNA. Figure adapted from (8).

Tumours cells are often profoundly hypoxic and therefore demonstrate resistance to radiotherapy treatment (71). The concept of 'reoxygenation' in the context of fractionated radiotherapy relates to the possibility that tumour cells which are hypoxic at the start of radiotherapy treatment may become less hypoxic, and therefore more radiosensitive throughout radiotherapy treatment. This may be partly due to the tumour shrinking and improving the oxygen supply to a proportion of the tumour cells.

1.7 Hypoxic radiosensitisation

The profound changes in radiosensitivity caused by hypoxic conditions have resulted in multiple different approaches to try to reverse tumour hypoxia. Initial attempts at improving tumour hypoxia involved patients breathing high-oxygen content gas under hyperbaric oxygen (HBO) conditions. A comprehensive Cochrane review of all clinical trials performed with HBO concluded that there was some evidence that HBO improved local control rates in cervix and head and neck cancer, but that these benefits may only arise with unconventional fractionation schemes. Importantly they found that HBO was associated with significant adverse effects, including oxygen toxic seizures and severe tissue radiation injury (72).

Other strategies have previously been employed to try to increase tumour oxygen levels. One particular approach has been to try to increase the oxygen that can be delivered to the tumour by increasing patient's haemoglobin levels. Anaemia is recognised as conferring a poor prognosis in many different tumour types (73). Although the association between anaemia and poor prognosis may simply reflect more advanced disease, previous studies have suggested that anaemia is an independent prognostic factor in patients receiving radiotherapy treatment (74). As a

result of this, multiple small studies have investigated whether reversing anaemia during radiotherapy treatment results in an improvement in clinical outcomes. These studies have been unable to consistently show that treating anaemia with blood transfusions results in an improvement in patient outcomes. Although some studies show an improvement in outcomes, other studies have shown that blood transfusions may have a positively detrimental effect on outcome, possibly by inducing mild immunosuppression (75). Alternative means of correcting anaemia without using blood transfusions have also been pursued. Most notably, a large phase III trial investigated the possibility of improving anaemia, and therefore response to radiotherapy by treating head and neck cancer patients with erythropoietin β. This study showed that erythropoietin increased haemoglobin levels, but caused a statistically significant detrimental effect on overall survival (76). Since erythropoietin receptors are known to be expressed on tumour cells, it is possible that erythropoietin treatment causes adverse clinical outcomes by inducing tumour cell progression and proliferation (77).

An alternative approach to overcoming radioresistance associated with tumour hypoxia has been to use ‘oxygen mimetics’. The origins to this area of research began with the identification that electron affinic compounds sensitised hypoxic cells to radiation (78). Misonidazole was one of the first electron affinic compounds shown to cause hypoxic radiosensitisation *in vitro* (79). Metronidazole (80) and misonidazole (81-84) were among the first agents to be used in clinical trials to assess the therapeutic uses of these hypoxic radiosensitisers. The misonidazole studies were performed in patients with a wide spectrum of tumour types. Although some studies found small sub-groups of patients who appeared to derive benefit

from the addition of misonidazole (85), the majority of the trials showed misonidazole did not cause a statistically significant benefit (81-84). It has previously been suggested that the disappointing results obtained with misonidazole arose because the side effect profile of the drug meant that it could not be used at doses high enough to exert a radiosensitising effect (86). This led to efforts to identify oxygen mimetics that did not cause the severe side effects associated with misonidazole treatment. Nimorazole was the most widely investigated of these drugs and was the subject of a large phase III study in Danish patients with cancer of the pharynx or supraglottic larynx. This study showed that the combined treatment of nimorazole and radiotherapy was associated with a statistically significant improvement in loco-regional control, compared with patients treated with radiotherapy alone (87). Despite these trial results, nimorazole is rarely used in routine practice outwith Denmark (88). The reasons for this are unclear, but may be due to the trial failing to show that the addition of nimorazole resulted in an improvement in patient survival (87). No other hypoxic radiosensitiser is currently in routine, widespread use.

It has been suggested that the disappointing results associated with attempts to correct tumour hypoxia are due to the fact that these treatments act against chronic hypoxia (9). More recent studies have used nicotinamide in an attempt to reverse perfusion-limited acute hypoxia, by preventing transient fluctuations in tumour blood flow (89). In particular, nicotinamide has been used as part of the ‘Accelerated Radiation, Carbogen and Nicotinamide’ (ARCON) studies. Carbogen (95% oxygen, 5% carbon dioxide) breathing commences five minutes prior to radiotherapy and is continued throughout. Nicotinamide is administered orally, 90 minutes prior to radiotherapy. Large phase II studies investigating the effects of ARCON have been published in head and neck (90) and bladder cancer patients (91) and have so far

showed promising results. Results from ongoing phase III studies will determine whether ARCON treatment may prove to be a successful means of reversing the poor prognosis associated with tumour hypoxia.

1.8 Intrinsic radiosensitivity.

The realisation that the intrinsic radiosensitivity of tumour cells varied significantly, and was of considerable importance in influencing the response of tumours to radiotherapy treatment led Steel to propose in 1989 that 'radiosensitivity' should be recognised as one of the '5Rs of radiobiology' (92). It is been recognised for many years that tumours differ significantly in their sensitivity to radiotherapy treatment and that the intrinsic radiosensitivity of different cancers correlates with their potential radiocurability. A 1981 study initially showed the correlation between *in vitro* radiosensitivity and clinical response to radiotherapy (93). A subsequent study three years later showed similar findings, and developed the idea of measuring intrinsic radiosensitivity based on the surviving fraction of tumour cells following 2Gy of radiation (SF_2) (94). This initial work showed that different histological tumour types had different intrinsic radiosensitivities and that this correlated with clinical radioresponsiveness. Subsequent work has shown that there are significant differences in tumour radiosensitivity within the same histopathological class of tumours, and that this has significant clinical relevance. Studies in cervix, and head and neck cancers have shown that those patients with radioresistant tumours (as measured by the surviving fraction at 2Gy) are more likely to develop local recurrences (95-97) and have poorer survival rates (96, 97) than patients with more radiosensitive disease.

Clinical use of radiosensitising drugs

Multiple different approaches have been used to try to render tumour cells more sensitive to IR. The most commonly used approach has been to deliver radiotherapy with concurrent chemotherapy treatment. Typically this has involved the use of agents that affect DNA or RNA processes, of which cisplatin is the most commonly used. Cisplatin interacts with DNA to form inter- and intrastrand cross-links, as well as DNA-protein cross-links, inhibiting DNA replication and RNA transcription and ultimately inducing mutagenesis or apoptosis (98). The precise mechanism by which platinum analogues induce radiosensitisation remains the subject of debate. One possible explanation is that oxygen free radicals generated by IR result in an increase in the number of toxic platinum intermediates when delivered concurrently (99). Alternative explanations include the suggestion that radiosensitisation occurs due to cisplatin inhibiting DNA damage repair in the presence of IR (100).

Despite the uncertainty as to its mechanism of action, there is substantial clinical evidence showing that concurrent cisplatin and radiotherapy improves clinical outcomes. In patients with locally advanced non-small cell lung cancer, the addition of cisplatin has been shown to cause a 30% reduction in two year mortality compared to treatment with radiotherapy alone (101). In cervical cancer, cisplatin was shown in a large randomised phase III study to cause a 39% relative risk reduction of death in patients treated with concurrent cisplatin and radiotherapy (102). In view of these striking results, the US National Cancer Institute issued an alert in February 1999 that chemoradiotherapy should be considered for all patients with cervical cancer. A subsequent large meta-analysis confirmed the findings that the addition of cisplatin chemotherapy resulted in large improvements in clinical

outcomes (2). Concurrent cisplatin chemoradiotherapy has been demonstrated to cause a 30% relative risk reduction of death in head and neck cancer patients compared to patients treated with radiotherapy alone (103). This has again been confirmed by a large meta-analysis (104).

Other conventional chemotherapies such as 5-Fluorouracil (5-FU) are also often used clinically to cause tumour radiosensitisation. 5-FU is a halogenated pyrimidine nucleoside that is phosphorylated by cellular thymidine kinase to form 5-fluoro-20-deoxy-uridine-monophosphate which inhibits thymidylate synthase. The intracellular pools of thymidine 5'-monophosphate and thymidine 5'-triphosphate subsequently become depleted, leading to the inhibition of DNA synthesis and interference of DNA repair (105). The mechanism by which 5-FU induces radiosensitisation is not clear, but it can be mediated by non-cytotoxic concentrations of 5-FU (106). Phase III trials of 5-FU and RT have demonstrated benefit in cancers of the oesophagus, cervix, and anal canal (107-109).

The numerous studies demonstrating improved patient outcomes have resulted in a large increase in the different cancers that are treated with concurrent chemoradiotherapy. Whilst these have shown improved outcomes in terms of local recurrence and overall survival rates, it should be noted that the addition of conventional chemotherapy is not without consequence, and that the addition of chemotherapy significantly increases the side effects caused by radiotherapy (2, 110).

The therapeutic index of radiotherapy

The increased toxicity associated with chemoradiotherapy reflects the fact that the addition of conventional chemotherapy has a non-specific radiosensitising effect, sensitising both tumour cells and normal cells to radiotherapy. The balance of risks and benefits of making alterations to radiotherapy treatment are often considered in terms of the therapeutic index or 'therapeutic window'. The therapeutic window of radiotherapy is the ratio between the harmful dose and the therapeutic dose of radiotherapy and can be altered by interventions such as altering fractionation or by the concurrent use of chemotherapy. Interventions that widen the gap between the 'tumour control probability' (TCP) curve and the 'normal-tissue complication probability' (NTCP) have the effect of increasing the therapeutic window (Fig. 1.7). Alterations in radiotherapy dose-fractionation schedules have previously been employed to improve the therapeutic window of radiotherapy.

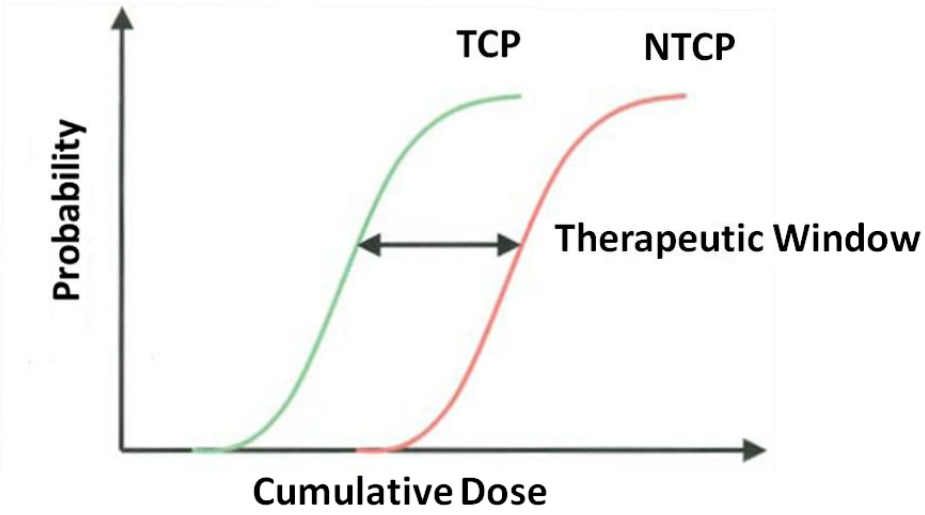

Figure 1.7 Representation of the therapeutic window. As the dose of radiotherapy is increased, the probabilities of both controlling the tumour (TCP), and of causing normal-tissue complications (NTCP) increase. The therapeutic window is the gap between the TCP and NTCP curves.

When delivering concomitant chemo-radiotherapy, the radiation dose–response curves of both the tumour and surrounding normal tissues will shift to the left (Fig. 1.7). Radiosensitisation due to conventional chemotherapies such as cisplatin induces a larger shift in TCP curve compared to that of the NTCP curve. Therefore, although chemo-radiotherapy results in increased side-effects, these are adequately offset by the benefits in tumour response and are indicative of the improved therapeutic index associated with chemo-radiotherapy treatment.

Tumour specific radiosensitisation

Potentially greater gains in the therapeutic ratio of radiotherapy could be made if treatments could be developed that selectively rendered tumour cells more sensitive to ionising radiation without altering the sensitivity of normal tissues. The best example of this approach being successfully utilised has come from the concomitant use of cetuximab and radiotherapy in the treatment of head and neck cancer. High levels of epidermal growth factor receptor (EGFR) expression, which is seen in the majority of squamous-cell cancers of the head and neck have been shown to correlate with worse clinical outcomes (111), decreased response to radiotherapy (112, 113), and increased loco-regional recurrence following definitive radiotherapy (114). Although the exact mechanism by which EGFR overexpression causes these effects is not clear, it appears to involve EGFR signalling via the Ras-PI3 kinase-Akt pathway (115). Cetuximab is a monoclonal antibody to the epidermal growth factor receptor that has been shown to radiosensitise tumour cells *in vitro* and *in vivo* (116). A phase III trial has investigated the potential benefits of concurrent treatment with cetuximab and radiotherapy in patients with locally advanced head and neck cancer (3). Patients were randomised to receive either radical radiotherapy alone or radical radiotherapy plus weekly cetuximab for the duration of radiotherapy. The study

reported a significant benefit from the addition of cetuximab. The median overall survival was 49.0 months among patients treated with combined therapy and 29.3 months among those treated with radiotherapy alone (HR for death, 0.74; P=0.03). The addition of cetuximab did not result in an increase in radiation induced side effects such as mucositis (3). The most common side effect associated with the addition of cetuximab is the development of an acneiform rash which occurs even in the absence of concurrent radiotherapy treatment (117). An updated analysis of this study with longer patient follow up has recently been published (4). This confirmed the improved clinical outcomes in patients treated with combined therapy. With the exception of acneiform rash and infusion reactions, the authors concluded that the addition of cetuximab does not increase the side effects associated with radiotherapy treatment. Interestingly they showed that for the patients treated with cetuximab, overall survival was significantly improved in those who experienced an acneiform rash and suggested that rash is a biomarker of an immunological response that is conducive for optimal outcome (4).

Rationale for performing a siRNA radiosensitivity screen

As previously discussed, delivering a potentially curative dose of radiotherapy is associated with the risk of developing significant side-effects due to the effects of radiation on normal tissues that surround the tumour. It is the risk of developing severe side effects that limits the dose of radiotherapy that we can deliver to tumours. The absence of excess normal tissue toxicity seen in the cetuximab study demonstrates the potential improvements that can be achieved by selectively rendering tumour cells more sensitive to radiation therapy (3). Such a strategy depends upon exploiting tumour specific molecular targets, many of which remain to be identified. The subject of this thesis will therefore attempt to identify and validate

novel targets involved in tumour cell radiosensitivity. The identification of novel molecular determinants of radiosensitivity will be based on a small interfering RNA (siRNA) screen of genes involved in DNA damage repair.

1.9 RNA interference

RNA interference (RNAi) is a post-transcriptional gene silencing mechanism that can be triggered by small RNA molecules such as microRNA (miRNA) and siRNA. The ability of short sequences of double stranded RNA to potently suppress specific genes was first identified in *Caenorhabditis elegans* (118). It has subsequently been demonstrated that RNAi is an important feature of eukaryotic cells including human cells, and that the introduction of synthetic siRNAs is capable of inducing profound gene suppression (119). It is now well recognised that a complicated system of endogenous RNAi complexes are produced within cells that target host RNA sequences resulting in gene silencing.

Mechanics of siRNA silencing

Endogenous siRNA is derived from longer dsRNA, whilst miRNAs are thought to arise from precursor RNA molecules that adopt a hairpin-and-loop structure (120). There are several distinct steps required for the formation and activation of endogenous siRNA. Firstly, long dsRNA strands are cleaved into siRNA dimers of between 21-25 nucleotides length with characteristic 2-nucleotide overhangs at the 3' ends. This function is performed by the enzyme Dicer (121) which is a endoribonuclease of the RNase III family. Dicer then aids in binding one of the siRNA strands (the 'guide' strand) onto a multiprotein complex called RNA-Induced Silencing Complex (RISC) (122). It has recently been shown that the guide strand is selected on the basis of the thermodynamic properties of the individual strands. The

strand whose 5' end is less tightly paired to its complement is the one that enters the RISC complex (123, 124). The remaining 'passenger' strand is then degraded during RISC activation (125).

The RISC complex then locates and cleaves complementary mRNAs resulting in degradation and silencing of the messenger RNA. The mechanism by which RISC locates the mRNA is not yet clear. The active catalytic, cleavage components of RISC have been identified as endonucleases called argonaute proteins (126). The pathways involved in RNAi are summarised in Figure 1.8

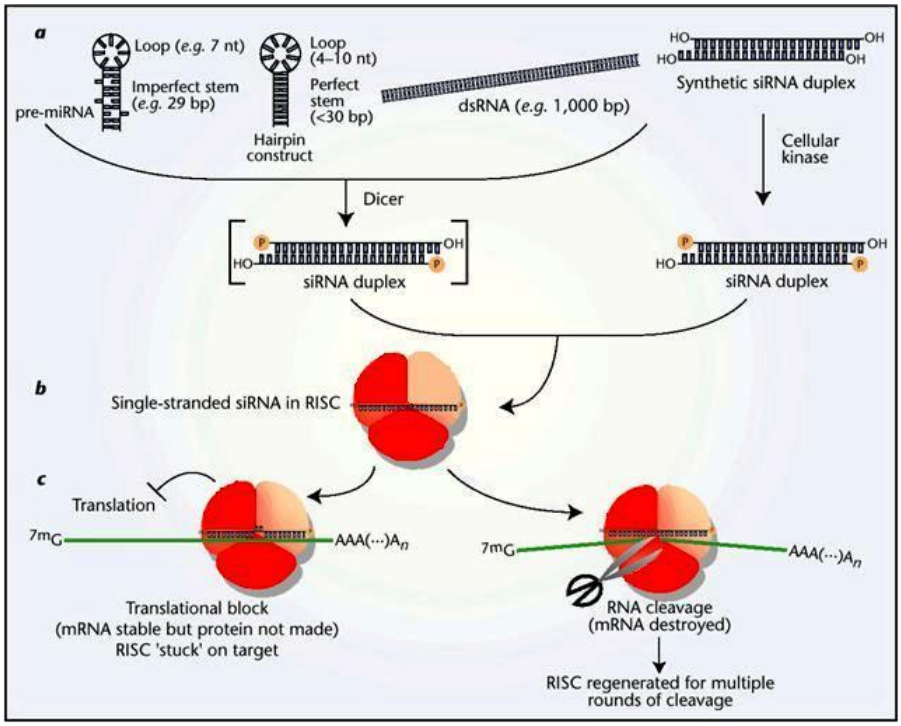

Figure 1.8. Mechanism of RNAi. A) Triggers of silencing. miRNAs are transcribed from non-coding genes, whilst dsRNA can be derived from sources such as viruses, and transgenes. These substrates are processed by Dicer to form siRNA duplexes. Synthetic siRNA mimics Dicer cleaved miRNA B) Incorporation of the guide strand into the RISC complex. C) RISC, guided by its small RNA, pairs with its mRNA target (green line), occasionally this can result in translational block but more typically results in cleavage and destruction of the mRNA. RISC is recycled with its guide strand intact to undertake additional cycles of cleavage. Adapted from (127).

siRNA screens

RNAi can be activated in mammalian cells by creating and introducing siRNAs that mimic Dicer-cleaved, endogenous microRNAs, resulting in potent gene silencing. The pairing of RNAi understanding with cDNA and genomic sequence data has made it possible to construct genome-scale libraries of siRNA reagents for performing high-throughput siRNA screens (128). The process of delivering siRNAs to cells *in vitro* typically involves a lipid mediated transfection, of which several are commercially available (119). Developing a successful RNAi screen requires awareness of the multiple potential problems that can occur with siRNA transfections.

Interferon response

The first problems relate to potential cytotoxicity occurring as a result of interferon activation. Interferons are cytokines that function as the host's first line of defence against viral infection. Activation of this innate immune response is triggered partly by dsRNA, a common viral replicative intermediate (129, 130). It has subsequently become apparent that the length of the RNA duplex is critical in determining the likelihood of an interferon response (131). Consequently most commercial companies now produce siRNA duplexes that are shorter than 24 nucleotide sequences long. Careful optimisation of the transfection reagents, combined with use of short RNA reagents means that this problem can usually be avoided.

Off-target effects

A more challenging problem arises with the phenomenon of 'off-target' effects'. Off-target effects occur when a siRNA is processed by RISC, and down-regulates unintended targets which share a degree of homology with the intended target. The

phenomenon was first described in 2003 (132). Using genome-wide microarray profiling as a method of detection, the authors identified modest, 1.5- to 3-fold changes in the expression of dozens of genes following transfection of individual siRNA. The levels of complementarity between the sense or antisense strand of the siRNA, and the off-targeted genes varied considerably. The overall off-target expression profile was unique for each siRNA, suggesting a sequence specific component to the phenomena. These off target effects can result in phenotypic changes that may result in the identification of genes which are false positives. Detecting false positives can lead to false leads and the unnecessary use of resources to explore non-productive research tracts. It is therefore of paramount importance to reduce the number of off-target effects.

Several strategies have been employed to successfully reduce off-target effects. Firstly, it has been shown that the concentration of transfected siRNA plays a key role in causing off-target effects, and demonstrates the importance of carefully optimising transfection conditions (132, 133). The intention of optimisation should be to use the lowest possible concentration of siRNA whilst still maintaining adequate knockdown. Another effective way of reducing the concentration of individual siRNAs is to use ‘pooled’ siRNA. Commercially available reagents typically use pools of four siRNAs designed to target the same gene. This technique enables strong on-target gene knockdown but minimises off-target effects by drastically reducing the concentration of individual duplexes. Commercial producers of siRNA reagents have also modified their reagents in light of evidence showing that 29-O-methyl ribosyl substitution at position 2 in the guide strand reduced off-target silencing of partially complementary transcripts (134).

The last approach toward eliminating off-target effects is associated with siRNA design. In two independent studies, investigators observed that off-targeted genes often contained matches between the ‘seed’ region of the siRNA (positions 2-7) and sequences in the 3' untranslated region (UTR) of the off-targeted gene (135, 136). Furthermore, they found that the likelihood of a gene being off-targeted is elevated by the presence of multiple 3'UTR seed matches. microRNAs also utilize the seed region to mediate gene knockdown, thus these findings intimate a strong mechanistic parallel between siRNA off-targeting and microRNA mediated gene regulation (137). The role of the 3’UTR seed match is now routinely taken into consideration during siRNA design, allowing for a further reduction in off-target effects.

The issue of off-target effects is of paramount importance when designing a siRNA screen. However, with careful optimisation of the transfection conditions and with the use of pooled siRNA, that has been designed using appropriate bioinformatics data, these unwanted effects can be significantly reduced.

1.10 Assay endpoints for radiosensitivity screens

The realisation that siRNA high-throughput screens are highly effective tools that can be used in the unbiased identification of novel genes involved in biological processes has led to a swift rise in the number of screening studies that have been published. Some of these studies have been able to identify novel proteins involved in DNA damage signalling; identifying important, and previously unexpected roles for proteins such as RNF8 (138) and RNF168 (139). Other studies have been able to identify synthetic lethal interactions in cancer cells. One such study found that cells

that are dependent on mutant KRAS exhibit sensitivity to knockdown of the serine/threonine kinase STK33 (140). HTS screens have also identified the mechanisms of tumour cell drug resistance. Such screens have been able to elucidate genes involved in tumour cell resistance to chemotherapies such as paclitaxel (128), to targeted therapy with poly (ADP-ribose)-polymerase-1 (PARP) inhibitors (141) and to endocrine therapy with tamoxifen (142). All of these screens used assay endpoints that were based on the quantification of short term cell viability following exposure to the drug of interest.

Cell viability assays

The use of cell viability assays is appropriate in siRNA screens of resistance to chemotherapy and endocrine agents, since they typically induce cell death via a rapid process of apoptosis (143, 144). Cell viability assays are less suitable for use in siRNA screens of tumour cell radiosensitivity since IR typically induces cell death via a more complicated process of mitotic cell death or 'mitotic catastrophe'. Although mitotic cell death may have some biochemical similarities to apoptosis, in that the final stages of cell death involve activation of the caspase pathway (49), there are many differences between the two processes. Cells which have been fatally exposed to IR, and which will undergo MCD, may continue to be metabolically active, and indeed continue to divide for several days or weeks after IR exposure (48-50). Key features of mitotic catastrophe include; the absence/delay of the G1/S checkpoint, the absence of interphase apoptosis coupled to this checkpoint, a delay in the G2 phase, and a sequence of aberrant mitoses forming abnormal, nonclonogenic daughter cells. The aberrant mitosis is morphologically characterised by the formation of cells containing micronuclei (MN) (145) or in the formation of multinuclear, giant cells (146).

Two previous studies have attempted to perform siRNA screens of tumour cell radiosensitivity using short term assays based on cell viability (147, 148). The delay in cell death that occurs following IR means that siRNA screens based on the use of short term viability assays as an endpoint are potentially flawed, as they may fail to distinguish between growth inhibition and clonal inactivation. Although one of these screens managed to successfully identify a gene called ‘tumour necrosis factor receptor–associated factor 2’ (TRAF2) whose depletion resulted in modest tumour cell radiosensitisation (147), it should be noted that the other study did not adequately validate the ‘radiosensitivity genes’ identified by their screen (148).

The choice of assay endpoint to use in a siRNA screen of tumour cell radiosensitivity is therefore a difficult one. The clonogenic survival assay is the ‘gold standard’ method for assessing intrinsic radiosensitivity (149). This *in vitro* cell survival assay is based on the ability of a single cell to grow into a colony (which is defined as consisting of at least 50 cells). The assay essentially tests every cell in the population for its ability to undergo ‘‘unlimited’’ division. Unfortunately, this assay is not suitable for use in large scale siRNA screens due to the highly labour intensive nature of the assay.

Quantification of micronuclei

HTS of tumour cell radiosensitivity therefore requires the use of an assay endpoint that can act as a reliable surrogate marker for tumour cell death following exposure to IR. One such possibility would be to perform a siRNA screen based on quantification of some of the morphological features of mitotic cell death. Micronuclei are one of the key features of MCD which are thought to represent chromatid fragments that detach from a chromosome, and do not integrate in the daughter

nuclei (145, 150). Micronuclei assays have most commonly been used as a test for genetic damage caused by environmental mutagens, and typically involved manual counting of micronuclei formation (151-153). Although there are some studies that have demonstrated a correlation between MN formation and intrinsic radiosensitivity (154, 155), other studies have failed to find a close correlation and have concluded that MN assays are not sufficiently sensitive to be used as a measure of radiosensitivity (156, 157). Other factors that limit the usefulness of MN quantification as an assay endpoint include the fact that MN quantification may be difficult to count in a HTS, and that it requires complicated assays that necessitate the induction of a cytokinesis block (158).

Like micronuclei formation, the presence of multinucleated cells is also characteristic of MCD (159). However, there are few studies demonstrating a correlation between intrinsic radiosensitivity and multinuclei formation (160). It may also be difficult to reliably detect multinucleated cells in a high throughput experiment.

Quantification of γH2AX foci

The critical role of DSBs and chromosome aberrations produced by ionising radiation in causing cell death has long been recognised (161, 162). DSBs result in the rapid phosphorylation of the histone 2A family member X (γH2AX) which can quickly enlarge to encompass a region spanning several megabases (163). H2AX is phosphorylated on the serine 139 residue by DNA-PKcs, ATM and ATR (164, 165). Phosphorylation of H2AX at the site of a DSB induces chromatin remodelling, further amplifying the DNA damage signal response, and resulting in downstream events such as cell cycle arrest and checkpoint activation (166). It has previously been shown that the number of DSBs can be determined by the number of γH2AX foci

present shortly after DNA damage (167). Most of these γH2AX foci resolve rapidly but a small proportion persists for many hours after irradiation (168). Previous studies have demonstrated a correlation between intrinsic radiosensitivity and the persistence of γH2AX foci 24 hours after radiation, (169-171) suggesting that γH2AX foci could be used as a surrogate marker for cell death. Although other studies have found that the quantitation of γH2AX foci is insufficiently sensitive to detect subtle changes in radiosensitivity (172-174), the fact that γH2AX foci can be readily visualized after antibody labelling (175) could potentially make it a good endpoint for use in HTS experiments that utilise high-throughput microscopy equipment.

1.11 Proposed siRNA screen

The known DNA repair defects that produce large differences in radiation sensitivity, are often associated with complex clinical syndromes such as ataxia-telangiectasia, Nijmegen breakage syndrome and Fanconi anaemia (176). The proteins identified by these repair defects do not represent potential therapeutic targets due to lack of tumour specificity. Therefore this thesis will be based on a siRNA radiosensitivity screen of a custom made library of 200 genes involved in DNA repair. The study will use the presence of γH2AX foci twenty-four hours after exposure to IR in order to identify novel genes involved in tumour cell radiosensitivity. Identifying novel molecular determinants of radiosensitivity could enable the development of inhibitors that could be clinically used to selectively render tumour cells more sensitive to radiotherapy without increasing normal tissue toxicity. The specific radiosensitisation of tumour cells could improve the therapeutic index of radiotherapy treatment.

1.12 Aims of the thesis

The aim of this thesis is to investigate the molecular determinants of tumour radiosensitivity with a view to identifying novel targets that may be clinically exploitable. The objectives are therefore:

1) To perform a siRNA radiosensitivity screen of 200 genes involved in DNA damage repair to identify novel determinants of tumour radiosensitivity (Chapter 3)

2) To examine whether depletion of the target gene identified by the siRNA screen induces tumour cell chemosensitisation, and if so, the mechanism by which this occurs (Chapter 4).

3) To investigate the clinical significance of tumour overerexpression of the identified target gene in cohorts of breast cancer patients (Chapter 5).

Chapter 2

MATERIALS & METHODS

2.1 Cell culture

Cell lines

The tumour cells used were the SQ20B (laryngeal squamous cell carcinoma), T24 (bladder transitional cell carcinoma), PSN1 (pancreas adenocarcinoma), HeLa (cervix squamous cell carcinoma) and U2OS (osteosarcoma) lines. The SQ20B cell line was obtained from Dr. Ralph Weichselbaum (University of Chicago, Chicago, IL) and has been described previously (115, 177). The other tumour cell lines were obtained from American Type Culture Collection (ATCC). Two types of normal human fibroblast cells (MRC5 and POC) were used at early passage. MRC5 cells were obtained from ATCC. POC fibroblast cells were established by our group and have been described previously (115).

Culture conditions

Cells were cultured in Dulbecco's Modified Eagle Medium (DMEM) containing 4.5 g/L glucose (Lonza) supplemented with 10% fetal bovine serum (FBS). All cultures were maintained at 37 °C in water-saturated 5% CO_2 / 95% air. Cells were regularly tested to ensure the absence of Mycoplasma contamination (MycoAlert; Lonza). Cell morphology was regularly checked to ensure the absence of cross contamination of cell lines.

Passaging of cells

Adherent cells were grown to confluence, washed with phosphate buffered solution (PBS), and incubated in 0.05% trypsin (Gibco) for 5 min at 37 °C. Lifted cells were resuspended in medium by gentle pipetting and divided into fresh tissue flasks.

Frozen storage of cells

Cells were detached using trypsin and resuspended in DMEM with 10% FBS. Cells were then centrifuged for 5 min at 1200 rpm, washed with PBS and incubated with trypsin. Cells were then resuspended in freezing medium (90% FBS, 10% DMSO) and transferred to cryo-vials (1 mL per vial) for storage at -80 °C or transferred to liquid nitrogen after 1-2 days at -80 °C.

Recovery of frozen cells

Cells were thawed by addition of pre-warmed medium to the cryo-vial prior to transfer to 10 mL of culture medium. Cells were centrifuged for 5 min at 1000 rpm, resuspended in culture medium and transferred to a culture flask.

Cell counting

Cells were washed with PBS, incubated with trypsin and resuspended as described above. Cell concentration was then determined using an automated cell counter (Nucleocounter, ChemoMetec) as per the manufacturer's instructions. Single cell suspensions were then made by diluting the cell solution to the required concentration and gently pipetting.

2.2 siRNA reagents and transfection conditions

siRNA resuspension

Individual genes were investigated using both individual and pooled siRNAs (ON-TARGET *plus*, Dharmacon). 5X siRNA buffer (Dharmacon) was diluted in RNase free water and then added to the siRNA vials to form 20 μM stock solutions and

stored at -80 °C. These were further diluted as required using 1X siRNA buffer to form 2 μM working solutions, which were also frozen at -80 °C.

siRNA transfection conditions

siRNA transfection can be performed in either a 'reverse' or 'forward' fashion. Reverse transfection involves plating a suspension of cells onto a plate containing a freshly prepared solution of siRNA and transfection reagent. This contrasts with forward transfection where the cells are plated and allowed to settle for one day prior to the addition of a siRNA and transfection reagent containing solution.

For 6 well plate transfections, 2 μM siRNA solution was mixed with serum-free medium (SFM) to give a total volume of 200 μL. This was incubated for 10 minutes at room temperature. Meanwhile, a separate 200 μL solution of diluted transfection reagent, Dharmafect 1, and serum free medium (SFM) was prepared and incubated at room temperature for 5 minutes. The two solutions were then gently and thoroughly mixed together and incubated for 20 minutes, allowing siRNA/Dharmafect complexes to form. The 400 μL siRNA/Dharmafect solution was then added to the cells. In the case of forward transfection it was added onto a plate that already contained adherent cells prior to the addition of 1.6 mL of antibiotic free complete medium (AFM). In the case of reverse transfection, the 400 μL siRNA/Dharmafect solution was added to a fresh plate and then 1.6 mL of cells suspended in AFM was added to it. The specific transfection conditions used for each cell line are shown in Table 2.1. The same technique was used for 96 well plate transfections, but the volume used at each step was reduced 20 fold.

Cell line	siRNA (µl)	SFM1 (µl)	DF (µl)	SFM2 (µl)	End conc (nM)	Number of cells plated
SQ20B	50	150	3	197	50	100 000
T24	50	150	3	197	50	70 000
HeLa	50	150	3	197	50	70 000
PSN1	50	150	3	197	50	100 000
MRC5	50	150	3	197	50	150 000
POC	50	150	3	197	50	150 000
U2OS	20	180	2	198	20	70 000

Table 2.1. Details of siRNA transfection for each cell line. Given volumes of 2 µM siRNA solution were mixed with stated volumes of serum-free medium (SFM1) which were then mixed with pre-incubated solutions of Dharmafect (DF) and serum-free medium (SFM2). The end-concentration of siRNA used and the number of cells transfected in each 6 well plate experiment are stated.

2.3 siRNA screen

siRNA library

The optimisation, development and analysis of the screen were performed in collaboration with Dr Remko Prevo and Dr Yin-Fai Lee. A custom designed DNA repair gene library of 200 pools of siRNA (Appendix. Supplementary Table 1) was used for the screen (siGenome, Dharmacon). Each pool contained four separate siRNAs. Each plate contained positive and negative control wells in addition to the library wells. Four replica wells contained non-targeting siRNA (NT) which acted as a negative control. A further four wells contained DNA-PKcs siRNA which acted as a positive control. DNA-PKcs plays a central role in NHEJ (14-17) and it is well recognised that disruption of DNA-PKcs results in an increase in γH2AX foci following exposure to DNA damaging agents (178).

Transfection conditions for the siRNA screen

For the siRNA screen, both SQ20B and MRC5 cells were ‘reverse’ transfected with siRNA in four replica 96 well plates. A suspension of cells was dispensed onto plates containing freshly prepared solutions of siRNA and Dharmafect. The same transfection technique was used for both cell types, although the SQ20B cells were transfected 48h prior to use whereas the MRC5 cells were transfected 66h prior to use. For each well, 2.5 µL of 2 µM siRNA solution was incubated with 7.5 µL of serum free medium. This was then mixed with 10 µL of SFM containing 0.15 µL of the transfection reagent Dharmafect 1 (Dharmacon), and incubated for 20 minutes in order to allow siRNA/Dharmafect complexes to form. Eighty microlitres of a SQ20B or MRC5 AFM cell suspension (containing 40000 cells/mL) was then added to each well containing the transfection mixture. This technique means that 3200 cells were added to each well and transfected with 50 nM siRNA. Forty-eight hours after transfection, the siRNA/Dharmafect containing medium was aspirated, and replaced with 200 µL of DMEM containing 10% FBS.

Cell irradiation

For both cell types, two replica plates were treated with 4Gy using an IBL634 caesium irradiator (CIS biointernational) at a dose rate of 0.66Gy/min and two plates were left unirradiated. Optimisation studies showed that this dose of radiation resulted in sufficiently large differences in γH2AX foci formation between positive and negative controls. The SQ20B cells were irradiated forty-eight hours, and the MRC5 cells sixty-six hours after transfection. After irradiation, the cells were returned to the incubator for 24 hours. Cells were then fixed using 3% paraformaldehyde (PFA) diluted in PBS prior to staining for γH2AX foci.

γH2AX foci staining and analysis

After fixation, the cells were permeabilised and blocked with 0.1% Triton (vol:vol) diluted in PBS containing 1% BSA (Sigma) for 1 hour at room temperature. Cells were incubated with a primary mouse monoclonal antibody to γH2AX (Millipore) 1:1500 overnight at 4 °C. Cells were then washed thrice with PBS prior to incubation with Alexafluor 488 conjugate secondary antibody (Invitrogen) 1:1200 for 1 hour at room temperature. Cells were again washed thrice with PBS for 5 min before 4',6-diamidino-2-phenylindole (DAPI) staining, 0.5 µg/mL diluted with PBS, for 10 min. The DAPI was replaced with PBS and the plate stored at 4 °C prior to image analysis. DAPI is a fluorescent stain that binds strongly to DNA and is therefore effective at marking the outline of the cell nucleus, enabling automated counting of foci (179).

γH2AX foci were detected using an IN Cell Analyzer 1000 automated epifluorescence microscope (GE Healthcare) with the following excitation and emission filters (Chroma): DAPI – excitation filter, 360 nm (D360_40x); emission filter, 460 nm (HQ460_40M); dichroic mirror 61002bs, Alexafluor 488 – excitation filter, 480 nm (HQ480_40x); emission filter, 535 nm (HQ535_50M); dichroic mirror, 61002bs. Four images were obtained per well. Foci quantitation was accomplished using IN Cell Analyzer Workstation software (v3.5). This software uses the DAPI images to identify a mask outline of the cell nucleus which it then superimposes onto the γH2AX foci images, enabling it to assess the number of foci per cell. For unirradiated cells, the read-out was the mean number of γH2AX foci per cell. For irradiated cells, this was the proportion of cells that contained >7 γH2AX foci per cell.

This was because optimisation studies (shown in Chapter 3) demonstrated that analysis based on this technique correlated best with results obtained from clonogenic survival assays.

Statistical analysis of the screen

Data was analysed using the CellHTS2 package (180) as follows. Sample values from each plate were first normalised using the median of the NT siRNA control wells for each plate. Z-scores for each gene in each replicate were then calculated using the formula: Z-score = $Sample_{norm}$ – $Median_{NT}$ / MAD_{NT}, where $Sample_{norm}$ is the normalised sample value, $Median_{NT}$ and MAD_{NT} are the median and the median absolute deviation (MAD) of all non-targeting control wells across all three library plates, respectively. The final Z-score was then calculated using the mean of the replicate Z-scores for each gene.

Individual siRNAs used

Candidate genes identified by the screen were investigated in more detail in separate experiments. For each of these genes, individual pools of siRNA were obtained from Dharmacon (On-TARGET plus). As with the 200 gene screen, NT siRNA or siRNA targeted against DNA-PKcs were used as negative and positive controls respectively. Each pool consisted of 4 individual siRNAs, the details of which are given in Table 2.2 below.

Gene	siRNA Strand details
NT	UGGUUUACAUGUCGACUAA
	UGGUUUACAUGUUGUGUGA
	UGGUUUACAUGUUUUCUGA
	UGGUUUACAUGUUUUCCUA
DNA-PKcs	GCAAAGAGGUGGCAGUUAA
	GAGCAUCACUUGCCUUUAA
	GAUGAGAAGUCCUUAGGUA
	GCAGGACCGUGCAAGGUUA
APEX2	GAGCCAUGUGUGAUGCGUA
	CAACAAUCAAACCCGGGUA
	GGACGAGCUGGAUGCGGAU
	GAGAAGGAGUUACGGACCU
RAD21	GCUCAGCCUUUGUGGAAUA
	GGGAGUAGUUCGAAUCUAU
	GACCAAGGUUCCAUAUUAU
	GCAUUGGAGCCUAUUGAUA
XAB2	ACGCAGCACUCUCGAAUUU
	CCAAAUUCAUUGCCCGCUA
	CCUUGCGGCUGCUGCGAAA
	AGGAGAGCUUCAAGGCGUA
POLQ	CAACAACCCUUAUCGUAAA
	CGACUAAGAUAGAUCAUUU
	ACACAGUAGGCGAGAGUAU
	CCUUAAGACUGUAGGUACU

Table 2.2. Details of the sequences of the siRNAs used in each individual pool. All siRNAs were obtained from Dharmacon.

2.4 Clonogenic assay technique

Cell resuspension

In all clonogenic survival experiments, cells were transfected with siRNA in 6 well plates 48h prior to plating for clonogenic survival. The medium from the 6 well plate was aspirated, the cells washed with PBS and then incubated with trypsin at 37 °C. The cells were then resuspended in DMEM containing 10% FBS and counted as previously described. In all cases, remaining cells from the transfection were used to confirm effective knockdown.

Clonogenic assays involving cell irradiation

All clonogenic assays involved irradiating at doses of 0Gy, 2Gy, 4Gy, and 6Gy. A suspension of known cell concentration was made for the 6Gy treatment. Accurate serial dilutions were derived from this solution so that the number of cells plated for all subsequent radiation conditions could be calculated. The medium was mixed gently to ensure it contained single-cell suspensions, prior to plating 4 mL of cell suspension to each plate. The cells were allowed to adhere to culture dishes before irradiation with an IBL634 caesium irradiator at a dose rate of 0.66Gy/min. The plates were then incubated at 37 °C until the colonies could be stained.

Clonogenic assays involving drug treatment

A suspension of known cell concentration was made and mixed gently to ensure the medium contained a single-cell suspension prior to plating 2 mL to each plate. After the cells had adhered, 100 μL of medium containing 21x the end concentration of drug was added. The medium containing the drug was gently mixed and the cells incubated at 37 °C for the duration indicated in each experiment. The medium was

then removed, the cells washed with PBS, and replaced with 4 mL of fresh medium. The plates were then incubated at 37 °C until the colonies could be stained.

Colony counting

A cell that retains proliferative capacity after radiation treatment is considered to have survived, whilst those that have lost the ability to regenerate are regarded as having been killed. Until recently, colony quantification was performed by manual counting. Colonies with more than 50 cells were identified and, having undergone at least 6 cell divisions, counted as viable (181). Since manual counting is time consuming and potentially subjective, colony counting is now usually performed with automated counters. Automated colony counting software enables the user to adjust the colony scoring parameters to detect colonies containing at least 50 cells and has been validated as being at least as reliable as manual counting (182, 183). Colonies were stained with crystal violet and counted 9 to 16 days after irradiation. Colony counting was primarily accomplished using an Oxford Optronics Colcount. Some primary cells formed diffuse colonies and required manual scoring. Each point on the survival curve represents the mean surviving fraction from four dishes. Clonogenic survival curves are representative of at least two independent replicate experiments.

The surviving fraction was derived using the formula:

$(\#\text{Colonies}/\#\text{ of cells plated})_{\text{treated}}/(\#\text{Colonies}/\#\text{ of cells plated})_{\text{untreated}}$.

Linear Quadratic Modelling

For clonogenic assays involving cell irradiation, the experimental data were fitted with the linear quadratic model (LQ) (184):

$S= \exp(-\alpha D-\beta D^2)$

where S is the survival probability, D the radiation dose (Gy), and α and β are the fit parameters (Gy^{-1} and Gy^{-2} respectively). KaleidaGraph software (Synergy Software) was used to calculate α and β values and to plot LQ curves.

The sensitisation enhancement ratio (SER) was used to quantify radiosensitisation (the SER_{10} was deduced from data by using $SER_{10} = D_{control}/ D_{treated}$, where $D_{control}$ and $D_{treated}$ doses yield 10% survival for controls and treated cells, respectively).

Statistical Analysis

For all clonogenic assays, unpaired t-tests were conducted at each radiation dose or drug concentration to assess differences in surviving fractions. Data points represent mean values, error bars the standard deviation *=$p<0.05$, **=$p<0.01$. All tests of significance were two-sided.

2.5 Protein Immunoblotting

Preparation of samples

Cell were rinsed with PBS and then incubated with radio immunoprecipitation assay lysis buffer (RIPA) for 5 minutes. The composition of RIPA is given below.

RIPA buffer

25 mM Tris pH 7.6

150 mM NaCl

1% NP40

1% Sodium deoxycholate

0.1% SDS

10 mM NaF

5 mM NaPPi

1 mM Na_3VO_4.

1x protease inhibitor cocktail

The cells were then sheared with a cell scraper and the lysate sonicated for 5 min to further increase protein extraction. The lysate was then centrifuged at 14000 rpm for 5 min. The supernatant was then removed and the protein concentration analysed. Protein concentration was determined using a bicinchoninic acid (BCA) assay according to the manufacturer's instructions. Briefly, 2 μL of the protein solution was mixed with 200 μL of the BCA solution and incubated at 37 °C for 30 mins. A standard curve was obtained with increasing concentration of BSA. The optical density 562 nm was then read in a microplate reader (Infinite M200, Tecan). Typically 10 μg of sample protein was mixed with 4x loading buffer (RunBlue LDS sample buffer, Expedeon) containing 200 mM dithiothreitol (DTT). The sample was then boiled at 70 °C for 10 min.

Sodium dodecyl sulphate-polyacrlyamide gel electrophoresis (SDS-PAGE)

Precast gels (Expedeon) were inserted into an electrophoresis tank (Invitrogen) which was filled with running buffer. The samples and pre-stained molecular weight markers (Biorad) were loaded onto the gel which was run at a constant voltage of 180V. The compositions of the buffers used are listed below.

Electrophoresis buffer	4x Loading buffer
40 mM Tricine	40% Glycerol
60 mM Tris	4% LDS, 0.8M Triethanolamine-Cl pH 7.6
0.1% SDS	4% Ficill-400
2.5 mM sodium bisulphite	0.025% Phenol Red
	0.025% Coomassie Brilliant Blue
	2 mM EDTA-2Na

Protein transfer and blocking

Gels were placed in a blotting tank (XCell SureLock Mini-Cell, Invitrogen) and the protein transferred at a constant voltage of 30V to nitrocellulose membranes (GE-Amersham) for 1h in 1x transfer buffer (25 mM Tris–HCl, 192 mM glycine, 20% methanol). The membrane was then blocked in incubation buffer (TBS, 0.1% Tween, 5% dried milk powder) and subsequently incubated with primary antibody overnight at 4 °C. After washing 4 times (TBS, 0.1% Tween) for 1h in total, the membranes were incubated with horseradish peroxidase (HRP) conjugated secondary antibody for 1h at room temperature. The membranes were then washed as before. Antibody binding was detected using an enhanced chemiluminescence (ECL) kit (either Millipore or Thermo Scientific). The antibody conditions used are summarised in

Table 2.3 below. Exposed film was digitised and figures were assembled using Microsoft PowerPoint.

Protein	Primary Antibody Details	Secondary Antibody Details	ECL used
DNA-PKcs	1:500 (BD Biosciences)	1:10000 anti-mouse (Pierce)	Thermo Scientific
RAD21	1:500 (Abcam)	1:10000 anti-rabbit (Pierce)	Thermo Scientific
XAB2	1:4000 (Abcam)	1:20000 anti-rabbit (Pierce)	Millipore
β-actin	1:30000 (Sigma)	1:70000 anti-mouse (Pierce)	Millipore

Table 2.3. Details of immunoblotting conditions. Concentrations of primary and secondary antibodies are as shown.

2.6 Quantification of gene silencing

Quantitative reverse-transcription PCR

Ideally, effective siRNA transfection should be demonstrated by Western Blotting to show protein knockdown. Although there are several commercial antibodies available for both POLQ and APEX2, all of them proved to be ineffective despite significant attempts at optimisation. For both of these genes, it was therefore necessary to demonstrate effective knockdown at the RNA level.

In each experiment, RNA was extracted and purified from cells at the times indicated using the QIAshredder (Qiagen) and RNeasy Mini Kit (Qiagen) as per the manufacturer's instructions. RNA concentration was determined using a Nanodrop nd-1000 spectrophotometer (Thermo Scientific). One step quantitative reverse-transcription PCR (qRT-PCR) was performed on 500 ng RNA using Superscript III Platinum SYBR Green One-step qRT-PCR kit (Invitrogen). Gene expression was normalised to glyceraldehyde-3-phosphate dehydrogenase (GAPDH) expression.

Each reaction mixture consisted of 25 μL (in water) and contained:

1) 500 ng RNA

2) 12.5 μL of 2X Reaction Mix (a buffer containing SYBR Green I, 0.4 mM of each dNTP, and 3.2 mM MgSO4)

3) 0.5 μL of Platinum Taq mix

4) Forward and reverse primer

The quantity of primer used for each gene was as stated below:

Gene	Forward primer	Reverse primer
GAPDH	0.4 μM	0.4 μM
POLQ	0.08 μM	0.08 μM
APEX2	0.2 μM	0.2 μM

Table 2.4. Details of primer concentrations used for each gene of interest.

The primers used for each gene are as stated below, and were obtained from Eurofins MWG.

POLQ Forward: TATCTGCTGGAACTTTTGCTGA

POLQ Reverse: CTCACACCATTTCTTTGATGGA

APEX2 Forward: CTGTAAGGACAATGCTACCC

APEX2 Reverse: ACACGTTGATTAGGGTCAAG

GAPDH Forward: CCACCCATGGCAAATTCCATGGCA

GAPDH Reverse: TCTAGACGGCAGGTCAGGTCCACC

qRT-PCR was achieved using a Stratagene Mx3005P system. cDNA synthesis was performed by heating the reagents to 42 °C for 30 mins followed by 95 °C for 10 minutes. The amplification was performed at the following conditions for all three genes of interest: 95 °C for 30 sec, 58 °C for 30 sec, 72 °C for 60 sec for 40 cycles. In addition, a melting curve was generated at the end of the 40 cycles to confirm that only a single amplicon had been produced.

Agarose gel electrophoresis

The DNA produced by the above qRT-PCR reactions was run on an agarose gel in order to verify that the amplified product was of the anticipated size. A 0.8% agarose gel containing 0.5 μg/mL of ethidium bromide was made in tris-acetate-EDTA (TAE) buffer. The samples were mixed with 6x DNA loading buffer (0.25% bromophenol blue, 30% glycerol) and ran under constant voltage (100V). The gel was then visualised using UV illumination.

2.7 Cytotoxic drug treatment

Preparation of drugs

All cytotoxic drugs were obtained from Sigma. Cisplatin, doxorubicin, mitomycin C and temozolomide were all dissolved directly into DMEM. Etoposide and docetaxel were initially dissolved in DMSO at a concentration of 10 mg/mL and subsequently diluted in DMEM to provide the required concentration. Cytotoxic drugs were added 48h after siRNA transfection for the duration stated in each experiment.

2.8 Flow cytometry analysis

Cell cycle analysis

Adherent cells were washed with PBS and incubated with trypsin at 37 °C. DMEM with 10% FBS was added once the cells had lifted. The cell suspension was then centrifuged at 1100 rpm for 5 min. The medium was aspirated and the cells washed with PBS. The cells were centrifuged as before and the PBS removed. The cells were then resuspended and fixed in 70% ethanol at 4 °C. The solution was again centrifuged at 1100 rpm for 5 min, washed again with PBS, and then recentrifuged at 2000 rpm for 10 min. The PBS was carefully removed and the cells resuspended in 0.5 mL of propidium iodide (PI) staining solution (50 μg/mL PI, 200 μg/mL RNase in PBS) one hour before fluorescence activated cell sorting (FACS) was performed (FACSort, Becton Dickinson). Cell cycle phase was assessed using Modfit Cell cycle Analysis software.

2.9 Homologous recombination assays

RAD51 Foci assay

U2OS cells were reverse transfected with NT or POLQ siRNA in 96 well plates with 20 nM siRNA. Forty-eight hours after transfection, cells were treated with 1 μM etoposide for 24h before being fixed in 3% paraformaldehyde, permeabilised in 0.1% triton and blocked in PBS 3% BSA. Cells were then incubated with RAD51 antibody (Santa Cruz) 1:1000 overnight. Cells were then washed with PBS, and incubated with Alexafluor 488 conjugate secondary antibody (Invitrogen) 1:1000 for 1 hour at room temperature. Cells were then washed, stained with DAPI, and imaged using the IN Cell Analyzer as described previously. Nuclei with more than 9 foci were classified as RAD51 positive.

I-Sce-I assay

The work relating to this assay was undertaken with the help of Dr Cecilia Lundin. The I-Sce-I assay involves the transfection of cells with a modified green fluorescent protein (GFP) gene containing the recognition site for the rare-cutting I-Sce-I endonuclease, and has been described previously (185). Expression of I-Sce-I results in the formation of a single DSB in the GFP gene, which, when repaired by homologous recombination results in the formation of functional GFP, which can be detected by flow cytometry. U2OS cells with stable integrated truncated GFP vector were transfected with siRNA as described previously. After 48h, cells were transfected with 0.25 μg I-Sce-I vector and 0.2 μg polyethylenimine in 150 μL OptiMEM/well. GFP-positive cells were analysed using FACS 48h after I-Sce-I transfection as previously described (185).

2.10 Clinical data analysis

This work was undertaken in collaboration with Professor Adrian Harris' group. In particular, statistical help was provided by Dr Francesca Buffa.

Details of the Oxford series of patients

Gene expression data was correlated with clinical outcomes in several retrospective series of breast cancer patients. Two of these series were of early breast cancer patients treated in Oxford. Data from the other studies was obtained by identifying published clinical series containing gene expression data from breast cancer patients.

The Oxford data was acquired from individual tumour samples obtained from retrospective series of patients with early primary breast cancer who were treated in Oxford, between 1989 and 1998. Two series of 152 (Series 1) and 127 (Series 2) samples respectively were analysed. Series 1 has been described previously (186, 187); this series had completed 7 years of follow-up for all but 4 patients, and the median follow-up time for patients leaving the study alive and without a relapse was 12 years. Series 2 is also part of a published series (188); the published cohort had 93 cases in common with Series 1, these have been excluded from this study so that Series 1 and 2 have no overlapping cases. Series 2 had completed 10 years of follow-up apart from one case. During the period when the tumour samples were obtained, patients were offered adjuvant systemic treatment on the basis of the following criteria. Patients who were <50 years of age, with lymph node positive tumours, or oestrogen receptor negative tumours (ER-), and/or a primary tumour >3 cm in diameter, were offered adjuvant cyclophosphamide, methotrexate, and 5-

fluorouracil (CMF) for six cycles, in a three weekly intravenous regimen. Patients ≥50 years of age with ER–, lymph node–positive tumours also received CMF. Tamoxifen was used as endocrine therapy for 5 years in oestrogen receptor positive patients.

The patient demographics, pathology details, and adjuvant treatment details for these two series of patients are given in the Appendix (Supplementary Table 2A and B). The main differences between the two series are that none of the patients in Series 1 received adjuvant chemotherapy, whilst 40% of patients in Series 2 received adjuvant CMF chemotherapy. This reflects the greater prevalence of lymph node involvement in the patients in Series 2. In addition, a larger proportion of the patients in Series 1 had ER positive disease.

RNA extraction and gene expression profiling

In Series 1, total RNA was isolated by Trizol method (Invitrogen, Carlsbad, CA) and in Series 2 by Tri-reagent (Sigma-Aldrich) and ethanol precipitation as per the manufacturer's instructions. More details regarding RNA extraction are given in the original studies that used these datasets (186, 188). mRNA expression was measured using Affymetrix U133 arrays for Series 1 and Illumina Human RefSeq-8 arrays (Illumina inc., San Diego, CA, USA) for Series 2. RNA was amplified using Ambion Illumina Amplification Kit. Methods for both protocols have been previously described (186, 188). After RNA samples are hybridized with arrays, they are scanned, and images are produced and processed to obtain an intensity value for each probe. These intensities represent the amount of hybridization for each oligonucleotide probe. However, part of the hybridization is non-specific and the intensities are affected by optical noise. Statistical techniques have been developed

to give accurate measurements of specific hybridization. For the Affymetrix data this was achieved using gcrma (189); for the Illumina arrays, the signal was background subtracted with local background subtraction (BeadStudio). Data from both series were quantile normalised in Bioconductor (190) and logged (base 2). The target sequence of the probes that corresponded to *POLQ* expression in Affymetrix and Illumina arrays are shown in the Appendix (Supplementary Table 3.)

Published clinical series

NCBI Gene Expression Omnibus (191) was searched for gene expression studies in cancer, published in peer-reviewed journals, where microarrays were performed on frozen material extracted before treatment with either chemotherapy, radiotherapy or endocrine treatment. Two datasets were identified (GSE3494 and GSE2034) that had survival data which could be used to validate the findings seen in the two Oxford series. GSE3494 is a heterogenous dataset that comprises samples from 251 patients with early breast cancer. This data was originally used for a study which identified a 32-gene expression signature that distinguished p53-mutant and wild-type tumours and which was used to predict prognosis and therapeutic response (192). The GSE2034 dataset comprises 286 samples from patients with node negative early breast cancer and was used to identify a gene signature that predicted the development of distant metastases (193).

A total of five data sets (187, 192, 194) that used latest generation Affymetrix 3' array platforms (Affymetrix U133 and plus2, www.affymetrix.com) of 1015 samples in total (Appendix. Supplementary Table 4) were selected that could be used to identify genes that were co and inversely expressed with *POLQ.* All handling and processing of the downloaded data was performed as previously described (195).

Data-mining of gene expression data

Seed-clustering with bootstrap resampling was applied, as previously described (195), in order to obtain genes co- and inversely expressed with *POLQ* in the 1015 published breast cancer samples. In short, the two probesets targeting *POLQ* were chosen as initial seeds (Appendix. Supplementary Table 4). Transcripts on the arrays showing significant association (Spearman Rank Test, Bonferroni multiple test correction) with each seed after bootstrap resampling of the breast cancer samples were considered. Amongst these, transcripts showing a concordant association with both seeds that was significantly higher than observed by random simulation were selected as *POLQ* co-/inversely expressed genes. A pathway enrichment analysis was thus performed using GeneCodis2 (196) to study the Gene Ontology classes and the KEGG pathways which are over-represented in *POLQ* co-/inversely expressed genes.

Survival analysis

The study endpoints used were, relapse free survival for Series 1; and distant-relapse free survival and recurrence free survival as defined by the STEEP criteria (197) for Series 2. For the other datasets the endpoints were considered as published. Univariate and multivariate analysis was performed for each dataset. Cox multivariate models were reduced using stepwise backward likelihood selection. In univariate analyses, expression of *POLQ* and other genes was considered either as binary variable, with median expression as binary cut-off, or as continuous variable, ranked and normalised between 0 and 1. In multivariate analysis the latter was always considered.

Chapter 3

POLQ DEPLETION CAUSES TUMOUR-SPECIFIC RADIOSENSITISATION

3.1 Abstract

The effectiveness of radiotherapy treatment could be significantly improved if tumour cells could be rendered more sensitive to ionising radiation without altering the sensitivity of normal tissues. However, many of the key, therapeutically exploitable mechanisms that determine intrinsic tumour radiosensitivity are largely unknown. A siRNA screen of 200 genes involved in DNA damage repair was conducted with the aim of identifying genes whose knockdown increased tumour radiosensitivity. Parallel siRNA screens were conducted in irradiated and unirradiated tumour cells (SQ20B) and irradiated normal tissue cells (MRC5). Using γH2AX foci at 24 hours after ionising radiation several genes were identified such as *BRCA2*, *Lig IV* and *XRCC5*, whose knockdown is known to cause increased cell radiosensitivity, thereby validating the primary screening endpoint. In addition, POLQ (DNA polymerase theta) was identified as a potential tumour-specific target. Subsequent investigations demonstrated that *POLQ* knockdown resulted in radiosensitisation of a panel of tumour cell lines from different primary sites, whilst having little or no effect on normal tissue cell lines. These findings raise the possibility that POLQ inhibition might be used clinically to cause tumour specific radiosensitisation.

3.2 Introduction

Radiotherapy is a vital tool in the management of cancer patients. It is often given with curative intent either alone or with chemotherapy in patients with diseases as diverse as head and neck, cervix, bladder, and non-small cell lung cancer. The radiation dose that can safely be delivered to patients is limited by the dose tolerances of surrounding normal tissues (51). It is anticipated that the effectiveness of radiotherapy would be improved if tumour cells could be rendered more sensitive to IR without altering the sensitivity of normal tissues. Such a strategy depends upon exploiting tumour specific molecular targets, many of which remain to be identified. A siRNA screen was therefore performed with a custom designed siRNA library of 200 genes involved in DNA repair aimed at identifying genes whose knockdown causes increased tumour radiosensitivity. The experimental design used both irradiated and unirradiated tumour cells as well as parallel siRNA screens in a radioresistant SQ20B tumour line and MRC5 normal tissue fibroblast line. By comparing the effects of siRNA treatment in each of these conditions, siRNAs that cause tumour specific radiosensitisation could be better identified.

siRNA screens aiming to identify novel determinants of tumour cell radiosensitivity have previously used short term assays based on cell viability (147, 148). This approach is potentially flawed as it may fail to distinguish between growth inhibition and clonal inactivation. Although the clonogenic survival assay is the ‘gold standard’ method for assessing intrinsic radiosensitivity in vitro (149), it is unsuitable for use in siRNA screens due to the highly labour intensive nature of the assay.

The critical role of DNA double-strand breaks and chromosome aberrations produced by ionising radiation in causing cell death has long been recognised (161, 162). DSB formation results in rapid phosphorylation of the serine 139 residue of the histone protein H2AX (γH2AX) (163). Typically, most of these γH2AX foci resolve within a few hours of irradiation. It was therefore reasoned that foci persisting at 24 hours may mark sites of delayed repair, and could correspond to the sites likely to lead to chromosome breaks. Previous studies have demonstrated a correlation between intrinsic radiosensitivity and the persistence of γH2AX foci 24 hours after radiation (169, 170) suggesting that γH2AX foci could be used as a surrogate marker for cell death. An important benefit of using γH2AX foci as the assay endpoint is that it is relatively straightforward to utilise for a HTS since the foci can be readily detected by a high-throughput, automated microscope (198).

This chapter describes the results of a siRNA screen of 200 genes involved in DNA damage repair aimed at identifying genes whose knockdown causes increased tumour radiosensitivity. Using γH2AX foci at 24 hours after IR, POLQ (DNA polymerase theta) was identified as a potential tumour-specific target whose knockdown led to tumour cell-specific radiosensitisation.

3.3 Results

The percentage of irradiated cells that contain more than seven γH2AX foci correlates with cellular radiosensitivity. Initial optimisation work using SQ20B cells treated with DNA-PKcs siRNA showed that measuring γH2AX foci in irradiated cells resulted in an underestimation of changes in cell radiosensitivity. A clonogenic assay was performed with SQ20B cells transfected with either DNA-PKcs or NT siRNA to determine the surviving fraction of cells following exposure to 4Gy irradiation. Effective knockdown of DNA-PKcs in the SQ20B cell line is shown in Figure 3.1. Depletion of DNA-PKcs resulted in an approximately 4.6 fold reduction in the surviving fraction compared with cells transfected with NT siRNA (Fig. 3.2). However, analysis of γH2AX foci in SQ20B cells treated with the same siRNAs and IR dose showed that there was only about a two-fold difference in mean γH2AX foci per cell between DNA-PKcs and NT treated cells (Fig. 3.2).

This finding represented a significant barrier to pursuing a siRNA screen of irradiated cells based on analysis of mean γH2AX foci per cell. It raises the possibility that differences in radiosensitivity caused by siRNA treatment would not result in significantly detectable differences in γH2AX foci. It was therefore possible that siRNAs that induce radiosensitisation would not be correctly identified by the screen. It was then examined whether the proportion of cells containing more than a certain number of foci was a better correlation with radiosensitivity than the mean foci number. The images were reanalysed having adjusted the IN Cell Analyzer Workstation software so that it identified the proportion of cells containing any given number of foci. It was found that identifying the proportion of cells which contained more than seven γH2AX foci per cell following 4Gy IR best correlated with underlying

changes in cell radiosensitivity. In DNA-PKcs depleted cells, there was an approximately four fold increase in the proportion of cells containing more than seven γH2AX foci compared to cells transfected with NT siRNA (Fig. 3.3). This analysis, based on the number of cells that reach a threshold of γH2AX foci, correlates most closely with the 4.6 fold change in underlying radiosensitivity, and is more likely to enable the correct identification of genes whose depletion causes an increase in radiosensitivity. In view of these findings, the siRNA screen of irradiated cells was based on an analysis of the percentage of cells containing more than seven γH2AX foci per cell. However for the screen of unirradiated cells, the mean foci number was still used due to the very low number of foci in these cells.

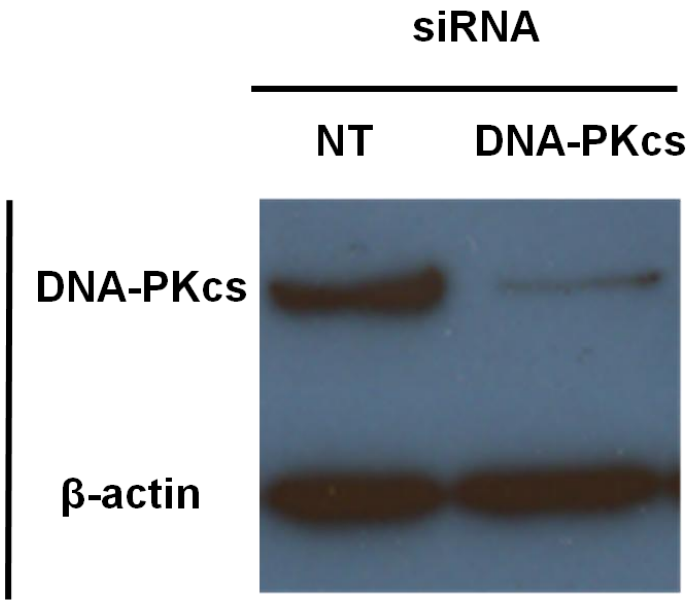

Figure 3.1 Western blot demonstrating the effective knockdown of DNA-PKcs in SQ20B cells 48h after siRNA transfection

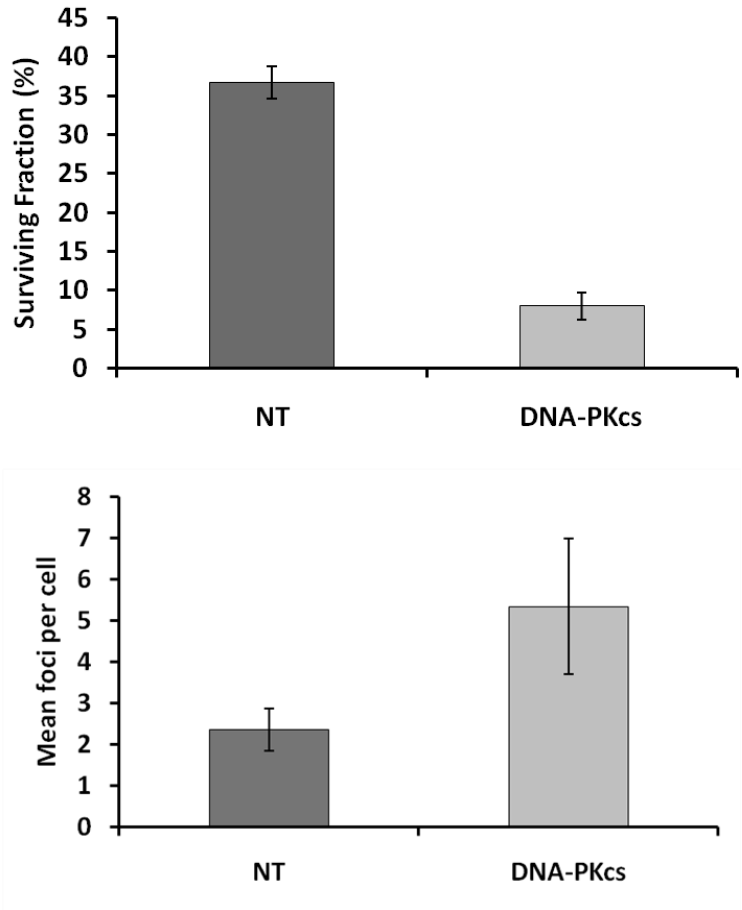

Figure 3.2. A comparison of clonogenic cell survival and residual γH2AX foci formation 24h after exposure to 4Gy IR. The profound differences in radiosensitivity following DNA-PKcs depletion (top) are not adequately reflected in changes to the mean γH2AX foci per cell (bottom) caused by 4Gy IR.

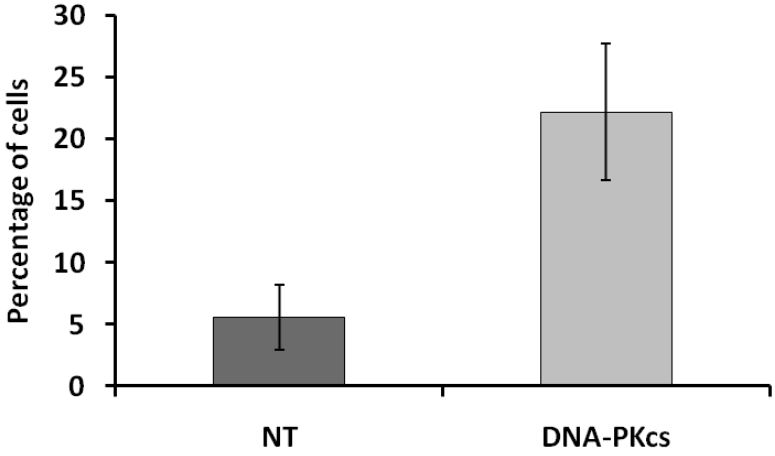

Figure 3.3. Analysis based on the percentage of irradiated cells containing more than seven γH2AX foci shows larger differences between cells transfected with DNA-PKcs and NT siRNA and more closely correlates with differences in radiosensitivity.

A siRNA screen identifies genes that are potentially involved in tumour cell radiosensitivity. A custom designed siRNA library of 200 genes involved in DNA repair was screened using the radioresistant SQ20B cell line as well as the MRC5 fibroblast line in order to identify novel tumour-specific radiosensitising targets. The screen of irradiated SQ20B cells was used to compile a list of genes that may be involved in tumour specific radiosensitivity.

Different techniques have been used previously to identify possible 'hits' from siRNA screens. Some studies have used defined Z-scores as a 'hit' threshold for candidate genes (141), whilst other studies have ranked the Z-scores obtained from the screen and defined the number of top-ranked siRNAs that were considered to be 'hits' (142). In this current work, the magnitude of the Z-scores obtained in each of the screens differed significantly, reflecting the different cell lines and irradiation conditions used. In view of this, it was decided that the most practical way to define genes of interest was to examine the top 30 genes with the highest Z-scores, rather than use a set Z-score threshold.

The Z-scores of the top 30 genes associated with elevated γH2AX foci in SQ20B cells twenty-four hours after 4Gy radiation are shown in Figure 3.4. Several of the genes identified in this screen are already known to increase cell radiosensitivity following knockdown. These included genes involved in homologous recombination such as *BRCA1* (199), *BRCA2* (200), and *RBBP8* (201) as well as genes involved in non-homologous end joining such as *Lig IV* (202), *XRCC5* (*Ku80*) (203) and *PRKDC*

(*DNA-PKcs*) (204). Genes involved in DNA damage response such as *53BP1* (205) which has been shown to be involved in cell radiosensitivity were also identified by the screen. Depletion of TIMELESS, which was also associated with a high Z-score, has previously been shown to increase radiosensitivity but through mechanisms that are less clear (206).

Of the remaining genes that have not previously been shown to be involved in tumour radiosensitivity, it was decided to investigate *POLQ*, *RAD21*, *APEX2* and *XAB2* in more detail as these genes were considered to have clinically exploitable potential if it was shown that their depletion caused tumour-specific radiosensitisation. APEX2 (AP endonuclease 2) is a secondary mammalian apurinic/apyrimidinic endonuclease that has previously been shown to be involved in repair of oxidative damage (207, 208). XAB2 (XPA binding protein 2) has previously been implicated in nucleotide excision repair (NER) due to its involvement in transcription coupled repair (TCR) (209) but has recently been implicated in sensitivity to PARP inhibition (210). RAD21 overexpression has been found in certain human tumours (211) and its depletion is associated with increased sensitivity to etoposide and bleomycin (212). POLQ (DNA polymerase theta) is a low fidelity DNA polymerase, whose normal physiological role is unclear at present (213, 214). It has limited expression in normal tissues but has been shown to be overexpressed in certain tumour types (215).

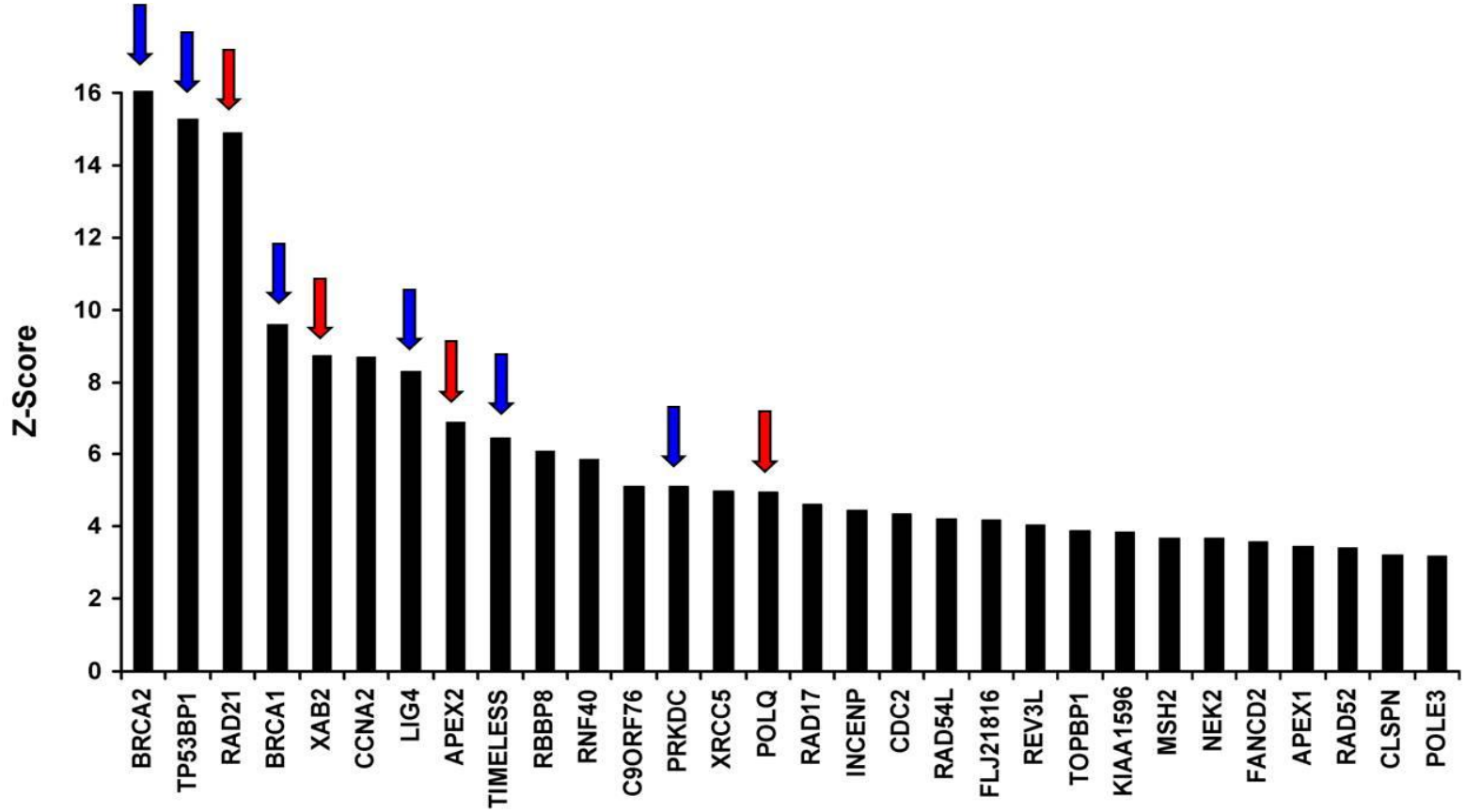

Figure 3.4. Irradiated SQ20B cells. Z-scores of the top 30 genes associated with elevated γH2AX foci twenty-four hours after 4Gy radiation. Blue arrows indicate genes already known to be involved in radiosensitivity. Red arrows indicate genes not previously known to be involved in intrinsic radiosensitivity that were investigated in more detail.

Knockdown of *POLQ* and *APEX2* can be assessed by qRT-PCR. Having identified four genes to pursue further, it was important that effective knockdown could be demonstrated for each of these genes. Commercially available antibodies for RAD21 and XAB2 were effective and therefore used to confirm knockdown at the protein level. The antibody details are given in Chapter 2 and demonstration of effective knockdown is shown in the relevant section below.

The commercially available antibodies for both POLQ and APEX2 were extensively tested, but were found to be insufficiently reliable to be able to demonstrate siRNA knockdown of these targets at the protein level. It was therefore decided that successful knockdown would be demonstrated at the mRNA level instead, using qRT-PCR. In each case the gene expression level was normalised to that of *GAPDH*. The details of the one-step qRT-PCR reactions used are given in Chapter 2.

Several measures were taken to ensure that the qRT-PCR reactions could be reliably used to confirm gene knockdown. Firstly it was verified that the amplified products were of the correct size. To demonstrate this, DNA produced by the qRT-PCR reactions was run on an agarose gel as described previously. Figure 3.5 illustrates that the qRT-PCR reactions for *GAPDH, APEX2* and *POLQ* produced DNA of the appropriate size (based on the positions of the primers).

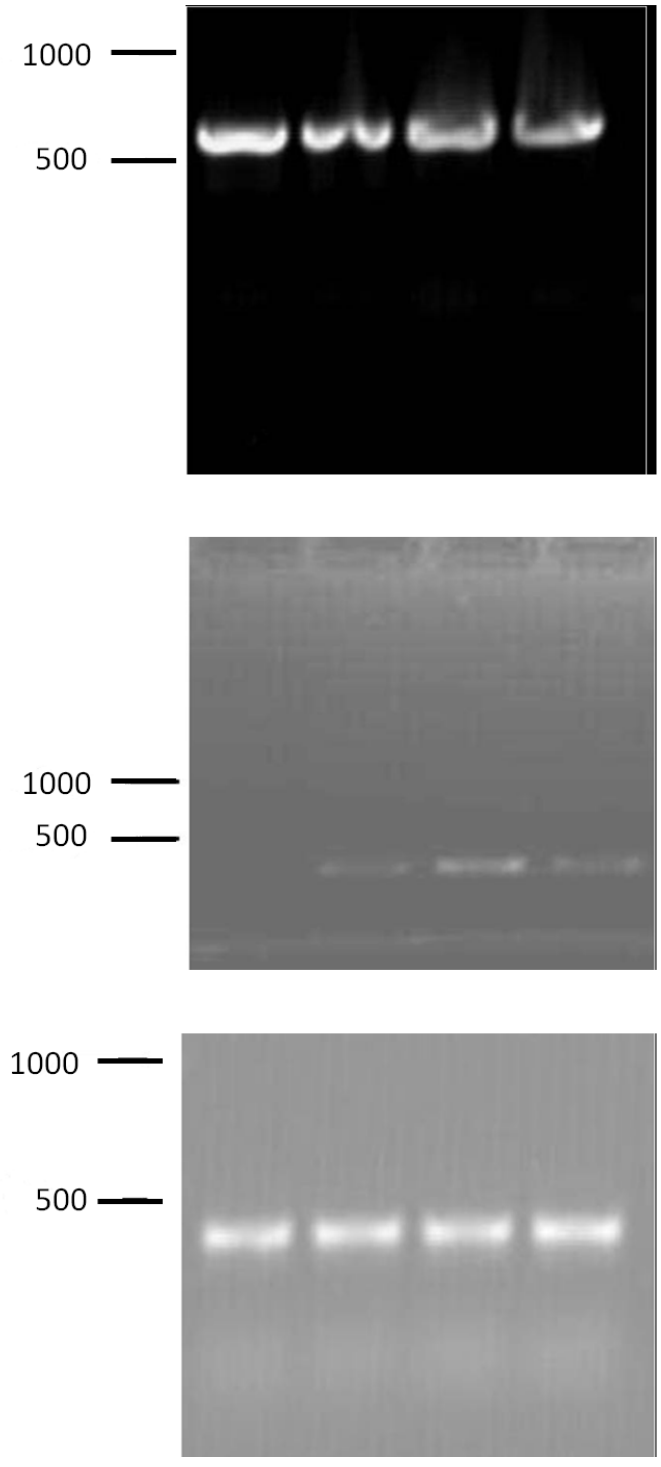

Figure 3.5. Agarose gel electrophoresis. The anticipated qRT-PCR product size for *GAPDH* (top) was 598 bps. DNA from four independent qRT-PCR reactions confirmed this was the case. The anticipated *APEX2* product size (middle) was 212 bps and this was confirmed by three independent qRT-PCR reactions. The anticipated *POLQ* product size (bottom) was 372 bps and this was confirmed on four independent qRT-PCR reactions.

To further validate the qRT-PCR techniques used, the (dissociation) melting curves for each of the reactions were assessed every time a qRT-PCR was performed. The melting curves can help evaluate the specificity of the qRT-PCR products produced. Ideally the reactions should show a sharp peak at the melting temperature of the amplicon. Such a result indicates that the qRT-PCR products are specific, and that the SYBR Green I fluorescence is a direct measurement of accumulation of the product of interest. If the dissociation curve shows a series of peaks it indicates that there is insufficient discrimination between specific and non-specific reaction products. Figure 3.6 illustrates that the melting curves for each of the amplicons produce single, sharp peaks. This suggests that the fluorescence measurement does not include non-specific reaction products.

A normal amplification plot typically consists of a horizontal baseline region, a log phase of amplification, then a linear amplification phase followed by a plateau. Gene knockdown can be assessed by qRT-PCR by comparing cycle threshold (Ct) values of RNA extracted from cells treated with different siRNAs. For accurate analysis of qRT-PCR, it is important that the reaction is quantified at the early part of the exponential phase of the reaction, whilst all reagents are still in excess. The Ct setting should also be in a range where all the amplification plots to be analysed are parallel, suggesting that the amplification efficiencies are equivalent for each reaction to be compared. Figure 3.7 illustrates that the Ct threshold for each of the qRT-PCR reactions is at the early part of the exponential phase, and that the curves being compared are parallel at this point. It also demonstrates the effective knockdown that was typically seen following transfection with either APEX2 or POLQ siRNA.

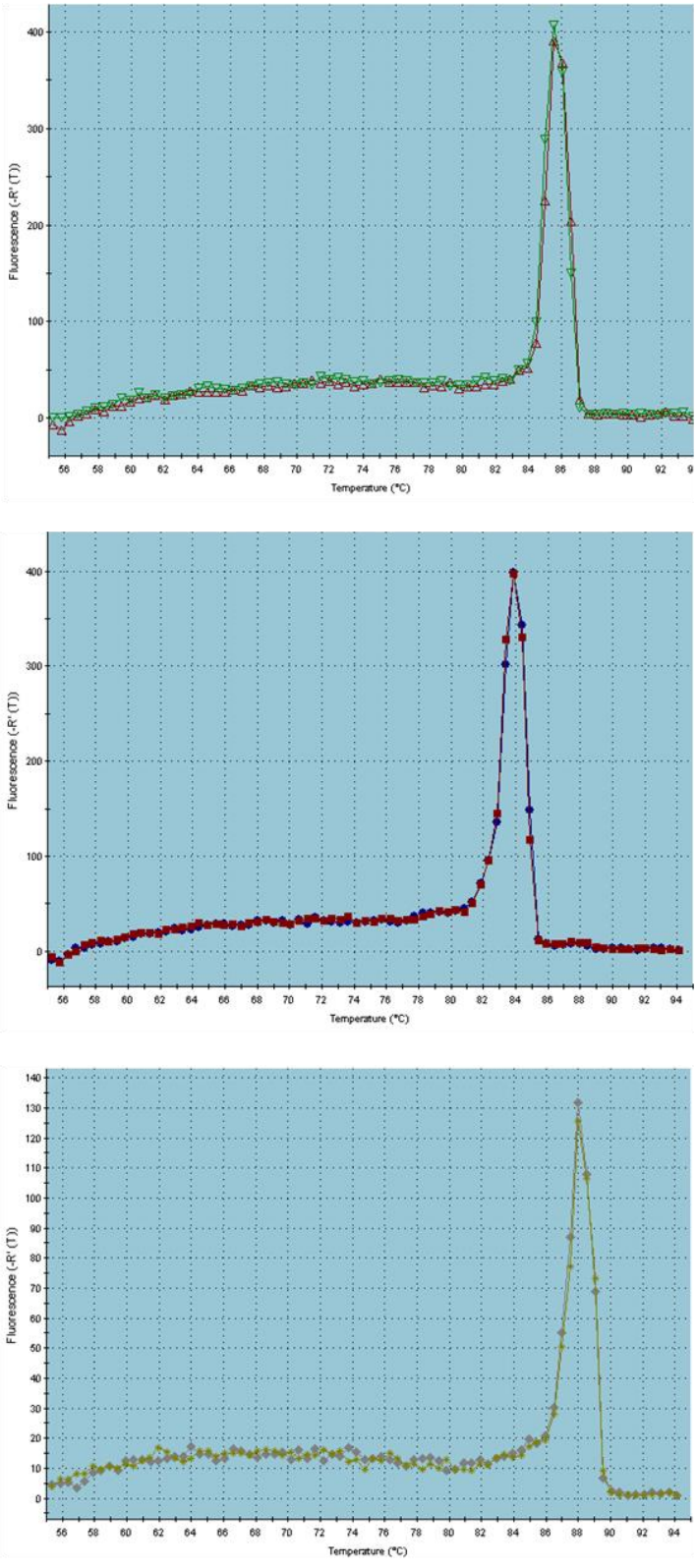

Figure 3.6. Dissociation curves for *APEX2* (top), *POLQ* (middle), and *GAPDH* (bottom). In each case the dissociation curves for two separate reactions are shown, in order to demonstrate that the single, sharp peaks are consistently produced. These sharp, essentially overlapping peaks, suggest that the fluorescence measurement does not include non-specific reaction products.

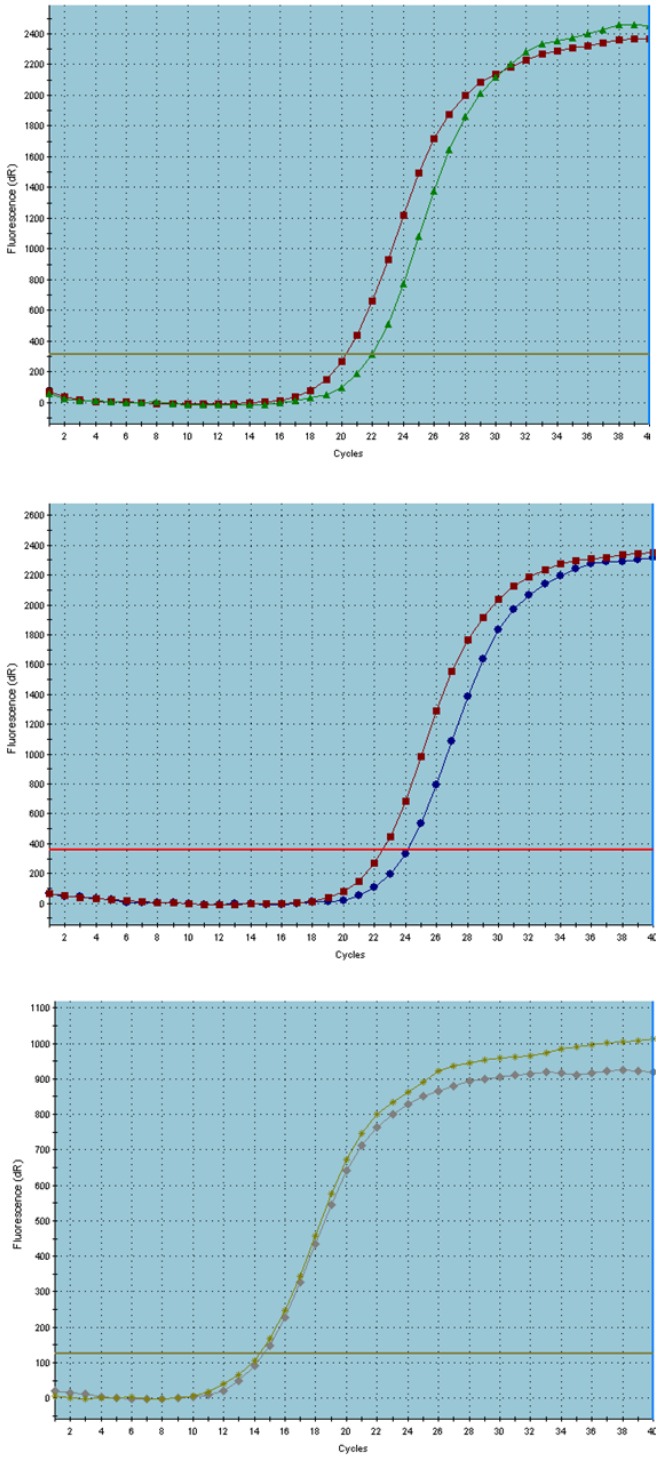

Figure 3.7. Amplification plots for *APEX2* (top), *POLQ* (middle), and *GAPDH* (bottom). Each plot contains curves for two separate reactions. The Ct threshold setting is represented by a horizontal line. In the plots for *APEX2* and *POLQ*, the left sided curve shows the reaction following NT siRNA transfection, whilst the right sided curve shows the reaction following transfection with *APEX2* or *POLQ* siRNA respectively. The top two curves therefore represent good knockdown of the genes of interest. *GAPDH* expression was used to normalise expression of *POLQ* and *APEX2*. The overlapping *GAPDH* curves suggest minimal differences in the concentration of RNA in these two reactions.

The screen of irradiated MRC5 cells was used to filter the list of candidate genes. In order to identify candidate genes whose depletion sensitised tumour cells to radiation without affecting normal tissue radiosensitivity, the MRC5 fibroblast cell line was screened with the same pools of siRNAs that were used to transfect the tumour cells. Figure 3.8 shows the top 30 genes associated with elevated γH2AX foci in irradiated MRC5 cells. One of the genes identified by this normal tissue screen was *APEX2* which also had a high Z-score on the screen of irradiated tumour cells (Fig. 3.4). As *APEX2* has not previously been shown to be involved in intrinsic radiosensitivity, clonogenic assays were performed with MRC5 cells depleted of *APEX2.* Figure 3.9 demonstrates that knockdown of *APEX2* did indeed cause increased cell radiosensitivity suggesting that APEX2 is unlikely to be a tumour-specific radiosensitisation target. This shows that performing a parallel screen in a normal tissue cell line is an effective way of identifying genes that induce normal tissue radiosensitisation and could be used in screens of larger siRNA libraries to avoid lengthy investigations of genes that do not have tumour-specific effects on cell radiosensitivity.

In addition to *APEX2* there were seven other genes which featured in the top 30 Z-scores of both the irradiated SQ20B and MRC5 cell line screens (Table 3.1). As a result, these were not investigated further as potential tumour-specific radiosensitisation targets.

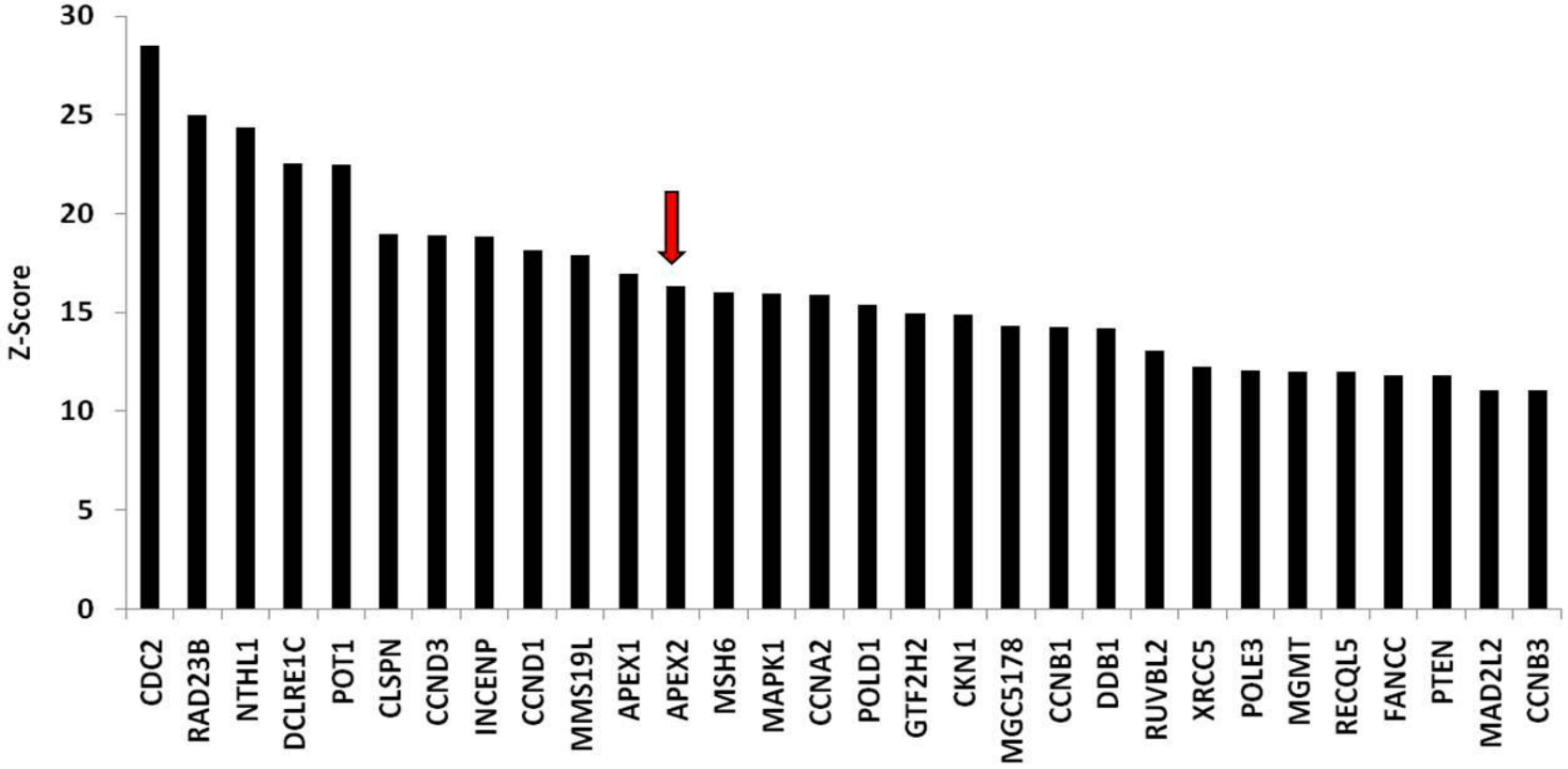

Figure 3.8. Irradiated MRC5 cells. Z-scores of the top 30 genes associated with elevated γH2AX foci twenty-four hours after 4Gy radiation. APEX2 siRNA was associated with a high Z-score in irradiated tumour cell and fibroblast screens.

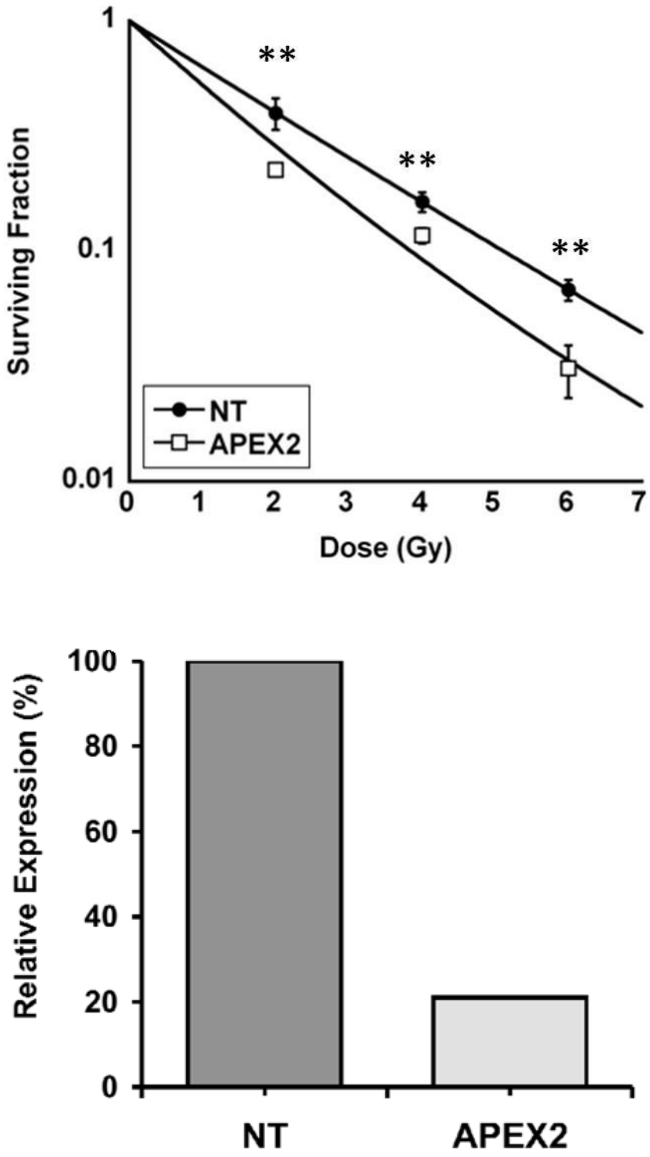

Figure 3.9. Radiosensitisation of MRC5 cells with *APEX2* depletion. Clonogenic assay in MRC5 cells treated with 50 nM NT or APEX2 siRNA. **, P < 0.01 unpaired two sided t-test (top). Demonstration of effective knockdown of *APEX2* by qRT-PCR (bottom). Gene expression normalised to cells treated with NT siRNA.

APEX1	CCNA2	CLSPN	POLE3
APEX2	CDC2	INCENP	XRCC5

Table 3.1 List of those genes which featured in the top 30 Z scores of both the irradiated SQ20B and MRC5 cell line screens.

Identification of genes important in tumour cell survival independently of radiation. Of the remaining candidate genes being investigated, the screen of unirradiated SQ20B cells was used as a filter to exclude those genes whose knockdown affected cell viability in the absence of exposure to IR. The Z-scores of the top 30 genes associated with elevated γH2AX foci in unirradiated SQ20B cells are shown in Figure 3.10. The effect of gene knockdown on cell survival has not previously been studied for several of these genes. Colony forming assays performed with unirradiated SQ20B cells transfected with siRNA pools against RPA and INCENP (Inner centromere protein) which both ranked highly in this unirradiated screen, resulted in widespread cell death and no colony formation. These colony forming assays were repeated in other tumour cell lines. The very low plating efficiency associated with knockdown of these two genes is summarised in Table 3.2.

These initial results suggested that the unirradiated tumour cell screen could be used as an effective filter for siRNAs which caused cell death in unirradiated conditions.

	SQ20B	T24	HeLa	PSN1
RPA	3.8%	0.1%	0.0%	0.0%
INCENP	2.1%	1.3%	N/A	N/A

Table 3.2. Low plating efficiency associated with knockdown of RPA and INCENP in several different tumour types.

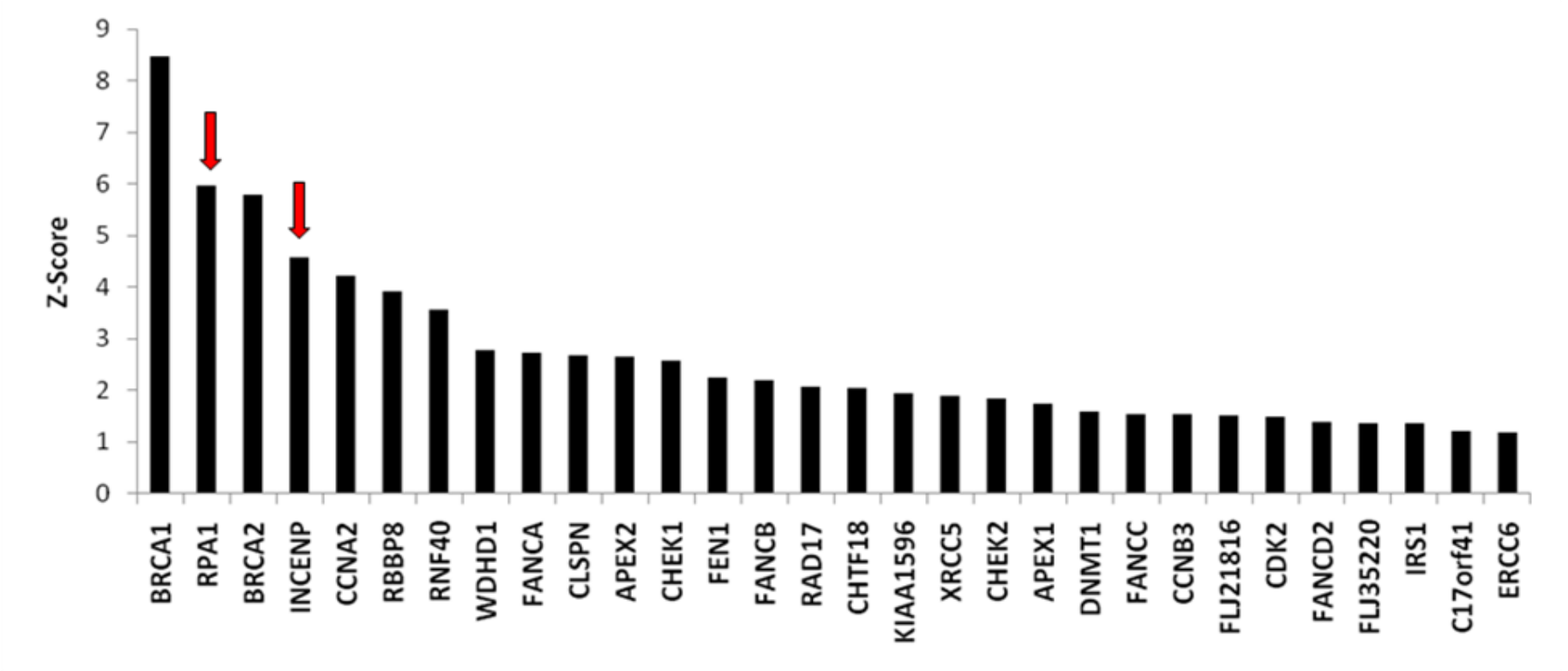

Figure 3.10. Unirradiated SQ20B cells. Z-scores of the top 30 genes associated with elevated γH2AX foci in cells transfected with siRNA pools. Red arrows indicate ranking of RPA and INCENP whose knockdown induces cell death in the absence of IR.

Table 3.3 lists those genes which featured in the top 30 Z-scores of the irradiated SQ20B but not in either the irradiated MRC5 screen, or the unirradiated SQ20B screen.

C9ORF76	NEK2	RAD21	REV3L	TP53BP1
LIG4	POLQ	RAD52	TIMELESS	XAB2
MSH2	PRKDC	RAD54L	TOPBP1	

Table 3.3 List of genes which featured in the top 30 Z-scores of the irradiated SQ20B screen but not in either the irradiated MRC5 screen or the unirradiated SQ20B screen.

None of the remaining genes being investigated as causing tumour specific radiosensitisation (*POLQ, RAD21,* and *XAB2*) were associated with high Z-scores in the screen of unirradiated tumour cells. However colony forming assays performed with a panel of unirradiated cells transfected with RAD21 and XAB2 siRNA demonstrated that knockdown of these genes resulted in widespread cell death in unirradiated cells (Fig. 3.11 and Table 3.4).

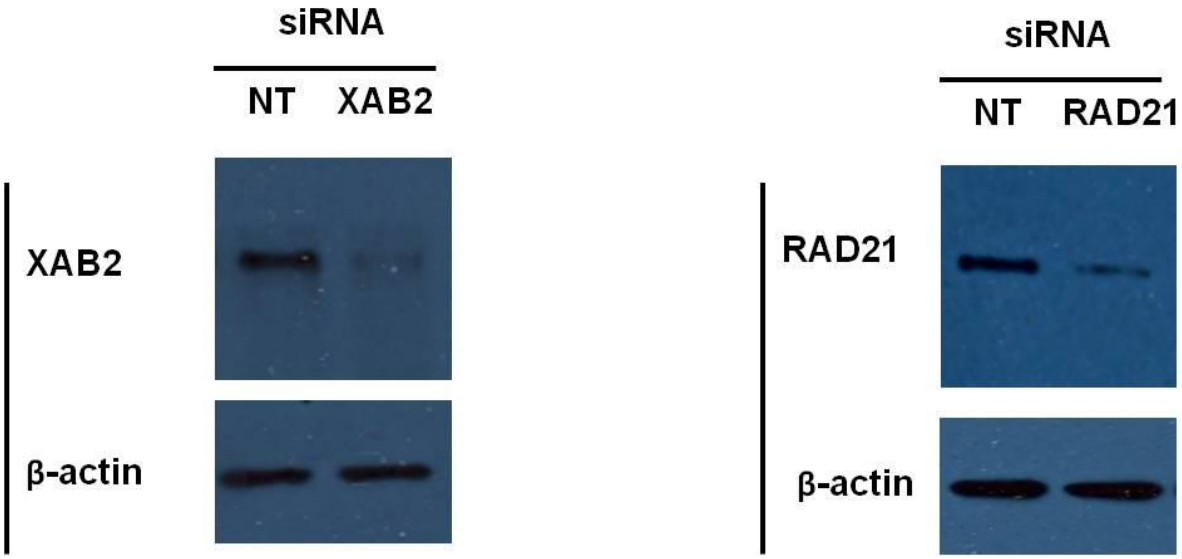

Figure 3.11. Western Blot of lysate obtained from SQ20B cells transfected with XAB2 (left) and RAD21 (right) siRNA demonstrating effective knockdown.

	Cell line			
siRNA pool	**SQ20B**	**T24**	**HeLa**	**PSN1**
NT	39.9%	43.9%	43.5%	23.9%
XAB2	0.3%	0.2%	0.1%	0.0%
RAD21	3.7%	4.1%	1.8%	0.2%

Table 3.4. Depletion of XAB2 and RAD21 resulted in widespread cell death in the absence of exposure to IR. Plating efficiencies for four different tumour cell lines are shown.

The results summarised in Figure 3.11 and Table 3.4 suggest that the absence of elevated γH2AX foci in unirradiated cells transfected with pools of siRNA cannot reliably be used to predict the survival of cells in the absence of IR. However, the exclusion of those genes which cause γH2AX foci in the absence of radiation may reduce the number of false positive genes in the screen of irradiated cells. Having excluded three of the four genes initially identified by the screen of irradiated SQ20B cells, the remaining gene, *POLQ* was investigated in more detail.

***POLQ* knockdown is associated with increased γH2AX foci following IR.** POLQ (DNA polymerase theta) is a low fidelity DNA polymerase with limited normal tissue expression, whose normal physiological functions are largely unknown (215, 216). *POLQ* featured in the top 30 Z-scores of the irradiated SQ20B screen but not in the screens using irradiated MRC5 cells or unirradiated SQ20B cells suggesting it does not affect MRC5 cell survival after irradiation or SQ20B cell viability in the absence of

irradiation. As *POLQ* knockdown has not previously been shown to sensitise human tumour cells to IR, this gene was investigated further. First, the results found in the screen were replicated. SQ20B cells were transfected in triplicate wells of two 96 well plates with either NT or POLQ siRNA. One plate was irradiated with 4Gy and the other left unirradiated. Twenty four hours after IR, cells were analysed for γH2AX foci. Unirradiated cells with *POLQ* knockdown did not have increased γH2AX foci compared to negative controls (Fig. 3.12). However the irradiated cells treated with POLQ siRNA had significantly increased residual γH2AX foci compared to irradiated cells treated with NT siRNA (Figure 3.13A and B). This confirmed the results seen in the screen and validated POLQ as an appropriate target to pursue further.

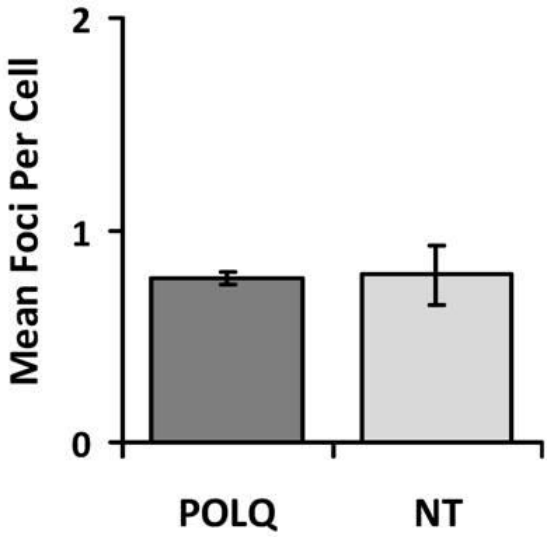

Figure 3.12. In unirradiated SQ20B cells, *POLQ* knockdown has no effect on γH2AX foci formation.

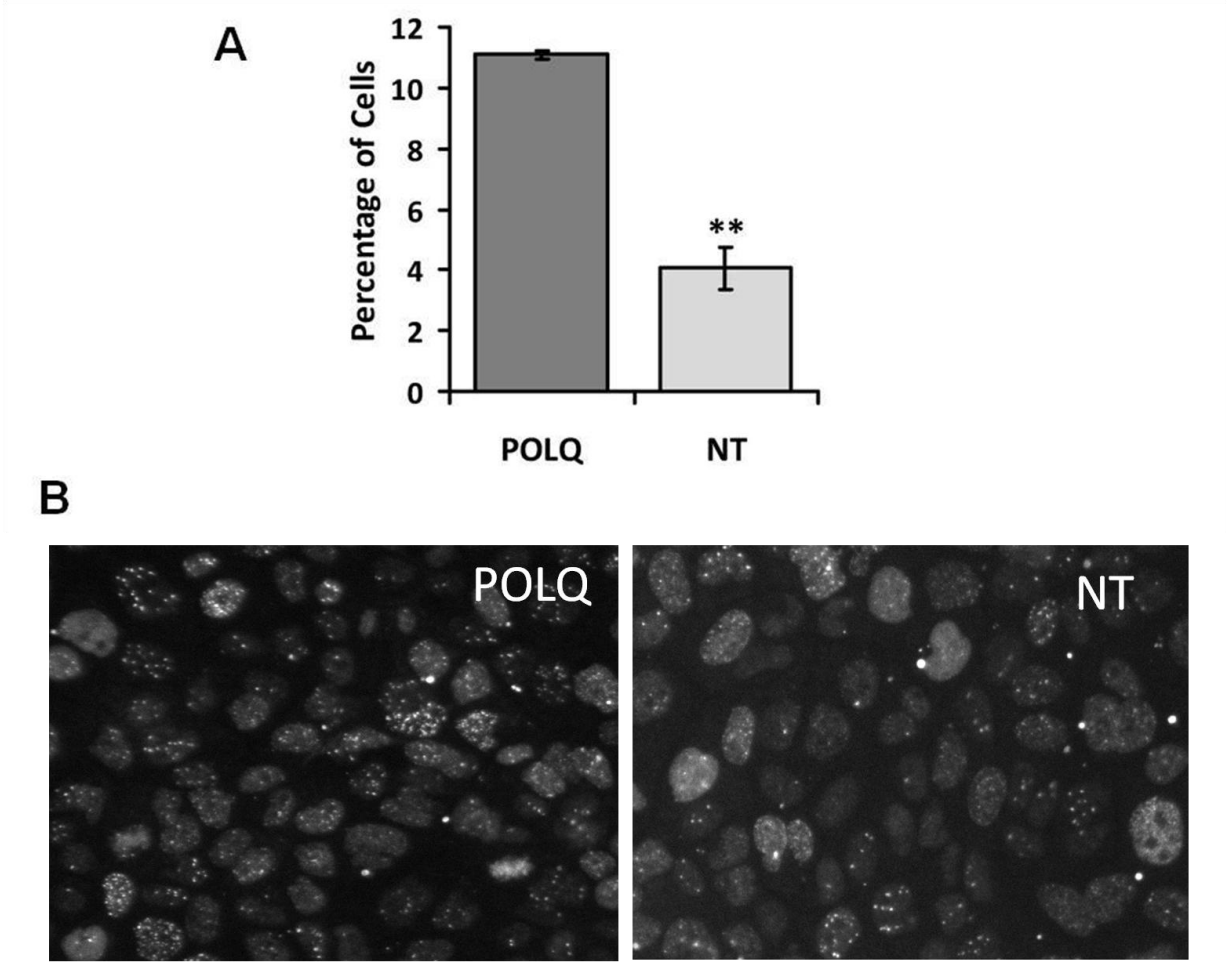

Figure 3.13. A) Increase in proportion of cells with >7 γH2AX foci in irradiated SQ20B cells with *POLQ* knockdown. **, P < 0.01 unpaired two sided t-test. B) Representative images showing the increase in γH2AX foci in irradiated SQ20B cells depleted of *POLQ* compared to those treated with NT siRNA.

***POLQ* knockdown sensitises several tumour cell lines to IR.** In order to confirm that the observed increase in γH2AX foci associated with irradiated SQ20B cells depleted of *POLQ* translated into an increase in tumour cell radiosensitivity, clonogenic assays were performed with the SQ20B cells used in the primary screen along with a second tumour line (HeLa) following transfection with either NT or POLQ siRNA (see Materials and Methods for transfection conditions). Figure 3.14

confirms that the transfection conditions were effective in causing *POLQ* knockdown in both cell lines and that knockdown resulted in significant radiosensitisation.

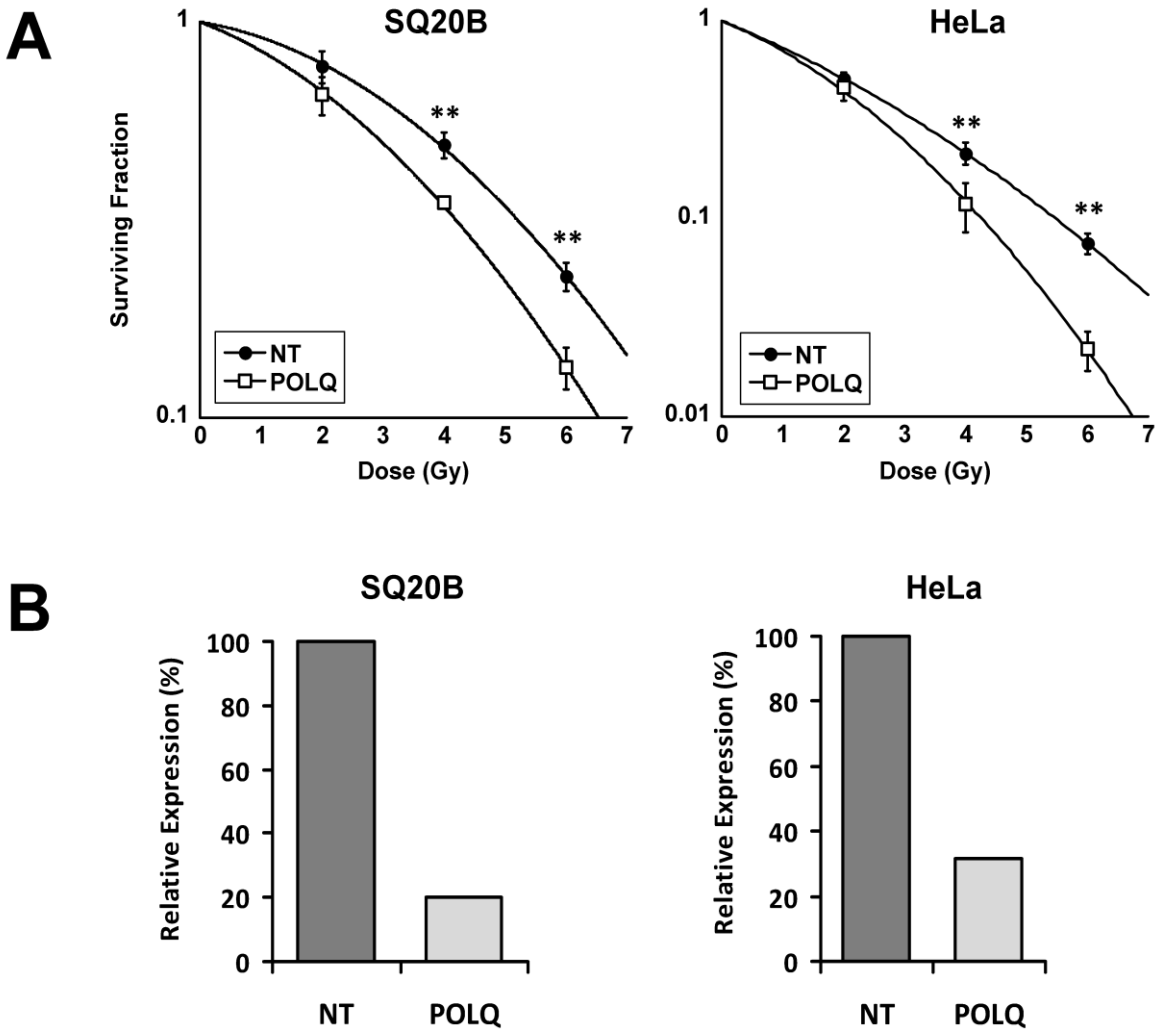

Figure 3.14. Radiosensitisation of tumour cells following *POLQ* depletion. A) Radiosensitisation of SQ20B (SER_{10}=1.18) and HeLa (SER_{10}=1.28) cells following POLQ siRNA transfection. **, P < 0.01 unpaired two sided t-test. B) Effective *POLQ* knockdown at the time of irradiation confirmed by qRT-PCR using the remaining SQ20B and HeLa cells.

In order to demonstrate that the radiosensitisation effects caused by depletion of POLQ were not just limited to squamous cell carcinomas, clonogenic assays were performed on a third tumour cell line (T24 transitional cell bladder carcinoma). As well as using pooled siRNA targeted against POLQ, clonogenic assays were also performed using each individual siRNA from the pool (Fig. 3.15). Several other published siRNA screens have also performed such deconvolution studies to validate targets identified by primary screening as true on-target effects (217, 218).

The individual siRNA strand transfections were performed with a final concentration of 25 nM siRNA. Three of the four siRNAs caused significant radiosensitisation and the degree of *POLQ* knockdown was well correlated with the magnitude of associated radiosensitisation. Of the four individual siRNAs, Strand '1' caused the most potent silencing and the most potent radiosensitisation (Fig. 3.15). These findings strongly suggest that the observed radiosensitisation associated with transfection with POLQ siRNA did not occur as a result of 'off target' effects.

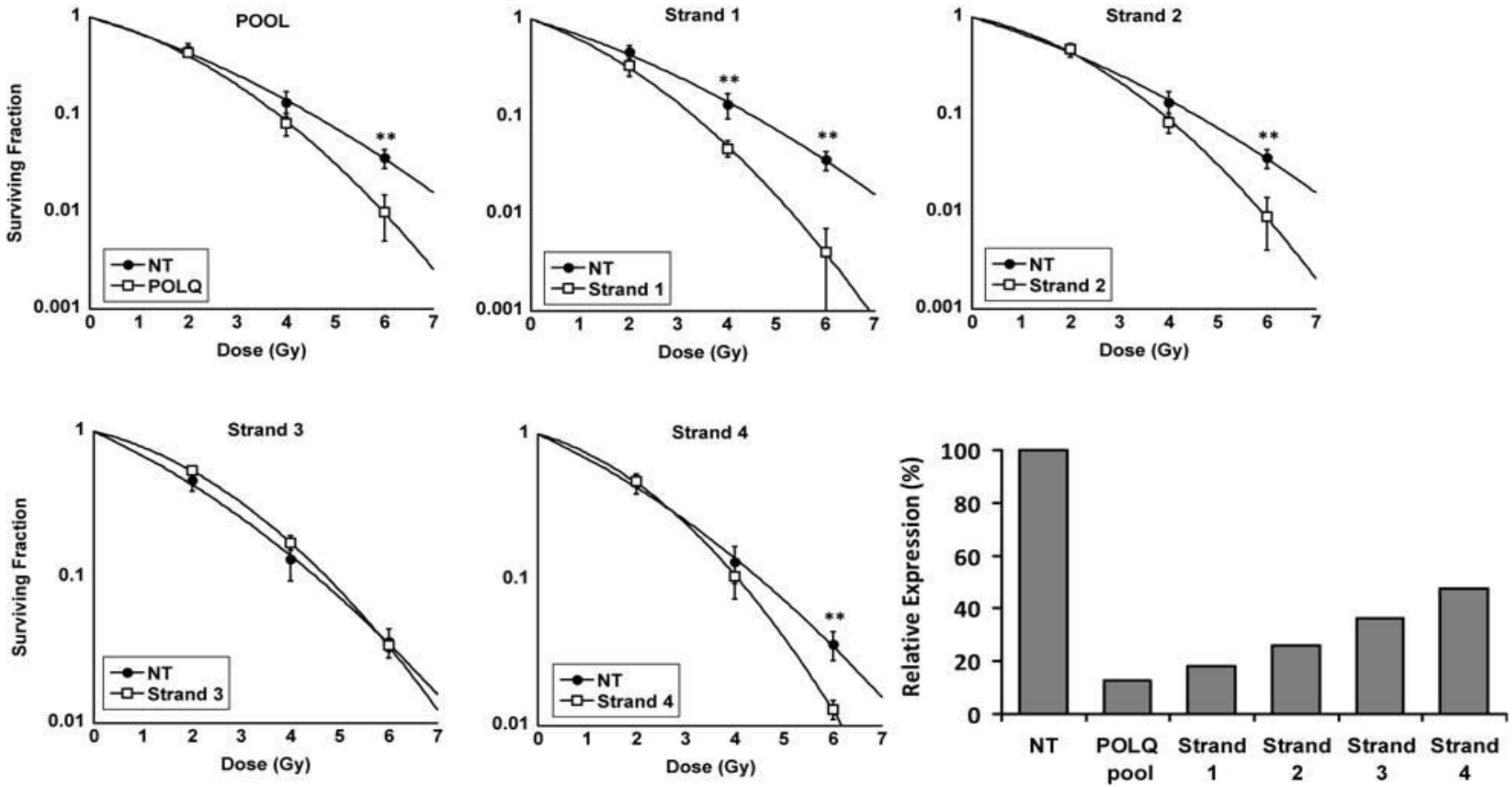

Figure 3.15. Demonstration of the absence of off-target effects. T24 cells transfected with either 50 nM POLQ pool of siRNA (SER_{10}=1.18), or 25 nM of each individual siRNA strand. **, P < 0.01 unpaired two sided t-test. Relative expression of *POLQ* normalised to cells treated with NT siRNA as determined by qRT-PCR (bottom right).

***POLQ* knockdown does not appear to alter cell cycle distribution in either irradiated or unirradiated cells.** To investigate the effects of POLQ depletion on cell cycle distribution, SQ20B cells were forward transfected in 6 well dishes with either NT or POLQ siRNA as previously described. Forty-eight hours after transfection, cells were exposed to either 0Gy or 4Gy IR, and then returned to the incubator until they were lifted and fixed for FACS analysis 24h after irradiation. Figure 3.16 illustrates that POLQ depletion does not alter cell cycle distribution in unirradiated cells. Twenty-four hours after IR, the SQ20B cells showed evidence of a G2 arrest as would be expected (219), however this arrest occurred with the same magnitude regardless of whether cells were transfected with either POLQ or NT siRNA.

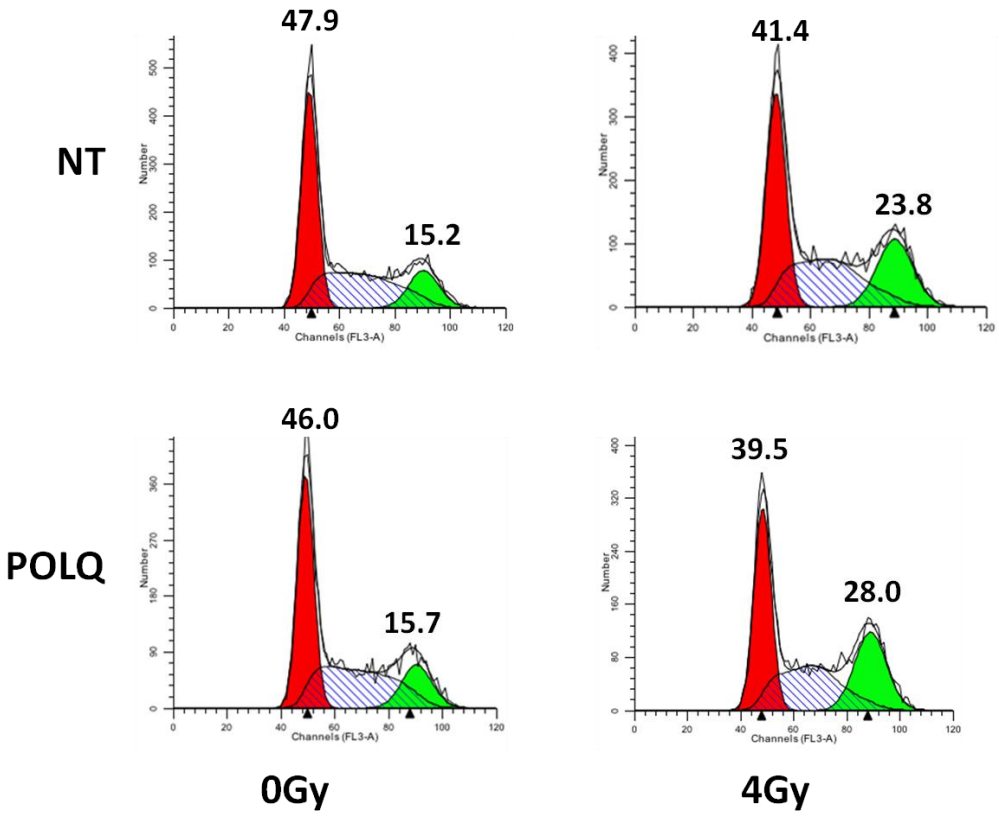

Figure 3.16. POLQ depletion does not alter cell cycle distribution in either irradiated or unirradiated SQ20B cells compared to cells transfected with NT siRNA. Numbers above G1 and G2-M peaks indicate the percentage of cells in each compartment.

***POLQ* knockdown causes minimal effects on normal tissue radiosensitivity.** Previous work has shown that *POLQ* expression is limited to only a small number of normal tissues, particularly lymphoid tissues such as the fetal liver, thymus and bone marrow (215). In order to confirm that treatment with POLQ siRNA did not significantly alter the radiosensitivity of normal tissue cell lines, clonogenic assays were performed on two fibroblast lines, MRC5 and POC cells. The POC cells did not express *POLQ* and treatment with POLQ siRNA had no radiosensitising effects (Fig. 3.17). As well as supporting the hypothesis that *POLQ* knockdown may cause tumour specific radiosensitisation, this also confirms that the observed effects did not occur as a result of off-target effects.

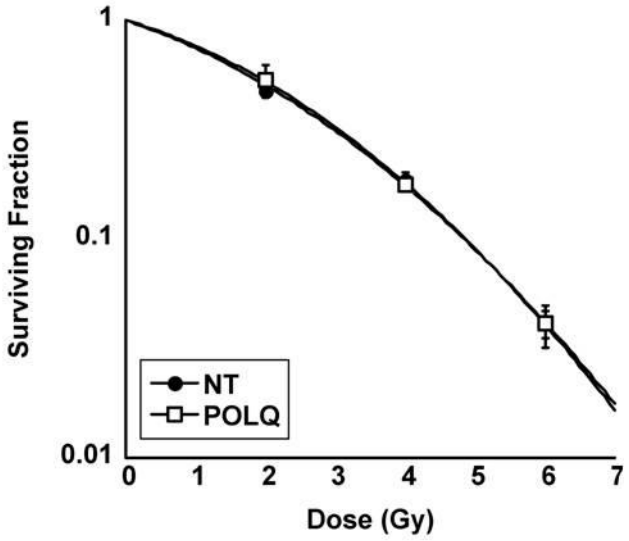

Figure 3.17. POC cells treated with POLQ siRNA were not sensitised to IR. POLQ expression could not be detected by qRT-PCR.

In the MRC5 cells, POLQ siRNA treatment caused only a marginal increase in radiosensitivity at very high doses of radiation (Fig. 3.18).

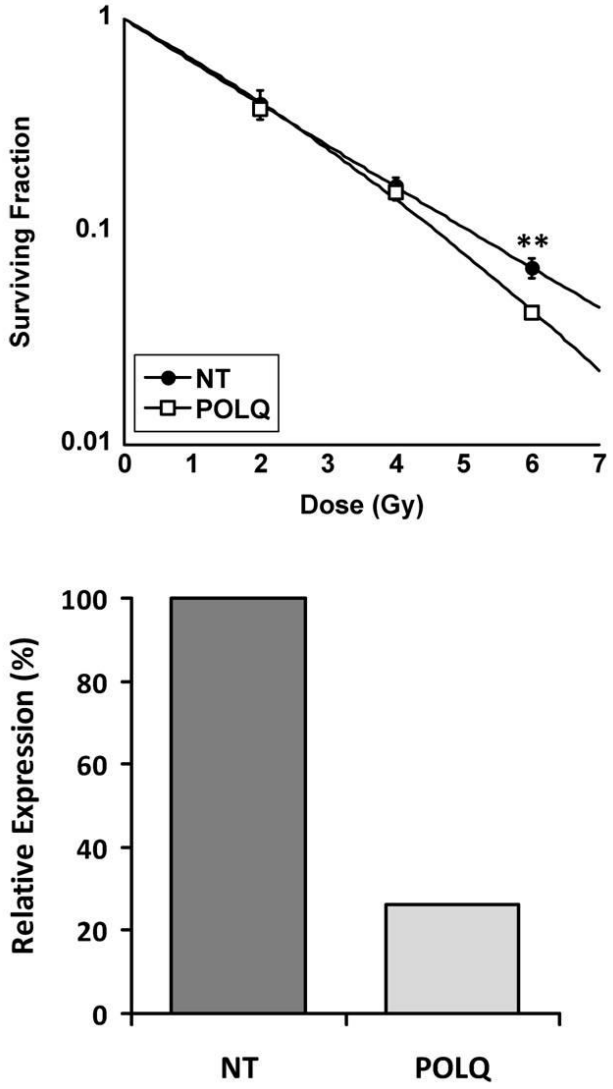

Figure 3.18. MRC5 cells show modest sensitisation to *POLQ* depletion only at high doses of IR (top). **, P < 0.01 unpaired two sided t-test. Effective knockdown of *POLQ* in MRC5 cells treated with 50 nM POLQ siRNA as determined by qRT-PCR (bottom).

A comparison between *POLQ* expression normalised to the expression of a housekeeping gene (*GAPDH*) in untransfected MRC5 and T24 cells showed that MRC5 cells express *POLQ* at a level approximately 50 times lower than the T24

tumour cell line (Fig. 3.19). In unirradiated cells, *POLQ* knockdown did not consistently reduce colony formation in either the normal tissue or the tumour cell lines (Table 3.5).

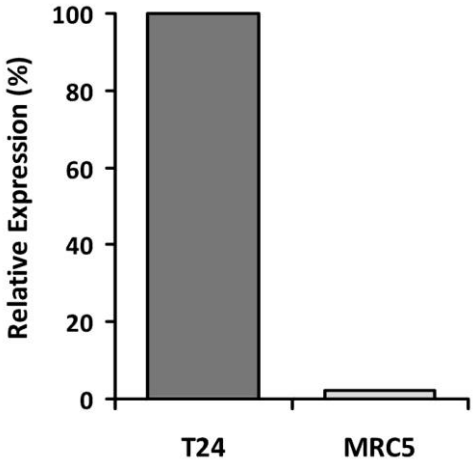

Figure 3.19. Relative expression of *POLQ* in untransfected T24 and MRC5 cells as determined by qRT-PCR. The expression of *POLQ* was expressed as a ratio relative to the presence of *GAPDH* in each cell line.

	Plating efficiency (SD)	
Cell line	**NT**	**POLQ**
HeLa	39.7% (4.5%)	30.9% (3.7%)
SQ20B	36.0% (1.9%)	34.7% (3.1%)
T24	51.2% (4.0%)	43.6% (5.0%)
POC	5.0% (0.4%)	4.2% (0.4%)
MRC5	5.2% (0.2%)	5.6% (0.8%)

Table 3.5. Percentage of cells capable of forming colonies following transfection with either NT or POLQ siRNA. Standard deviations are shown in brackets.

***POLQ* knockdown has no effects on cell response to temozolomide, with or without IR.** Temozolomide is an orally available alkylating agent that has an established role in the treatment of glioblastomas (220). It has previously been shown that a significant proportion of the DNA damage caused by temozolomide is repaired by the base excision repair (BER) pathway, and that cells with deficiencies in the BER pathway have increased sensitivity to temozolomide (221). As it has previously been suggested that POLQ plays a role in BER (222, 223), it was examined whether *POLQ* knockdown rendered cells more sensitive to temozolomide. Clonogenic assays performed on SQ20B cells treated with either POLQ or NT siRNA showed no difference in sensitivity to drug treatment with temozolomide (Figure 3.20).

For both unirradiated (Fig. 3.21A) and irradiated conditions (Fig. 3.21B), SQ20B cells treated with temozolomide were found to have elevated γH2AX foci twenty-four hours after drug exposure compared to cells not exposed to the drug. However, this occurred with the same magnitude regardless of whether cells had been transfected with either NT or POLQ siRNA. These findings would suggest that the mechanism by which *POLQ* knockdown causes increased radiosensitivity are independent of BER.

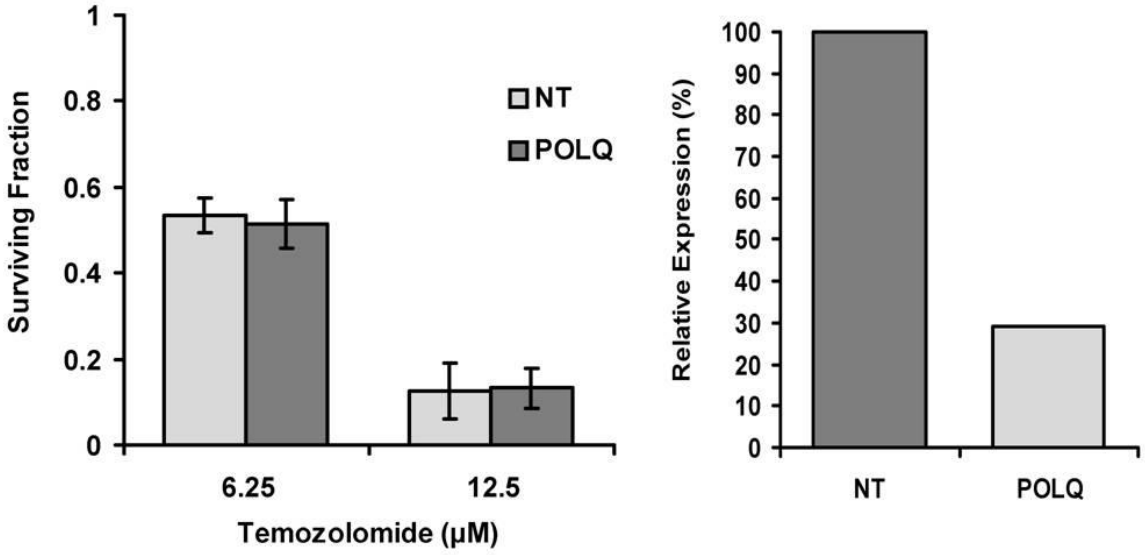

Figure 3.20. Clonogenic assays performed with SQ20B cells transfected with either NT or POLQ siRNA. Survival following 2h temozolomide treatment at the stated doses expressed as a fraction relative to cells not exposed to temozolomide (left). Confirmation of effective knockdown of *POLQ* in SQ20B cells as determined by qRT-PCR (right).

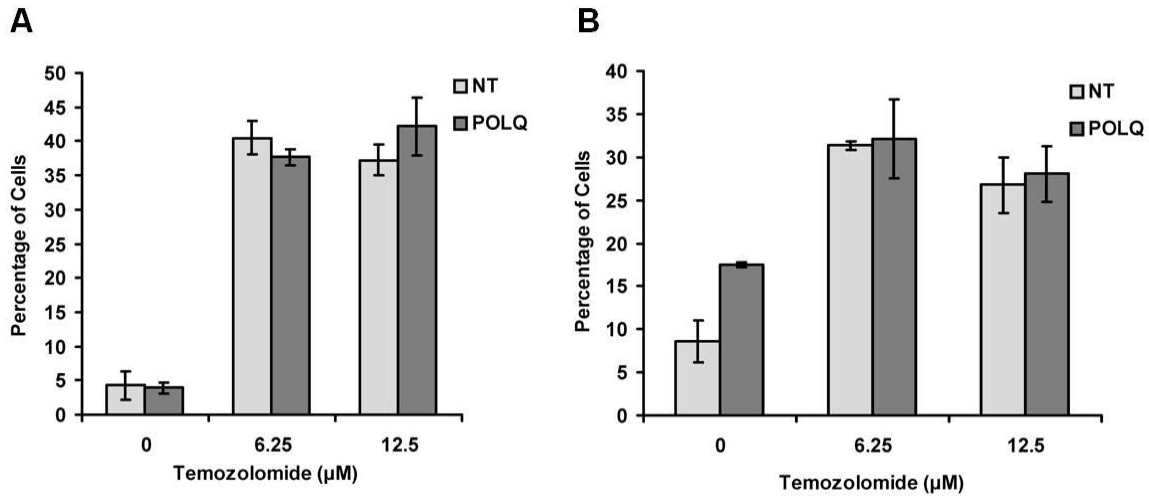

Figure 3.21. A) Effects of temozolomide treatment on the percentage of unirradiated SQ20B cells containing >7 γH2AX foci per cell. B) Percentage of SQ20B cells containing >7 γH2AX foci per cell following 4Gy irradiation. In all cases, cells were exposed to temozolomide for 2h at the stated doses.

3.4 Discussion

Syndromes such as ataxia-telangiectasia, Fanconi anaemia and Nijmegen breakage syndrome result from DNA repair defects that cause radiation sensitivity in addition to other complex clinical problems. (176). The proteins responsible for these repair defects are not appropriate therapeutic targets due to their lack of tumour specificity. Many of the key, therapeutically exploitable mechanisms that determine intrinsic tumour radiosensitivity are largely unknown. The clinical importance of understanding these mechanisms is shown by the known correlation between increased tumour radioresistance and adverse patient outcomes (95-97).

The EGFR pathway is the most widely studied contributor to tumour cell radioresistance. Recent trials have demonstrated the large benefits that can potentially be derived from biological treatments that selectively render tumour cells more sensitive to radiation by manipulation of this pathway, and illustrate the need for greater understanding of the molecular basis for tumour radioresistance (3, 224).

This siRNA screen of genes involved in DNA repair was based on the critical role that unrepaired DSBs play in cell death following IR. Of the genes whose knockdown was associated with increased γH2AX foci in SQ20B cells following IR, several have already been shown to be associated with increased cell radiosensitivity (199-205) thus validating the primary screening endpoint. The experimental design used both irradiated and unirradiated tumour cells as well as parallel siRNA screens in a tumour line and normal tissue line. The aim of this design was to enable the identification of siRNAs that cause tumour specific radiosensitisation.

The siRNA screen utilised γH2AX foci as an assay endpoint and was successful in identifying a novel gene whose depletion leads to tumour specific radiosensitisation. Our experience with this screen would suggest that γH2AX foci are an appropriate endpoint to use for radiosensitivity screens of larger siRNA libraries. A potential disadvantage of using this endpoint is that γH2AX foci do not appear only at sites of damaged DNA, but also appear at sites of stalled replication forks in S-phase. Since 53BP1 foci are better defined than γH2AX foci, and do not occur at stalled replication forks (225) it could be argued that this would be a better endpoint. However, there is insufficient evidence showing a correlation between 53BP1 foci and intrinsic radiosensitivity (173), and like γH2AX, this endpoint would still have the problem of identifying genes whose knockdown induced cell death in the absence of IR.

High throughput screens will inevitably feature both false positive and false negative results. Failure to cause sufficient gene knockdown is one of the most common causes for obtaining false negative results. *ATM* is widely recognised as being involved in cell radiosensitivity (226, 227) and was included in this 200 gene library. However *ATM* was notably not in the top 30 Z-scores of the irradiated cell screens. In this case it is probable that this occurred because *ATM* is one of the genes involved in causing H2AX phosphorylation in response to DSB formation (228). Therefore depletion of *ATM* limited the number of γH2AX foci formed in response to IR and thus is a false negative in this assay.

The screen of irradiated SQ20B cells identified several genes, whose knockdown was associated with elevated γH2AX foci post IR, that were not previously known to be involved in tumour cell radiosensitivity. Genes that were felt to be clinically exploitable if it was shown that gene depletion caused tumour specific radiosensitisation were selected for further investigation. These were *APEX2, RAD21, XAB2,* and *POLQ*

Rationale for selection of candidate genes, *APEX2, RAD21, XAB2,* and *POLQ* .

APEX2 (AP endonuclease 2) is a secondary mammalian apurinic/apyrimidinic endonuclease. In humans, it has approximately 1% of the endonuclease activity of its paralogue APEX1 (229). However, APEX2 is a multifunctional enzyme, which has strong 3'-phosphodiesterase and 3'–5' exonuclease activities and has previously been shown to be involved in repair of oxidative damage (207, 208). The finding that mice deficient in APEX2 are viable, and other than demonstrating a degree of growth retardation, are phenotypically normal, suggested that APEX2 may not be essential for most normal tissues (230). It was therefore felt that APEX2 was a reasonable gene to investigate further. Unfortunately APEX2 depletion also caused increased γH2AX foci in irradiated MRC5 cells, suggesting that APEX2 depletion may cause normal tissue radiosensitisation. Colony forming assays confirmed that this was the case (Fig. 3.9). Previous Northern blot studies on human tissues have shown widespread APEX2 expression in stomach, thyroid, spinal cord, lymph node, trachea, adrenal gland, bone marrow, spleen, thymus, prostate, testis, uterus, small intestine, colon, peripheral blood leukocyte, heart, brain, placenta, lung, liver, smooth muscle, kidney, and pancreas (229). It was therefore decided not to pursue this gene further since it was felt that APEX2 inhibition was unlikely to be clinically useful.

XAB2 (XPA binding protein 2) has previously been implicated in nucleotide excision repair due to its involvement in transcription coupled repair (TCR) (209). TCR is involved in the removal of transcription blocking lesions from transcriptionally active genes and is most likely triggered by lesion-stalled RNA polymerase II. A siRNA screen recently demonstrated that XAB2 depletion rendered CAL51 breast tumour cells significantly more sensitive to PARP inhibition (210). This unexpected finding suggested that XAB2 may have functions beyond NER, which was felt to warrant further investigation. Unfortunately it was found that XAB2 depletion led to cell death in unirradiated cells and was therefore not explored further. Since XAB2 knockout mice are embryonically lethal at an early stage, it is quite possible that XAB2 plays a crucial role in normal physiology and is therefore unlikely to be a clinically exploitable target (231).

RAD21 was another of the genes associated with a high Z-score in the irradiated SQ20B screen which was investigated in more detail. The full functions of RAD21 are not yet known, although it is recognised as being involved in ensuring cohesion of sister chromatids in mitotic cells (232). The yeast homologue of RAD21 has previously been implicated in DSB repair via homologous recombination (233), whilst RAD21 depletion of human tumour cells has been shown to increase their sensitivity to etoposide and bleomycin (212). Several studies have previously been published linking RAD21 function to the development of cancer, and to the cellular response to cancer treatment. It has previously been suggested that elevated RAD21 levels in oral squamous cell carcinoma correlate with increased potential for tumour invasion and metastasis (211). A previous study identified three separate RAD21 single nucleotide polymorphisms (SNPs) which were found to be inversely associated with

the risk of developing breast cancer, although the authors did not elucidate on the functional significance of the SNP (234). Another clinical study identified 19 patients who had previously developed severe radiosensitivity reactions during treatment and found that 6 of these patients had a T1440C SNP (235). Although this polymorphism is not associated with an amino acid change, the authors suggested that this SNP was biologically active and that homozygous mutations of this gene could contribute to increased radiosensitivity (235). Following on from this work, a separate group also found an increased incidence of RAD21 SNPs amongst patients who had previously developed a severe radiosensitivity reaction (236). In view of this suggestion of a link between RAD21 function and intrinsic radiosensitivity, it was felt that this gene should be investigated further. Unfortunately colony forming assays showed that RAD21 depletion resulted in widespread cell death in unirradiated cells. Interestingly, another group have performed clonogenic assays in tumour cells depleted of RAD21 (212). Although they noticed a significant reduction in colony formation following RAD21 knockdown, it was much less pronounced than the level that we observed in four different tumour lines (Table 3.4). The reason for this difference is not clear, but it is possible that the experiment described here resulted in more potent RAD21 knockdown, and therefore more cell death. In view of the finding that RAD21 depletion resulted in such poor colony formation in unirradiated cells, it was felt that RAD21 was not a suitable gene to pursue further.

It had previously been hoped that the screen of unirradiated tumour cells could identify genes whose depletion resulted in cell death in the absence of IR. However, the results obtained from XAB2 and RAD21 knockdown showed that the absence of

elevated γH2AX foci in unirradiated cells transfected with pools of siRNA cannot reliably be used to predict the survival of cells in the absence of IR.

Of the targets that were identified in this screen, it was decided to investigate *POLQ* further. POLQ (DNA polymerase theta) will be discussed in more detail in the introduction to the next chapter, but in brief, POLQ is a member of the A family of DNA polymerases which, unusually for this class of polymerases, synthesises DNA with very low fidelity (213, 214). The normal physiological functions associated with this protein are currently unclear. It has previously been suggested that POLQ plays a significant role in the process of somatic hypermutation of immunoglobulin genes (237, 238), however this remains contentious (216).

A key reason for electing to investigate POLQ in more detail stems from previous work showing that POLQ is overexpressed in a variety of different human cancers (such as lung, gastric and colon cancer) but has very limited normal tissue expression (215). Interestingly, expression was primarily limited to lymphoid tissues such as the fetal liver, thymus and bone marrow. Critical normal tissues such as the lung, liver, small intestine, kidney, heart, brain and spinal cord that typically limit the radiation dose that can be delivered to patients, did not appear to express *POLQ* (215). It was felt that this difference in expression meant that POLQ inhibition could potentially be exploited clinically since POLQ inhibition would not be expected to alter the radiation sensitivity of these tissues.

The results presented in this chapter confirm that *POLQ* is overexpressed in tumour cells derived from a variety of primary sites, and that *POLQ* knockdown causes increased intrinsic radiosensitivity of these tumour cells. It was found that transfection of POLQ siRNA had little or no effect on normal tissue cells. These results are consistent with the limited normal tissue expression of *POLQ*, and suggest that depletion of *POLQ* might cause much less radiosensitisation of normal tissues compared with tumours. These findings raise the possibility that POLQ inhibition could be used clinically to cause tumour specific radiosensitisation.

This is especially true since the relatively small differences observed in single irradiation colony forming assay experiments are exponentially increased during a course of fractionated radiotherapy. The *in vitro* and clinical data relating to cetuximab provides the best illustration of this. Cetuximab, (an EGFR monoclonal antibody) showed modest radiosensitisation *in vitro* (116), but when used with fractionated radiotherapy in head and neck cancer patients, resulted in significant tumour radiosensitisation leading to large improvements in overall survival (3, 4). Since the *in vitro* radiosensitisation associated with POLQ depletion (SER 1.18-1.28) is larger than that seen with Cetuximab treatment it is possible that POLQ disruption induces radiosensitisation that is of a magnitude that could be clinically beneficial.

The mechanism by which POLQ depletion induces tumour cell radiosensitisation is not clear at present. It appears that the effects are not related to redistribution of the cell cycle since POLQ depletion does not alter cell cycle distribution compared to cells transfected with NT siRNA either in irradiated or unirradiated cells. It has previously been suggested that POLQ plays a role in BER (222), but this is currently

unresolved (223). The work presented here shows that *POLQ* knockdown does not alter the sensitivity of cells to temozolomide either with or without IR (Fig. 3.20). We have interpreted this to mean that the mechanism by which *POLQ* knockdown causes increased sensitivity to IR is independent of BER, although it remains possible that POLQ facilitates repair via BER of a lesion that is produced by IR but not by temozolomide.

Chapter 4

DEPLETION OF POLQ DOWNREGULATES HOMOLOGOUS RECOMBINATION EFFICIENCY AND INDUCES TUMOUR CELL CHEMOSENSITISATION

4.1 Abstract

Work contained in the previous chapter demonstrated that tumour cells depleted of POLQ are rendered significantly more sensitive to IR. Normal cells treated with POLQ siRNA were not sensitised to radiation, reflecting the limited normal tissue expression of POLQ. Ionising radiation causes cell death as a result of DSB formation. Since many chemotherapy agents also cause DSB formation, this chapter contains work that examined whether POLQ depletion increases sensitivity not only to radiation but also to cytotoxic drugs. It was found that POLQ depletion rendered tumour cells significantly more sensitive to several classes of DNA damaging cytotoxic agents. The ability of cells deficient in POLQ to repair DNA double strand breaks was examined. It was found that POLQ does not appear to play a role in non-homologous end joining in tumour cells. Conversely, following exposure to etoposide, tumour cells depleted of POLQ were found to have reduced RAD51 foci formation suggesting that POLQ is involved in homologous recombination. A homologous recombination assay was used to confirm that POLQ depletion does indeed result in reduced homologous recombination efficiency. These facts, combined with the limited normal tissue expression of POLQ, and the poor prognosis associated with its overexpression in tumours, could make POLQ an attractive target for clinical manipulation.

4.2 Introduction

The previous chapter contained the results of a siRNA screen investigating the molecular determinants of tumour radiosensitivity. This study showed that POLQ knockdown rendered tumour cells significantly more sensitive to IR, but had little or no effect on normal tissue cells. This chapter will investigate the effects of tumour cell depletion of POLQ in more detail. Prior to this, the background details of POLQ are discussed below.

Identification of POLQ

POLQ was first identified in *Drosophila* as the *mus308* gene product in 1996 (239). The *mus308* (mutagen sensitive 308) mutant was originally identified by its sensitivity to interstrand crosslinking agents but normal resistance to alkylating agents (240).

The mouse homologue of *mus308* was identified by forward genetic mutation screening. This is an established tool for identifying gene functions and has been described previously (241). By observing the number of micronuclei present in the peripheral blood of offspring of mice that had been injected with *N*-ethyl-*N*-nitrosourea (ENU), it was possible to identify a mutation that induced chromosomal instability. This mutation, named *chaos1* (chromosome aberration occurring spontaneously), exhibited elevated levels of spontaneous micronuclei in reticulocytes and appeared to arise from a T-to-C base substitution in the *POLQ* gene, which caused a serine-to-proline substitution in the central domain region at amino acid residue 1932 (242). It was confirmed that the *chaos1* phenotype arose from loss of

POLQ function when it was shown that POLQ deficient mice have the same phenotype as *chaos1* mice (243).

In 1999, the human POLQ cDNA was cloned, sequenced and shown to have sequence homology to *mus308*. As this was the eighth DNA polymerase to be identified, the authors named it DNA polymerase θ (244). In 2002 a group purified a polymerase from HeLa cells that they believed to be full-length POLQ and found that it conducted high fidelity translesion synthesis (TLS) (245). However other authors have claimed that the purified polymerase was not POLQ since it was of the incorrect size and had features very different to those observed by other groups (214, 246). Studies published in 2003 demonstrated that human POLQ (246) has structural similarities to the *Drosophila* homologue in that they have a helicase domain at the N terminal region and a polymerase domain in the C terminus.

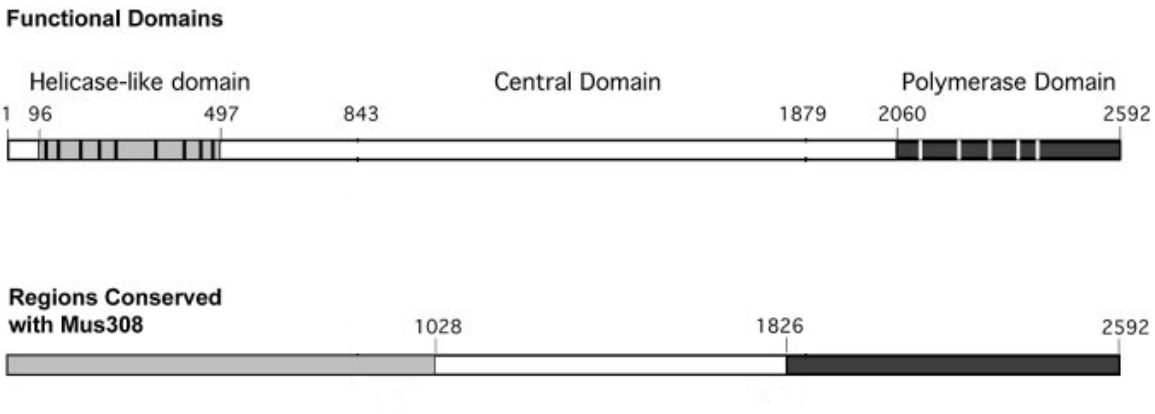

Figure 4.1. Structural representation of human POLQ (top) and comparison with *mus308* (bottom). The N-terminus contains the helicase domain (dark vertical lines represent conserved motifs) and the C-terminus contains the polymerase domain (white vertical lines represent conserved motifs). The shaded areas at both ends of the protein represent the regions that are most highly conserved. Figure adapted from (246).

Two further *mus308* POLQ paralogs have been identified in vertebrates; HEL308 has homology to the helicase domain of POLQ but has no polymerase domain (247), whilst POLN has homology to the polymerase domain, but does not have a helicase domain (248). These proteins will not be considered further since they have been shown to have different functional activities to POLQ (249, 250)

Physiological functions of POLQ

The normal physiological functions associated with POLQ are currently unclear. POLQ is a member of the A family of DNA polymerases which, unusually for this class of polymerases, synthesises DNA with very low fidelity (213, 214). One important feature of POLQ is its ability to tolerate damage arising from apurinic sites. Endogenous DNA damage resulting in hydrolytic loss of apurinic/apyrimidinic (AP) bases is extremely common. It has previously been estimated that 10,000 AP sites arise per cell every day (251, 252). Failure to adequately repair AP sites prior to DNA replication may induce mutagenesis (253) or cell death (254) and therefore TLS polymerases have evolved to bypass AP sites. The first step involves the intervention of a polymerase such as POLH (DNA polymerase eta) that incorporates a nucleotide across from the lesion (mispair inserter) (255), and another polymerase such as DNA polymerase zeta (256) that elongates past the mispair from the newly created primer end (mispair extender). This process allows cells to replicate through damaged DNA in either an error prone, or an error free fashion.

It has previously been shown that POLQ is able to efficiently perform translesion DNA synthesis at an AP site (214). Moreover, it is the only known enzyme that efficiently carries out both the insertion and extension steps required for AP bypass

(214). POLQ frequently misincorporates bases on both damaged and non-damaged DNA (with a frequency in excess of 1%) and therefore has been compared to the error-prone, Y family of DNA polymerases (214). Additional work has examined the role of POLQ in repairing UV induced damage. Although POLQ cannot by itself bypass a cyclobutane pyrimidine dimer, or a thymine-thymine (6-4) photoproduct, it is able to extend primers after a base has been inserted opposite these UV lesions by DNA polymerase iota (257).

POLQ and somatic hypermutation

It has previously been suggested that POLQ plays a dominant role in the process of somatic hypermutation (SHM) of immunoglobulin genes. SHM is a form of directed hypermutation that allows for the selection of B cells that express immunoglobulin receptors possessing an enhanced ability to recognise and bind a specific foreign antigen. B cell receptor (BCR) stimulation causes cell proliferation, during which time the rate of somatic mutation in the BCR locus is approximately one million fold greater than in most other genes (258). The first step in this process involves the mutation of a cytosine:guanine pair to a uracil:guanine mismatch. This deamination of cytosine to uracil in DNA is processed by an enzyme called ‘Activation-Induced (Cytidine) Deaminase’ (259). The uracil bases are then removed by the repair enzyme, uracil-DNA glycosylase (260). Error-prone DNA polymerases such as POLH (261) are then recruited to fill the gap and create mutations. The introduction of mutations in the rapidly proliferating population of B cells results in the production of thousands of B cells, possessing slightly different receptors of varying specificity for the antigen.

Although POLQ has been implicated as one of the error prone polymerases involved in the final step of the SHM process, this is currently a contentious issue. This suggestion originally arose from the observation by Masuda *et al* that mice with mutant POLQ containing an inactive polymerase, had significantly decreased C-G mutations (but not A-T mutations) in their immunoglobulin genes (262). A paper published concurrently by Zan *et al* found different results (237). They found that mice deficient in POLQ had a much greater reduction (~80%) in the overall mutation frequency of immunoglobulin genes than seen by Masuda *et al* but they did not observe a specific reduction in C/G mutations (237). A second paper by Masuda *et al* also examined the SHM rates in POLQ null mice (238). Although the overall reduction in mutation rates in immunoglobulin genes was less than that seen by Zan *et al,* they no longer saw the specific C/G mutations that they observed when using mice with mutant POLQ (238). This group concluded that the complete absence of POLQ may result in other polymerases acting as functional substitutes, resulting in a mutation pattern different from that found in POLQ inactive mice. They suggested that the differences in total immunoglobulin gene mutations rates seen between the two groups arose from differences in the tissues analysed, the methodology used, and the genetic background of the mice (238). The same group then assessed hypermutation in mice deficient in both POLQ and POLH (263). They found that the absence of POLQ did not change the frequency or pattern of mutation caused by the lack of POLH (i.e. a substantial decrease in mutations of A:T pairs) and therefore concluded that POLQ and POLH function in the same pathway (263).

A separate group also looked at the mutation types and frequencies seen in wild type, *POLQ*(-/-), *POLH*(-/-), and *POLQ*(-/-)/*POLH*(-/-) mice (216). They found that the

types of substitutions were similar between wild type and *POLQ*(-/-) clones, and between *POLH*(-/-), and *POLQ*(-/-)/*POLH*(-/-) mice. Accordingly this group suggested that POLQ does not play a significant role in the hypermutation pathway (216).

Very recent *in vitro* work conducted in the chicken DT40 B lymphocyte cell line has shown that POLH(-/-)/POLN(-/-)/POLQ(-/-) cells have significantly reduced immunoglobulin hypermutation rates (264). Given the ambiguous data that already exists on this topic, the authors acknowledged that further studies are required to support these *in vitro* data (264). This is especially true since the interactions of these polymerases may be even more complex *in vivo*.

POLQ and base excision repair

It has also been suggested that POLQ has a role in BER but this also remains unresolved. Base excision repair is a well orchestrated process by which base damage can be eliminated. The first step involves a lesion-specific DNA glycosylase which hydrolyses the N-glycosylic bond between the target base and deoxyribose, releasing a free base and resulting in an AP site (265). The phosphodiester bond 5’ to an abasic site is then cleaved by an AP endonuclease resulting in the 5’ terminus containing a deoxyribose phosphate (5’ dRP) residue (266). The resulting single strand break can then be processed by either short patch (where a single nucleotide is replaced) or long-patch BER (where 2-10 new nucleotides are synthesised). DNA polymerase beta (POLB) is the main protein involved in the final steps of short patch BER and has both polymerase and lyase activity. POLB inserts a single nucleotide and then removes the 5' dRP left behind by AP endonuclease cleavage (267, 268). DNA ligase III then seals the repaired DNA (269).

Long patch repair is initiated by the recruitment of POLB to the site cleaved by AP endonuclease (270). The strand synthesis is then continued by polymerases δ and ε (271). The strand displacement polymerisation produces a flapped substrate that is ligated by flap structure-specific endonuclease 1 (FEN1) (272). The activity of FEN1 has been shown to be regulated by scaffold proteins such as proliferating cell nuclear antigen (PCNA) (273). Long patch BER is then completed by DNA ligase I sealing the DNA strand (269).

It has previously been shown by Yoshimura *et al,* that mutation of *POLQ* in the DT40 chicken B cell lymphocyte cell line, increases sensitivity to hydrogen peroxide (222), which induces oxidative stress that is repaired by BER (274, 275). In addition they found that *POLQ*/*POLB* mutants had significantly higher sensitivity to methyl methanesulfonate than either single mutant. Extracts obtained from this cell line were used to show that *POLQ* mutant cells have markedly reduced single nucleotide BER capacity *in vitro* and that this reduction was of a similar magnitude to cells deficient in *POLB* (222). These findings led to the suggestion that POLQ and POLB cooperate in BER.

In view of these findings, subsequent biochemical work has looked at the *in vitro* activity of cloned human POLQ (223). It was shown that full-length, wild-type POLQ has 5’-dRP lyase activity. A C-terminal fragment of POLQ was also shown to carry 5’-dRP lyase as well as polymerase activity. The 5’-dRP lyase activity appears to be

independent of the polymerase activity since it was shown that full-length POLQ, with an inactivated polymerase, also retained 5'-dRP lyase activity (223). Furthermore, the full-length protein and the C-terminal fragment were shown to have short patch BER activity *in vitro*. Although these findings have been used to support the argument that POLQ may have a role in BER *in vivo*, it should be noted that the rate of 5'-dRP lyase activity of POLQ is approximately 40 fold slower than that of POLB, the main polymerase involved in short patch BER. The significance of POLQ mediated BER *in vivo* remains unclear.

In the previous chapter we found that *POLQ* knockdown did not alter the sensitivity of cells to temozolomide either with or without IR. Temozolomide is an orally administered alkylating agent that is routinely used in the management of glioblastomas (220). It has previously been shown that a significant proportion of the DNA damage caused by temozolomide is repaired by the BER pathway and that cells deficient in the key BER polymerase POLB have markedly increased sensitivity to temozolomide (221).

We interpret the finding that POLQ deficient cells are not rendered more sensitive to temozolomide to mean that the mechanism by which *POLQ* knockdown causes increased sensitivity to IR is independent of BER. However, it remains possible that POLQ could facilitate repair via BER of a lesion that is produced by IR but not by temozolomide.

Interaction between POLQ and ATM

The suggestion that POLQ may be involved in DNA damage repair prompted a research group to investigate the effects of producing mice with mutations in both ATM and POLQ. They found that double-homozygous mutations caused synthetic semi-lethality with an embryonic lethality rate of over 90% (243). Although the nature of the interaction is unclear, the authors suggested that POLQ may be involved in DSB repair. In view of the suggestion of a possible interaction between POLQ and ATM, a recent study looked at the effect of treating POLQ (-/-) mouse bone marrow stromal cells with an ATM inhibitor. They hypothesised that ATM kinase activity may be particularly important for survival of cells with POLQ deletion after irradiation, however, they found that ATM inhibition did not radiosensitise POLQ deficient cells any more than normal cells (276).

Expression of POLQ in normal tissues and in tumours

A previous study by Kawamura *et al* has assessed *POLQ* expression in a variety of different normal human tissues by RT-PCR (215). Interestingly, *POLQ* expression was primarily limited to lymphoid tissues such as the fetal liver, thymus and bone marrow. Other authors have suggested that the finding that POLQ is highly expressed in lymphoid tissues and in the germinal centres of B cells lends support to the notion that it plays a role in SHM (213).

Critical normal tissues such as lung, liver, small intestine, kidney, heart, brain and spinal cord that typically limit the radiation dose that can be delivered to patients do not appear to express *POLQ* (215). Intriguingly this study also found that *POLQ* was

overexpressed in a large proportion of tumours derived from patients with colon, lung and gastric cancer (215). It is therefore possible that POLQ inhibition could sensitise tumour cells to IR, but not alter the intrinsic sensitivity of these critical, normal tissues.

As discussed above, the physiological roles of POLQ are currently unclear, but the limited normal tissue expression in humans (215), and the finding that POLQ knockout mice are viable, and other than having elevated micronucleus formation are phenoytypically normal, (243) suggests that POLQ may not have an essential physiological role.

There have been no reported human syndromes resulting from germline mutations of POLQ. The only publication reporting a germline mutation of POLQ was published by a group investigating novel mutations of DNA repair genes in breast and pancreatic cancer (277). They identified a germline, truncating mutation (c.3605delT) of POLQ in a single breast cancer patient whose mother had also developed breast cancer. The single-nucleotide deletion caused a frameshift mutation that is expected to exclude the C-terminal resulting in loss of polymerase activity. The authors concluded that *POLQ* may therefore function as a tumor suppressor gene but acknowledged that larger genetic studies of breast cancer patients were required to confirm this (277). Unfortunately it was not possible to investigate the causal association between this germline mutation and the patient's cancer in any more detail as it was not possible to obtain tissue from the patient's mother. In addition loss of heterozygosity analysis of the mutation could not be conducted as the authors did not have enough remaining tumour tissue (277). It is therefore entirely

possible that this mutation may be coincidental, and that this SNP did not predispose the individual to developing breast cancer. There is no other data suggesting that *POLQ* mutations result in an increased predisposition to breast cancer or any other malignancy.

The previous chapter contained the results of a siRNA screen investigating the molecular determinants of tumour radiosensitivity. This work showed that POLQ knockdown rendered tumour cells significantly more sensitive to IR but had little or no effect on normal tissue cells. This radiosensitisation did not appear to be mediated by a reduction in BER efficiency. In this chapter, the clinical potential of POLQ inhibition is assessed further by examining the effect of POLQ knockdown by siRNA on cell sensitivity to cytotoxic agents. The ability of tumour cells depleted of POLQ to repair DSBs is also examined. Non-homologous end joining is assessed by analysing the kinetics of disappearance of γH2AX foci, and HR assessed by quantifying RAD51 foci formation following exposure to cytotoxic agents and by using a HR assay (185).

The results presented here show that POLQ knockdown results in tumour cell chemosensitisation to drugs such as topoisomerase inhibitors, anthracyclines, and platinum agents and that this occurs as a result of reduced homologous recombination. These findings provide further evidence that POLQ may be an appealing target for clinical exploitation.

4.3 Results

siRNA knockdown of POLQ. This work used three different tumour cell lines (HeLa, SQ20B, U2OS). A pool of 4 siRNAs was used to successfully knockdown *POLQ*. The transfection details are given in Chapter 2. As previously discussed, an effective POLQ antibody was not available, and knockdown was therefore quantified by qRT-PCR using the same technique as that used in Chapter 3. Successful *POLQ* knockdown is demonstrated for all three cell lines in Figure 4.2.

POLQ knockdown renders tumour cells more vulnerable to DNA damaging agents. In view of the previous evidence showing that POLQ knockdown causes radiosensitisation of tumour cells (Chapter 3), it was examined whether POLQ depletion caused increased tumour cell sensitivity to cytotoxic agents. Agents representative of several different classes of DNA damaging drugs were used. These included etoposide (a topoisomerase II inhibitor), doxorubicin (an anthracycline antibiotic and topoisomerase II inhibitor that generates free radicals), cisplatin and mitomycin C (DNA inter and intrastrand cross-linking agents).

Clonogenic assays were performed with HeLa cells depleted of POLQ. Cells were plated in single cell suspensions and allowed to settle prior to the addition of drug at the concentration and times stated. POLQ depletion rendered cells significantly more sensitive to all of the DNA damaging cytotoxic drugs tested, compared to cells transfected with NT siRNA (Fig. 4.3).

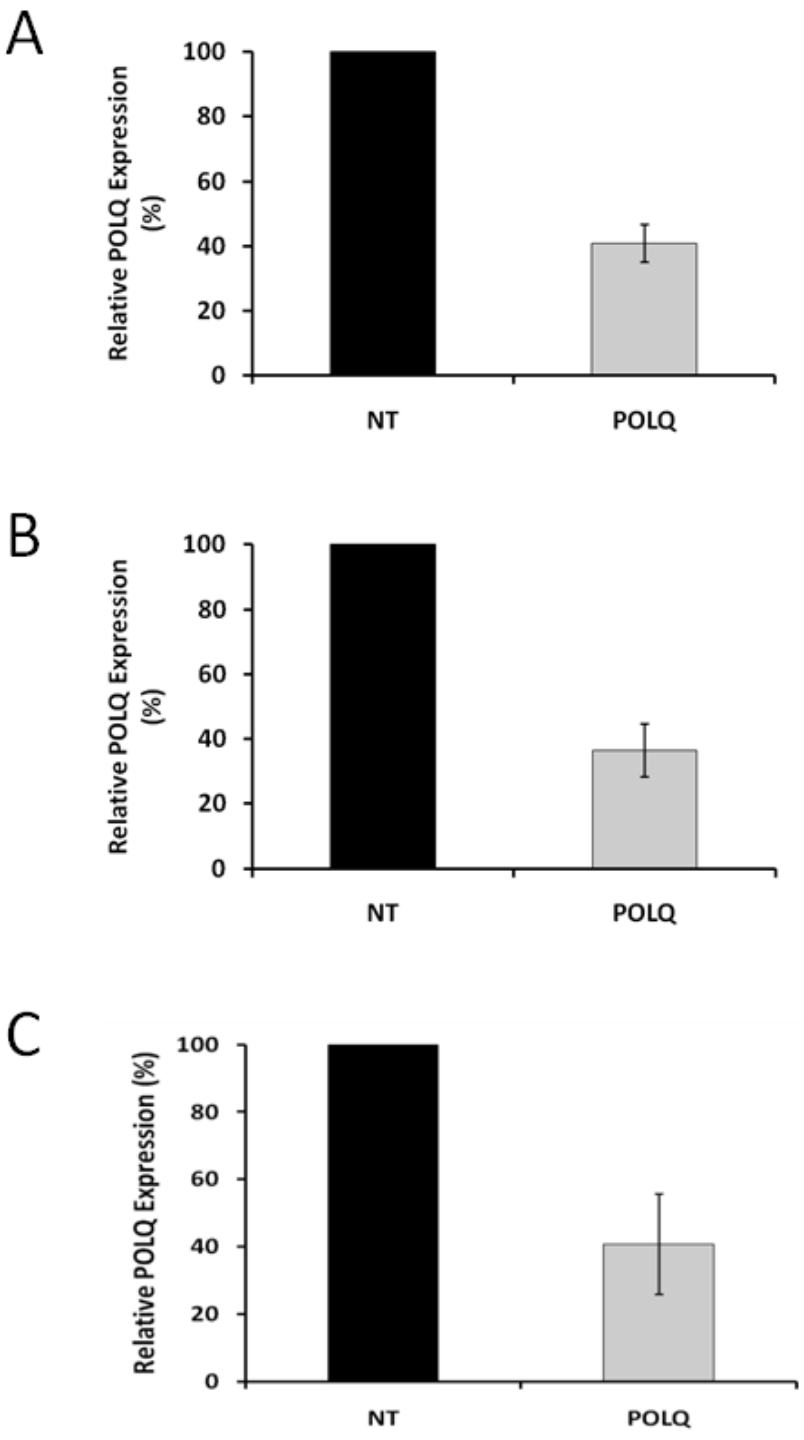

Figure 4.2. qRT-PCR showing successful knockdown of *POLQ*. A) HeLa, B) SQ20B and C) U2OS tumour cells 48h after siRNA transfection. *POLQ* expression normalised to cells transfected with a pool of 4 NT siRNAs. Mean and standard deviations shown from three separate q-RT-PCR reactions.

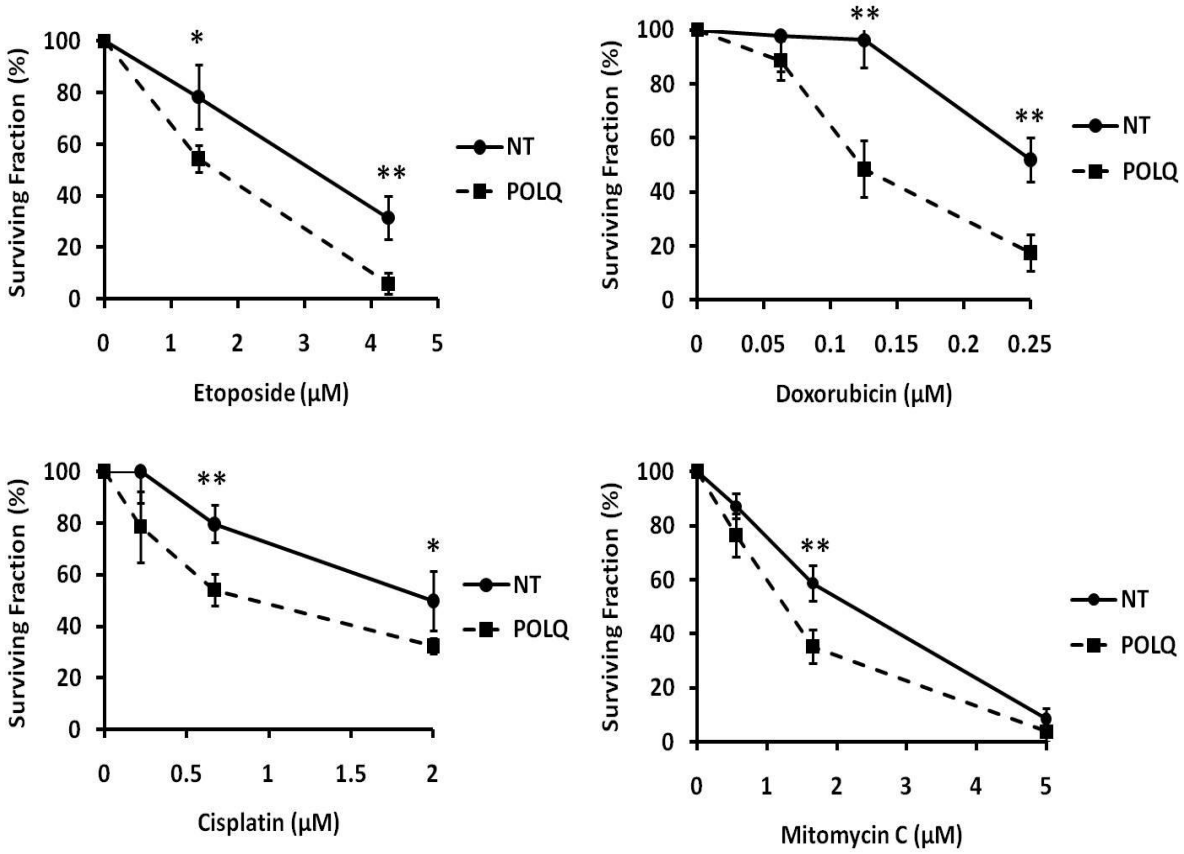

Figure 4.3. Colony forming assays showing chemosensitisation of HeLa cells depleted of POLQ. Surviving fractions after exposure to etopside (top left), doxorubicin (top right), cisplatin (bottom left), and mitomycin C (bottom right), for 1h at dose concentrations stated. *, $P < 0.05$, **, $P < 0.01$ unpaired two-sided t test.

Particularly pronounced chemosensitisation was observed following treatment with doxorubicin and etoposide. Etoposide induces DSBs as a result of its inhibition of topisomerase II (278), whilst doxorubicin induces DNA damage via a variety of mechanisms including free radical damage, topoisomerase II inhibition (279) and DNA adduct formation (280). It was therefore hypothesised that POLQ depletion induces chemosensitisation by preventing repair of DSBs and that POLQ depletion would not sensitise cells to cytotoxic agents that do not induce DNA damage.

Clonogenic survival assays were therefore conducted with HeLa cells exposed to docetaxel, since it is well recognised that this cytotoxic agent does not directly induce DNA damage, but induces cell death by hyperstabilising microtubules, and thereby inhibiting microtubular disassembly (281). As anticipated, it was found that cells depleted of POLQ were not rendered more sensitive to this mitotic spindle poison (Fig. 4.4). This supports the proposal that POLQ depletion induces chemosensitisation as a result of a reduction in DSB repair.

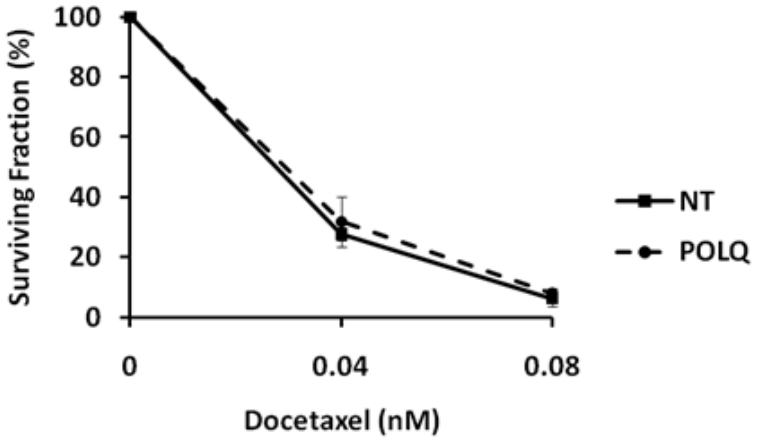

Figure 4.4. POLQ depletion does not sensitise HeLa cells to docetaxel after 24h exposure at dose concentrations stated.

POLQ depletion does not alter the cell cycle distribution of cells exposed to etoposide. HeLa cells transfected with either NT or POLQ siRNA were exposed to 4.25 μM etoposide for 1h. FACS analysis was performed on cells at multiple time points after drug exposure. Cells depleted of POLQ that have not been exposed to cytotoxic drugs do not have altered cell cycle distribution. This is consistent with the results obtained in unirradiated SQ20B cells previously described in Chapter 3 (Fig. 3.16). HeLa cells treated with etoposide underwent a significant G2 arrest; however,

this occurred with the same magnitude regardless of whether cells had been transfected with either NT or POLQ siRNA (Fig. 4.5)

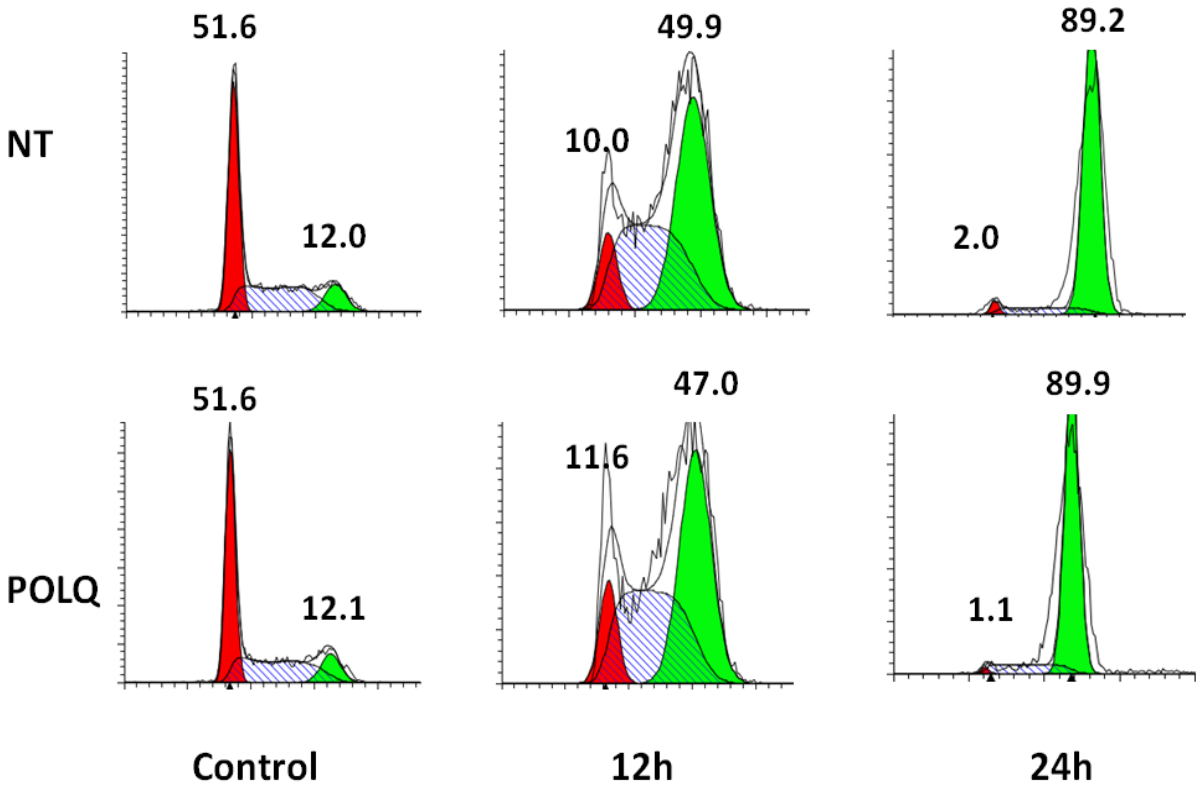

Figure 4.5. POLQ depletion does not alter cell cycle distribution. HeLa cells treated with either NT or POLQ siRNA were treated with 4.25 μM etoposide for 1h. Samples were harvested for flow cytometry following etoposide exposure at the time points indicated. No difference was observed in cell cycle distribution in untreated cells depleted of *POLQ* (left). Treatment with etoposide resulted in a large G2 arrest, but this occurred with the same magnitude regardless of siRNA treatment (middle and right). Numbers above G1 and G2-M peaks indicate the percentage of cells in each compartment.

γH2AX kinetics suggests that POLQ is not involved in NHEJ. Etoposide, doxorubicin and IR (161, 278, 282) produce DNA double strand breaks that are central to the ability of these agents to cause tumour cell death. The finding that POLQ knockdown renders cells more sensitive to these treatments, suggests that POLQ may enable tumour cells to repair DSBs more efficiently. We therefore

investigated the effect of POLQ knockdown on the two key processes by which DSBs are repaired: non-homologous end joining and homologous recombination (13).

It has previously been shown that the process of NHEJ repairs DSBs extremely quickly, whilst HR repairs DSBs over a longer time course (283). These differences mean that cells with defective NHEJ pathways show a higher number of residual γH2AX at early timepoints after exposure to IR (168, 284). In the previous chapter, it was shown in SQ20B cells that POLQ knockdown results in increased numbers of unresolved γH2AX foci 24h after exposure to ionising radiation. For this reason, SQ20B cells were again used to assess the time course of resolution of γH2AX foci. Cells were transfected with pools of NT, POLQ or DNA-PKcs siRNA. Forty-eight hours after transfection, SQ20B cells were treated with 4Gy and fixed at the time points indicated in Figure 4.6A. Cells with DNA-PKcs knockdown had higher numbers of γH2AX foci at the early time points after IR compared to cells treated with NT siRNA (Fig. 4.6A). This is the anticipated result for a gene that is involved in NHEJ (285). As shown in the previous chapter, POLQ depleted cells showed a higher proportion of cells with >7 γH2AX foci at twenty-four hours after IR compared with cells treated with NT siRNA (Fig. 4.6B). However, at early timepoints there were no significant differences between POLQ and NT siRNA treated cells. This suggests that POLQ is not directly involved with NHEJ (Fig. 4.6A), and points instead to a role in HR.

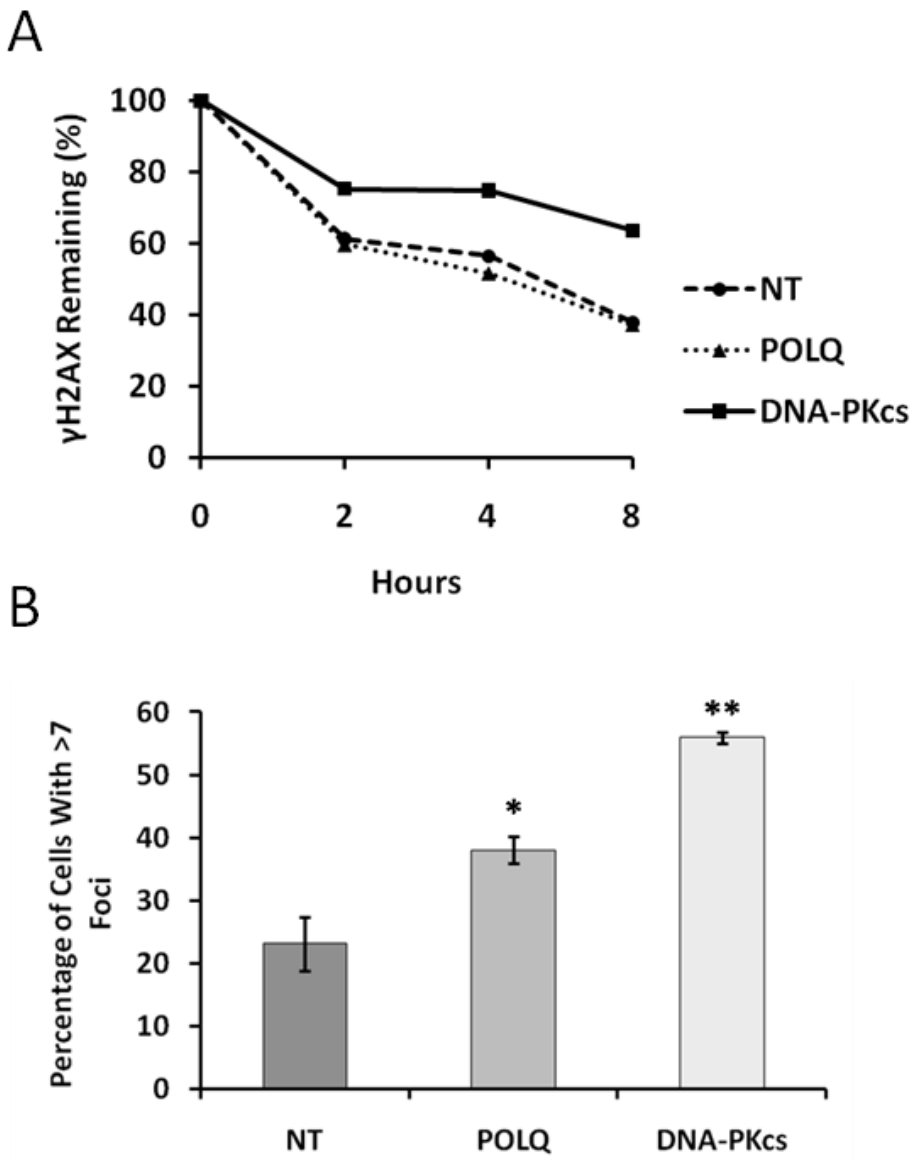

Figure 4.6. DNA double strand break repair kinetics post irradiation do not support a role for POLQ in NHEJ. A, SQ20B cells were transfected with NT, POLQ, or DNA-PKcs siRNA. Forty-eight hours after transfection, cells were treated with 4Gy and fixed at the time points indicated. POLQ knockdown does not result in an early increase in residual γH2AX foci; DNA-PKcs was used as a positive control. Mean foci number per cell relative to the number at 5 min after IR is shown. B, SQ20B cells fixed at 24h after treatment with 4Gy show differences in the proportion of cells with >7 γH2AX foci following POLQ knockdown. *, $P < 0.05$, **, $P < 0.01$ unpaired two-sided t test.

POLQ knockdown causes reduced HR activity. Two separate assays were conducted to assess whether the chemosensitisation of tumour cells depleted of POLQ occurs as a result of reduced HR. Firstly, RAD51 focus formation was measured after U2OS cells had been exposed to 1 μM of etoposide for 24h. RAD51 plays a central role in HR, and a reduction of RAD51 foci is indicative of impaired HR (286, 287). It was found that cells transfected with POLQ siRNA had significantly reduced levels of RAD51 foci after etoposide treatment compared to cells treated with NT siRNA (Fig. 4.7 A and B). This suggested that POLQ depletion resulted in a reduction in HR.

To assess whether POLQ depletion directly inhibits the process of homologous recombinational repair, an I-Sce-I assay was used to assess endogenous HR. This assay involves the use of cells expressing modified and truncated GFP cDNA that contains the I-Sce I restriction site. Transient expression of the I-Sce I endonuclease results in DSB formation, which, if repaired by HR using a linked donor GFP gene fragment as a template, restores functional GFP expression. This expression is then measured by flow cytometry. Transfection of U2OS cells with the I-Sce-I expressing plasmid treated with NT siRNA resulted in a HR frequency of 6.4%. This was reduced to 1.8% in cells transfected with POLQ siRNA ($p<0.01$) and indicates that HR activity is reduced following depletion of POLQ (Fig. 4.8).

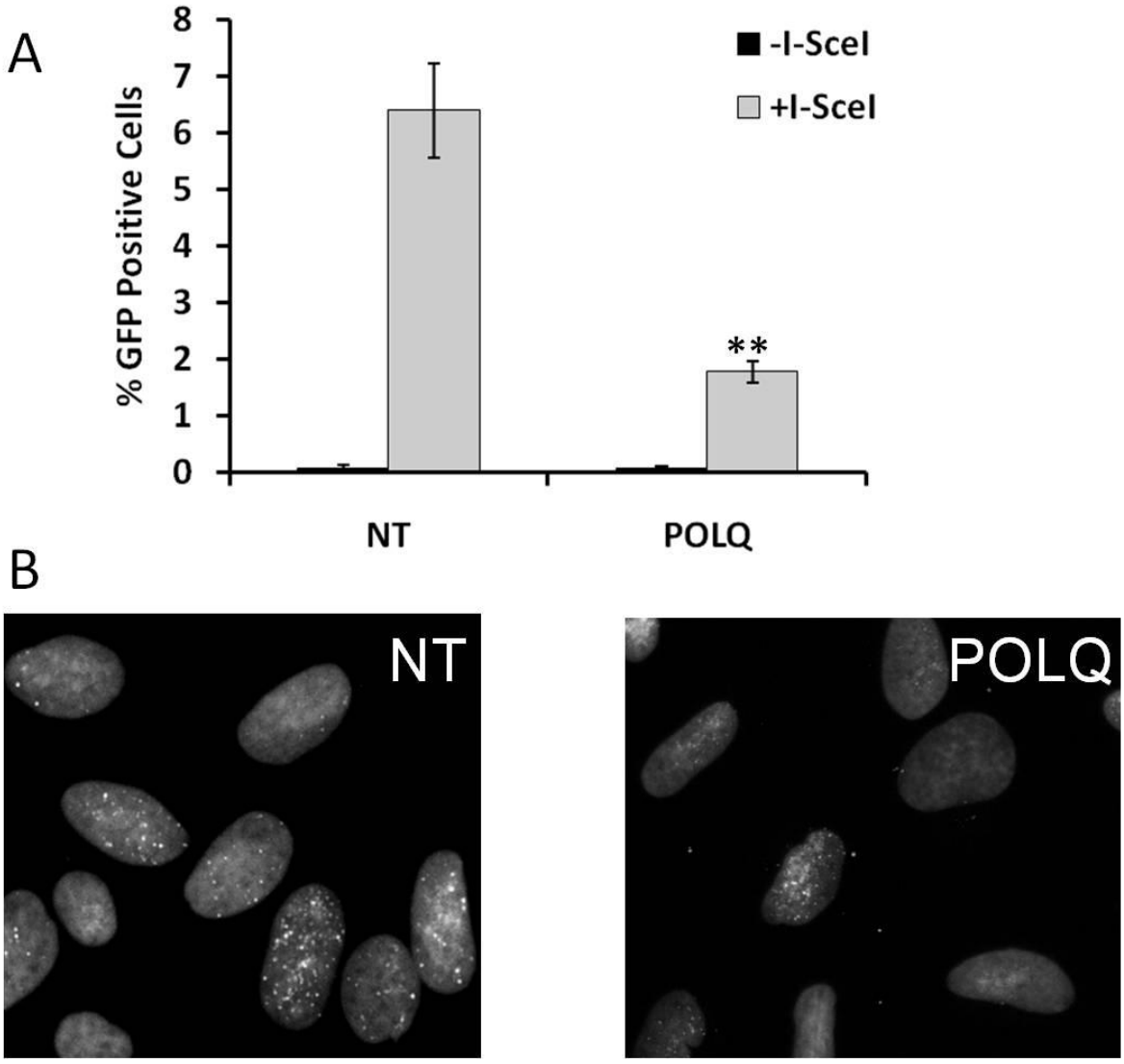

Figure 4.7. POLQ depletion results in reduced RAD51 Foci formation. A) U2OS cells were treated with 1 μM of etoposide for 24h. Nuclei with >9 foci were classified as RAD51 positive. Cells with POLQ knockdown show a significant reduction in RAD51 foci after etoposide treatment. Data points represent mean values, error bars the standard error of the mean. **, $P < 0.01$ unpaired two-sided t test. B) Representative images of U2OS cells after exposure to etoposide showing a decrease in RAD51 foci in cells depleted of POLQ.

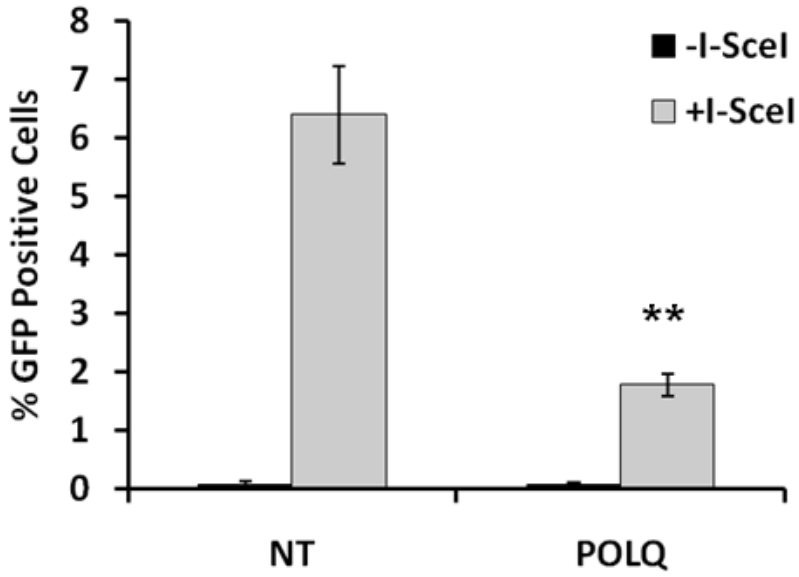

Figure 4.8. The I-Sce-I GFP assay shows POLQ depletion decreases the number of GFP expressing cells as a result of reduced HR. **, P < 0.01 unpaired two-sided t test.

4.4 Discussion

The previous chapter contained the results of a siRNA screen to identify novel genes involved in tumour radiosensitivity. This work showed that tumour cells depleted of POLQ were rendered significantly more sensitive to IR (288). The data shown in this chapter demonstrates that POLQ depletion also renders tumour cells more sensitive to several different classes of DNA damaging agents. Particularly pronounced sensitisation effects were seen after cells were exposed to etoposide and doxorubicin. DNA double strand break formation is the key cytotoxic insult induced by ionising radiation and several chemotherapy agents (161, 278, 282). The suspicion that POLQ depletion reduced DSB repair efficiency was supported by the finding that POLQ depleted cells are not sensitised to a non-DSB inducing chemotherapy (Fig. 4.4).

The kinetics of γH2AX foci resolution following exposure to etoposide provides indirect evidence that POLQ is not involved in NHEJ (Fig. 4.6), whilst analysis of RAD51 foci formation post-etoposide suggests it is involved in HR (Fig. 4.7). The I-Sce-I GFP assay (Fig. 4.8) supported the hypothesis that the mechanism by which POLQ depletion induces chemo and radiosensitisation arises from a reduction in homologous recombination.

Homologous recombination is a vital repair mechanism that allows for error-free repair of double strand breaks (289, 290). It has been shown previously that POLQ knockout mice are viable, and other than having elevated micronucleus formation are phenoytypically normal (243). This, combined with the limited normal tissue expression of POLQ (215), suggests that POLQ is not an essential component of HR.

To the best of my knowledge this is the first study to demonstrate chemosensitisation of tumour cells depleted of POLQ. However it is interesting to note that studies on different species have previously examined the role of POLQ homologues in DNA damage repair. In *Drosophila,* the *mus308* gene is a homolog of *POLQ*. Flies with homozygous mutant *mus308* are hypersensitive to several different crosslinking agents including cisplatin (240). Microhomology-mediated end joining (MMEJ) is a recently identified, error-prone mechanism by which DSBs can be rejoined, and appears to be distinct from the classical HR and NHEJ pathways. The main feature of MMEJ is that 5-25 bp microhomologous sequences are used during the alignment of the broken ends prior to joining, thereby resulting in deletions flanking the original

break (291). Very recent work has suggested that mutant *mus308* induces increased sensitivity through a reduction in MMEJ with the authors concluding that POLQ is not involved in HR (292, 293). Although the data presented in this chapter shows that human POLQ is involved in HR, further investigation into the role of human POLQ in MMEJ is warranted.

Work conducted in *C. elegans* has also suggested that POLQ plays a role in repair of damage induced by inter-strand cross linking agents such as cisplatin (249). However it should be noted that following exposure to a crosslinking agent, these researchers found that cells with *polq-1* mutation had an initial increase in RAD51 foci but that the kinetics of foci resolution were the same as in *wt* cells. The authors therefore concluded that POLQ was not involved in HR. Separate studies in cell lines derived from other species have shown that disruption of POLQ does not alter cell sensitivity to cytotoxic agents. Work conducted in CH12 mouse B lymphoma cells (294) and DT40 chicken lymphoma cells (222) found that disruption of POLQ did not result in increased sensitivity to either IR or cytotoxic drugs such as cisplatin. These inconsistent findings could suggest that POLQ functions differently in different species.

The evidence presented in this chapter lends support to the theory that POLQ may be an attractive target for clinical manipulation by inducing tumour cell radio and chemosensitisation. It is conceivable that tumour overexpression of POLQ may result in increased HR efficiency, thereby conferring tumour cell resistance to

treatment with radio or chemotherapy and therefore conferring a poor prognosis. This will be examined in the next chapter.

Chapter 5

POLQ OVEREXPRESSION CONFERS A POOR PROGNOSIS IN PATIENTS WITH EARLY BREAST CANCER

5.1 Abstract

As shown in the previous two chapters, depletion of POLQ renders tumour cells more sensitive to radiotherapy and several different classes of chemotherapy due to a reduction in the efficiency of homologous recombination. In view of these findings, it was investigated whether tumours that overexpress *POLQ* are associated with an adverse outcome. The clinical outcomes of two retrospective series of patients with early breast cancer were correlated with the expression levels of *POLQ*, as determined by microarray gene expression analysis. It was found that a significant number of tumours overexpressed *POLQ,* and that overexpression was correlated with ER negative disease (p=0.047) and high tumour grade (p=0.004), both of which are associated with poor clinical outcomes. *POLQ* overexpression was associated with poor relapse free survival rates on both univariate (HR 5.80; 95% CI, 2.220 to 15.159; p<0.001) and multivariate analysis (HR 8.086; 95% CI 2.340 to 27.948 p=0.001). Analysis of other published clinical series confirmed that *POLQ* overexpression is associated with adverse clinical outcomes. The poor prognosis associated with *POLQ* is independent of other clinical or pathological features. The mechanism that causes this adverse outcome remains to be elucidated but may in part arise from resistance to adjuvant treatment. These findings, combined with the limited normal tissue expression of POLQ, make it an appealing target for possible clinical exploitation.

5.2 Introduction

Pathologists routinely estimate the prognosis of patients with early breast cancer on the basis of classification systems such as the Nottingham prognostic index (295). These systems use pathological features such as tumour size, grade, lymph node involvement and lymphovascular invasion to assess the risk of an individual developing recurrent disease, and are routinely used to make decisions regarding the adjuvant treatment offered to patients (296). Additional pathological features used to assess prognosis include the oestrogen receptor (ER) and HER2 receptor status, which are also used to determine the need for adjuvant endocrine or trastuzumab therapy respectively (297-301). Recently, gene-expression profiling has been used to develop genomic tests that may provide better predictions of clinical outcome than the traditional clinical and pathological standards used. In breast cancer, gene expression signatures may enable more accurate and sophisticated decisions to be made about adjuvant treatment. Expression profiling may make it possible to identify the drugs that an individual will derive most benefit from. Additionally, expression signatures may be better able to identify those patients with low risk of recurrent disease who do not require systemic therapy. Such patients can therefore avoid the side effects associated with potentially unnecessary treatment. In 2007, the American Society of Clinical Oncology guidelines for the use of tumour markers in breast cancer stated that the evidence supporting a commercially available gene expression assay (Oncotype Dx) was sufficiently strong to support its use in deciding which patients should receive adjuvant chemotherapy (302). Gene expression profiles have been developed for many different clinical scenarios. Profiles have been used to predict the outcomes of patients with non-small cell lung cancer (303), head and neck cancer (304, 305), and colon cancer (306). In addition,

profiles have been created to predict tumour cell radiosensitivity (307) and tumour hypoxia (308).

In view of the *in vitro* data that POLQ depletion sensitises tumour cells to radiotherapy, and to several different chemotherapy agents, it was hypothesised that patients whose tumours overexpress POLQ may be resistant to adjuvant treatment and that they may therefore have an adverse prognosis. The clinical significance of tumour expression levels of *POLQ* has not previously been examined in detail. We therefore correlated the clinical outcomes of two series of breast cancer patients (n=279 in total) with the expression levels of *POLQ* as determined by microarray gene expression analysis. We also analysed the pathways associated with *POLQ* expression *in vivo* by data-mining gene expression data from published breast cancer studies (n=1015 samples). Although *POLQ* overexpression has previously been demonstrated in lung, gastric, and colorectal cancers (215), this is the first study to demonstrate that *POLQ* is overexpressed in breast cancer. This is also the first study to provide evidence that *POLQ* overexpression confers a significant adverse prognosis, and that it is associated with key cancer pathways.

5.3 Results

We identified two retrospective series of patients with early primary breast cancer who were treated in Oxford, UK, between 1989 and 1998. Series 1 contained 152 patients (187), and Series 2 contained 127 patients (188). Both series are part of previously published studies. Patient details are given in Chapter 2 (Section 2.10) and in the Appendix (Supplementary Table 2A and B). In addition, we identified two datasets (GSE3494 and GSE2034) that we used to validate the results obtained

from the two Oxford series. GSE3494 is a heterogenous dataset that comprises samples from 251 patients with early breast cancer (192). The GSE2034 dataset comprises 286 samples from patients with confirmed node negative early breast cancer (193).

***POLQ* is overexpressed in breast cancer compared to normal breast tissue.** In order to assess *POLQ* expression, we identified two independent gene expression datasets that were obtained using arrays from different manufacturers: Affymetrix and Illumina arrays for series 1 and 2 respectively. *POLQ* expression was normalised to the lowest level of tumour expression in the Affymetrix series, and to a panel of normal breast tissue samples for the Illumina series. *POLQ* was shown to be upregulated in a large proportion of breast tumour samples from both series (Fig. 5.1).

***POLQ* overexpression is independently associated with significantly worse relapse free survival (RFS) rates.** In order to assess whether POLQ expression is associated with an adverse outcome we initially performed a simple analysis on the data from Series 1. The samples from Series 1 were divided into the top and bottom 50^{th} centiles and a univariate analysis of the differences in RFS was conducted (Fig. 5.2). We found that on univariate analysis, *POLQ* overexpression was associated with a markedly increased risk of disease relapse (HR 5.80; 95% CI, 2.220 to 15.159; $p<0.001$).

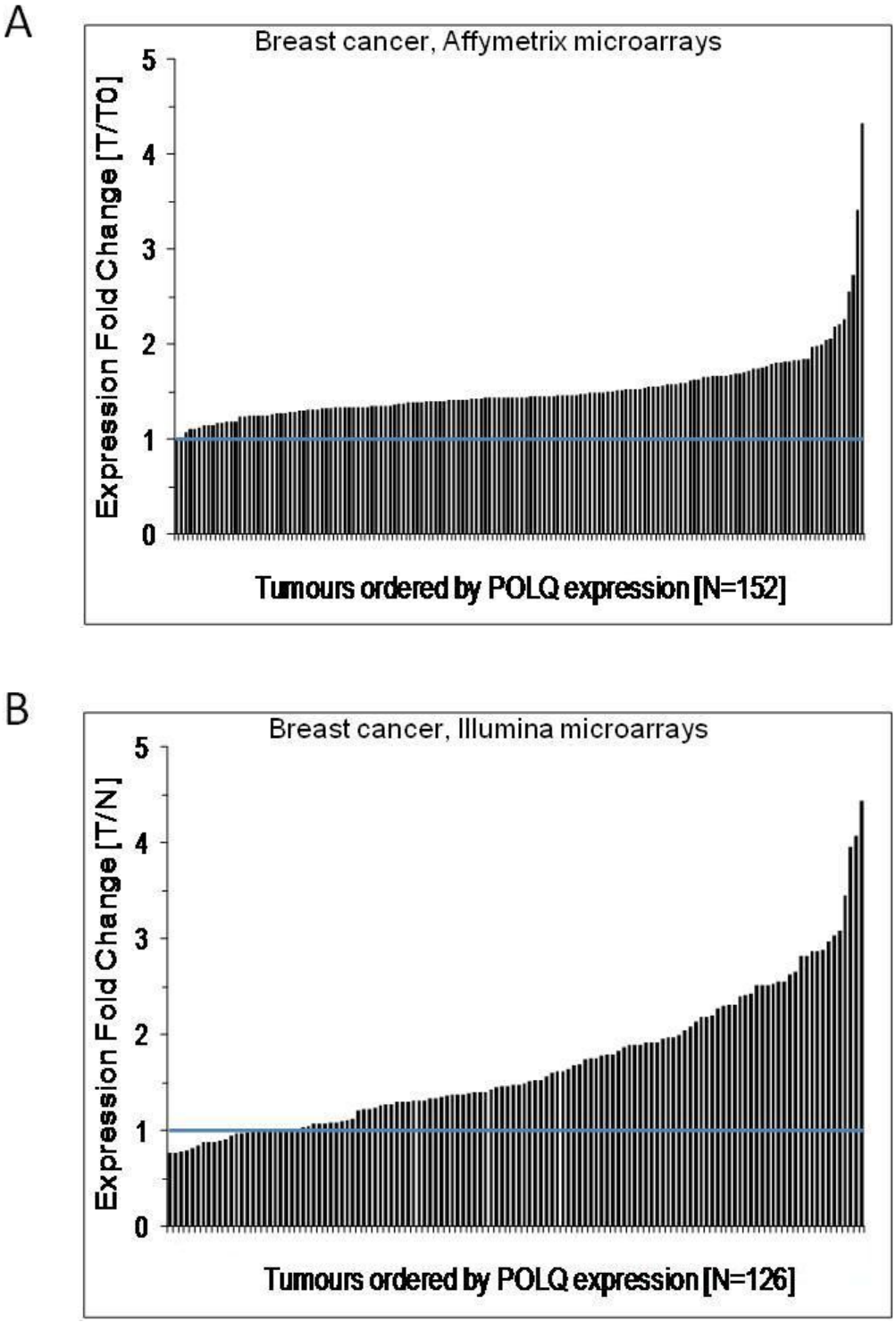

Figure 5.1. *POLQ* expression in breast cancer. A) Breast cancer samples, Series 1, described in this study (N=152). No normal breast tissue samples were available for Series 1 so *POLQ* data were normalised to the sample with the lowest expression of *POLQ* (named T0). Expression fold change (FC) between all other tumours and T0 is shown for *POLQ* (207746_at). B) Breast cancer samples, Series 2, described in this study (N=127). The FC between *POLQ* (ILMN_1450687) expression in each tumour and the median expression of 10 normal pools is shown.

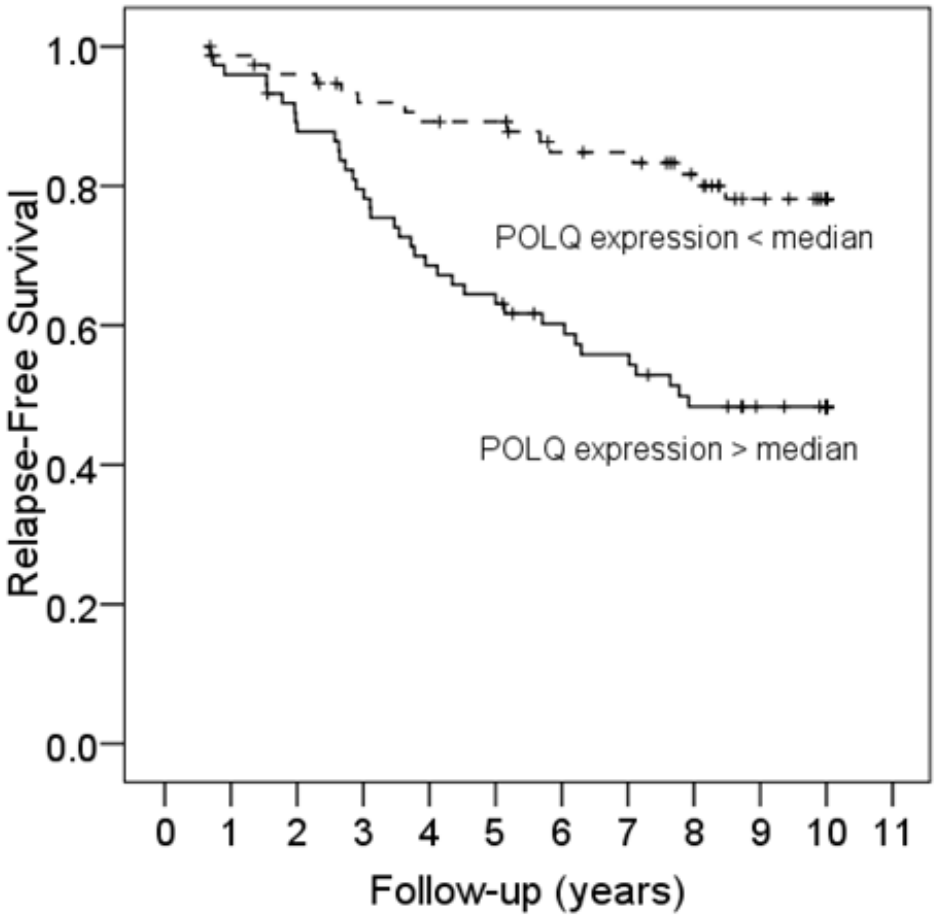

Figure 5.2. Univariate analysis on data obtained from Series 1 showing POLQ expression is associated with a significantly increased risk of disease relapse.

The level of *POLQ* expression was then correlated with multiple pathological and demographic features such as patient age, tumour grade and tumour size using data from Series 1, Series 2, GSE3494 and GSE2034. It was found that *POLQ* overexpression strongly correlated with both ER negative disease (Fig. 5.3) and high tumour grade (Fig. 5.4). Both of these features are recognised as being associated with poor clinical outcomes (300, 301, 309).

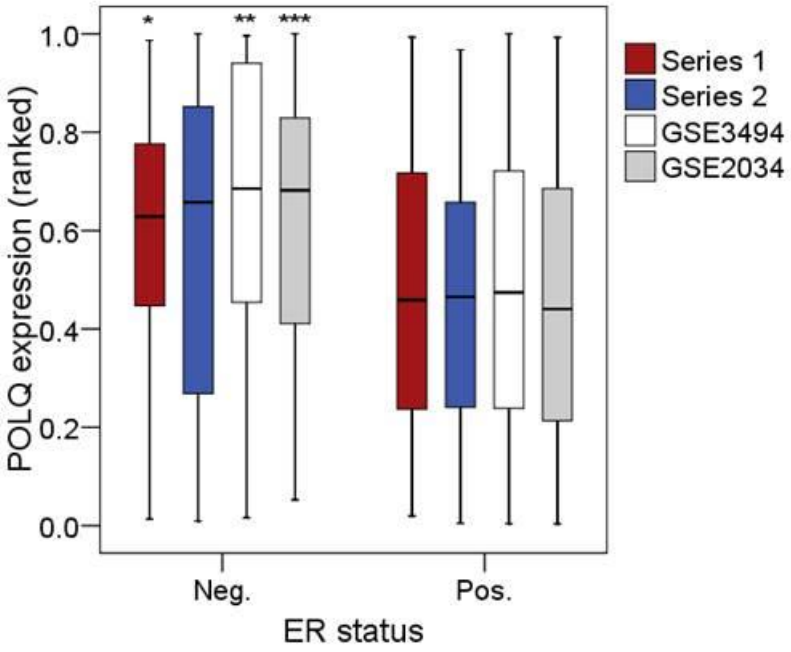

Figure 5.3. *POLQ* expression is correlated with ER status. Association with ER status in Series 1 and 2 and two separate published series. Boxes summarise the median, quartiles and extreme values of *POLQ* expression. Mann-Whitney test for the null hypothesis of *POLQ* not varying with ER *=p<0.05, **=p<0.01, ***=p<0.001.

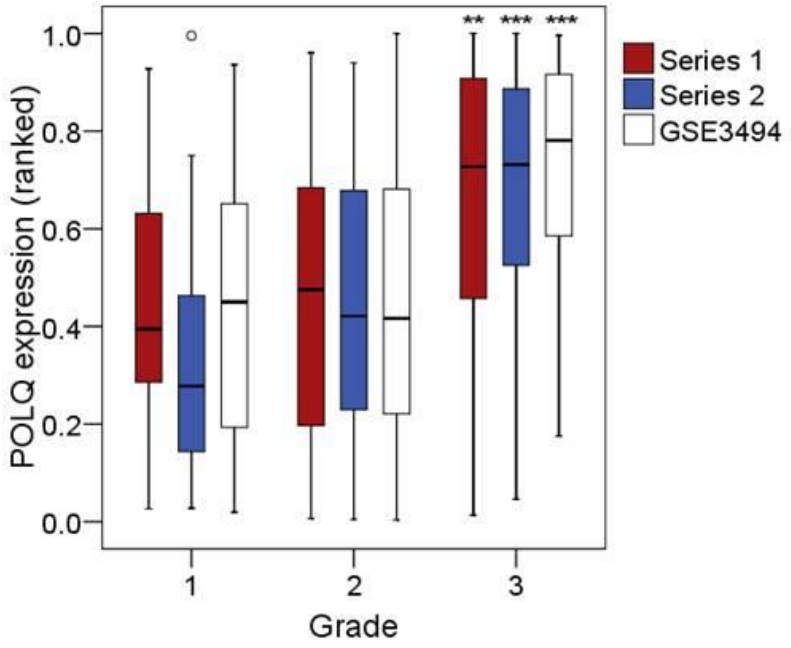

Figure 5.4. *POLQ* expression is correlated with high tumour grade in Series 1, Series 2 and GSE3494; grade information was not available for GSE2034. One outlier is shown (defined as case with values between 1.5-3 box lengths from the edge of the box). Spearman Rank Association significance levels for the null hypothesis of *POLQ* expression not varying with grade **=p<0.01, ***=p<0.001.

In view of this, it was possible that the previous univariate analysis showing that *POLQ* expression conferred a poor prognosis may simply reflect the association between *POLQ* expression, and high grade, ER negative disease. To assess this in more detail a multivariate analysis was performed that included all clinico-pathological details (ER status, lymph node status, patient age, tumour grade, tumour size). Multivariate analysis is a robust statistical tool that involves analysing more than one statistical variable at a time. It is frequently used when data includes several, potentially dependent variables, and is used to assess the effects of a given variable independently of all others. The multivariate analysis performed on data from Series 1 showed that *POLQ* expression confers a poor prognosis which is independent of any other clinical feature (HR 8.086; 95% CI 2.340 to 27.948; p=0.001).

Having performed a multivariate analysis on the data from Series 1, it was decided to validate the finding that *POLQ* expression confers an adverse prognosis by performing univariate and multivariate analyses on Series 2 and the two additional datasets previously described. The results of the multivariate analyses are shown in detail in the Appendix (Supplementary Table 5) and summarised in a Forest plot in Figure 5.5. In total, three out of the four datasets analysed demonstrated that *POLQ* overexpression was strongly associated with significantly worse survival outcomes (Fig. 5.5). The remaining dataset (GSE3494) showed a trend for *POLQ* to be associated with poor prognosis but this did not quite reach statistical significance (HR 2.239; 95% CI 5.712 to 0.877).

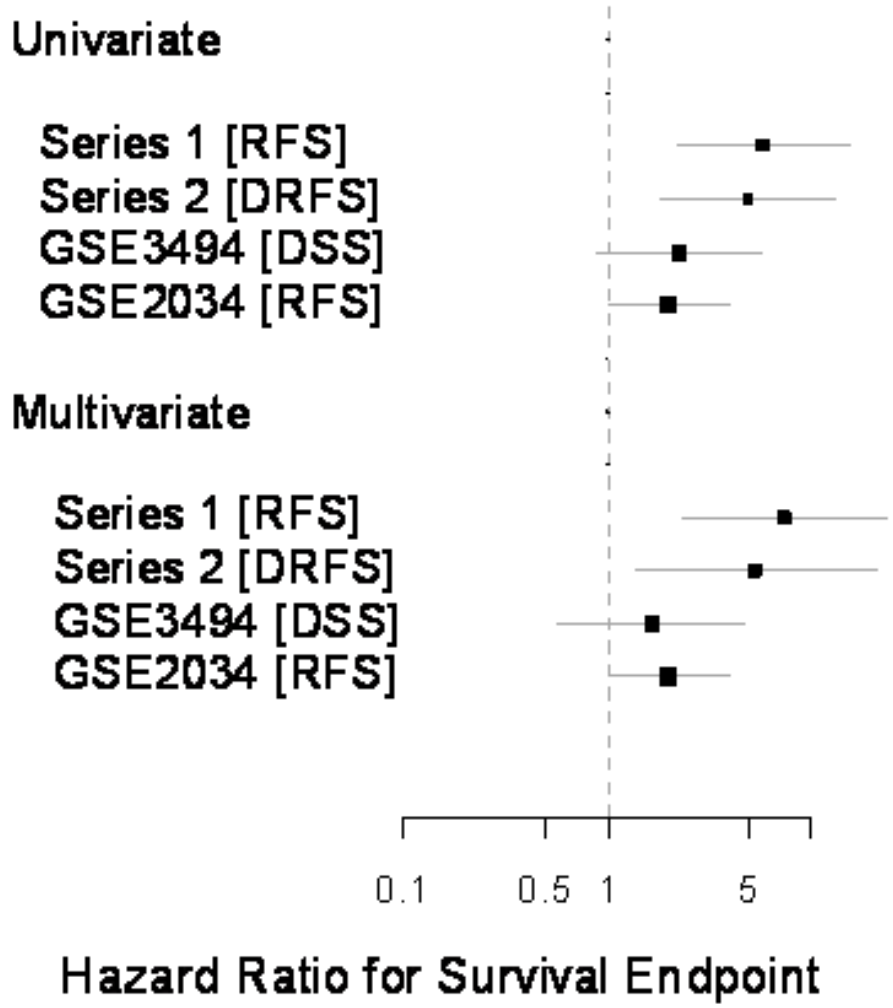

Figure 5.5. Forest plot summarising the results of the univariate and multivariate analyses performed on all four datasets. *POLQ* expression was strongly associated with adverse prognosis in three of the four datasets studied.

Clustering analysis identifies genes co-expressed with *POLQ* with functions in key cancer pathways. In order to identify genes which were co-expressed with *POLQ*, a seed-clustering analysis was performed on gene expression data obtained from five different breast cancer data sets (n=1015, details of datasets in Appendix. Supplementary Table 4). This identified a total of 97 genes that were strongly associated with *POLQ* overexpression in breast cancer (Appendix. Supplementary Table 6). Pathway analysis of these genes showed that genes co-expressed with *POLQ* are involved in several pathways that have been associated with cancer

development and progression such as cell cycle regulation, p53 signalling, Wnt signalling and DNA replication (Fig. 5.6A and B).

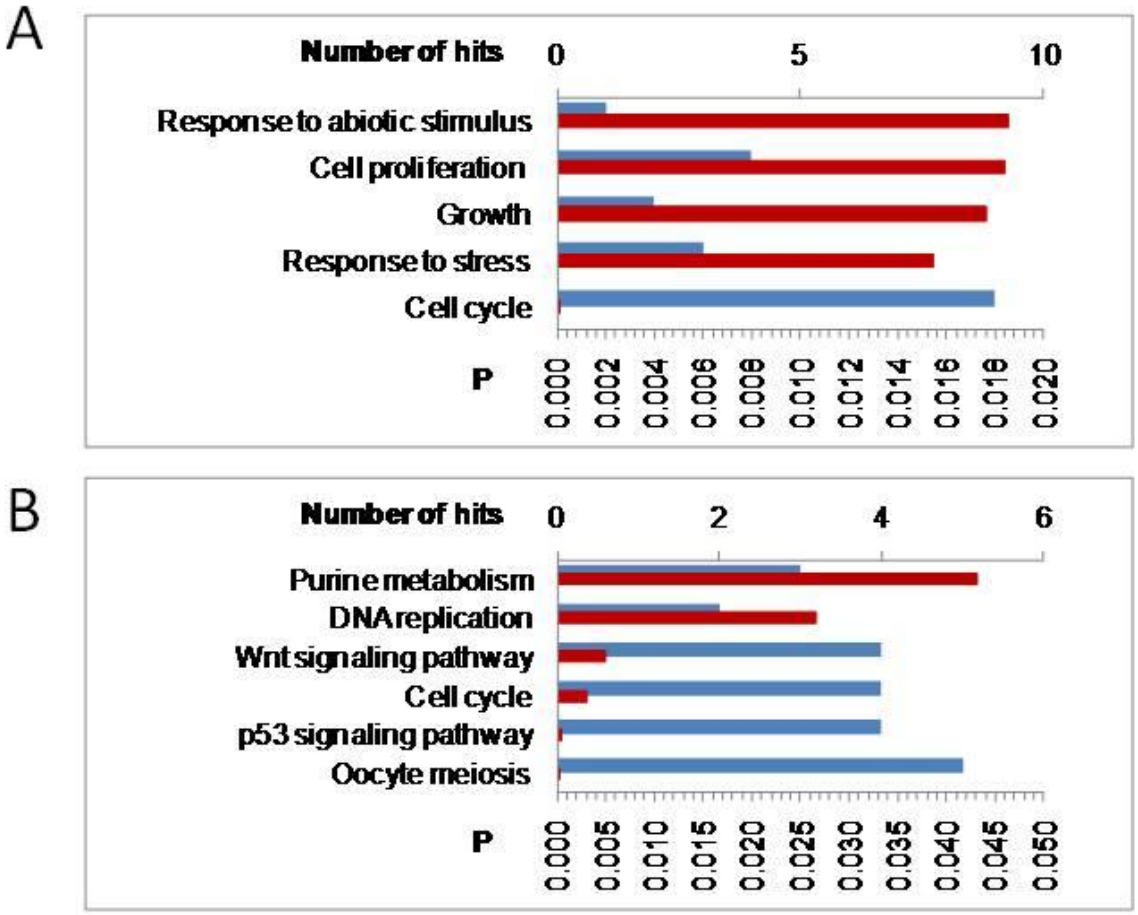

Figure 5.6. Pathway analysis of *POLQ* co-expressed genes. Seed-clustering was used in 1015 breast cancer samples to identify genes whose expression was co- and inversely associated with *POLQ* expression. A) Over-represented KEGG pathways and B) GO Biological processes amongst genes co-expressed with *POLQ*. The number of genes in each pathway is shown in blue, top x-axis, and a hypergeometric test p-value (FDR adjustment for multiple testing) is shown in red, bottom axis.

Genes co-expressed with *POLQ* overlap with several genes that comprise the Gene expression Grade Index (GGI). As discussed in the introduction to this chapter, several studies have previously identified gene expression signatures that predict clinical outcome of patients with breast cancer. The genes co- and inversely

expressed with *POLQ* were examined to see whether there was overlap with genes that comprise the '70-gene' signature, the '76-gene' signature, and the GGI.

The '70-gene' signature is a gene expression profile that predicts the prognosis for patients with early breast cancer and was first described in 2002 (310). It has subsequently been validated as being a reliable predictor of clinical outcome regardless of patient's lymph node or ER status (311). Recently, patients defined by the 70 gene signature as being at high risk of developing disease recurrence have been shown to benefit from the addition of adjuvant chemotherapy (312).

The '76-gene' signature was identified as being able to assess the risk of distant metastases developing in patients with early, lymph node negative breast cancer (193). This study used tumours derived from patients who did not receive adjuvant systemic therapy, thereby eliminating potentially confounding predictive factors occurring as a result of systemic treatment. The resulting '76 gene' signature was shown to predict both distant failure as well as overall survival. Further studies have reinforced the prognostic accuracy of this gene signature (313, 314).

The histological grade of breast cancer is typically graded from 1-3 and provides important prognostic information that determines whether adjuvant chemotherapy should be offered to patients (309). However between 30-60% of tumours are classified as 'grade 2', which is of limited use in decision making since it implies an intermediate risk of recurrence. The GGI (315) was established to see whether a gene expression signature could better assess the risk of those patients with 'grade 2' disease. The signature was based on differential expression of 97 genes between

low and high grade breast carcinomas. This signature was then shown to give a more accurate and refined assessment of the risk of disease recurrence in patients with intermediate grade disease. Subsequent studies have confirmed the ability of the GGI signature to accurately predict disease relapse (186, 316).

Although *POLQ* expression has not previously been shown to be independently associated with clinical outcome, it is interesting to note that *POLQ* is included in both the GGI (315), and the '76-gene' signature (193). The correlation between *POLQ* expression, with tumour grade and prognosis (Fig. 5.3 and 5.4) led us to assess whether genes that are co-expressed with *POLQ* are included in these validated gene expression signatures. The overlap is shown in a Venn diagram (Fig. 5.7) illustrating the number of genes that overlap between altered POLQ expression and each of the gene expression profiles.

Eighteen of the genes significantly co-expressed with *POLQ* (Appendix. Supplementary Table 6) are components of the GGI index (Fig. 5.7). These genes are listed in Table 5.1. The large number of genes that overlap between these two groups may account for the clinical correlation between *POLQ* expression and high tumour grade.

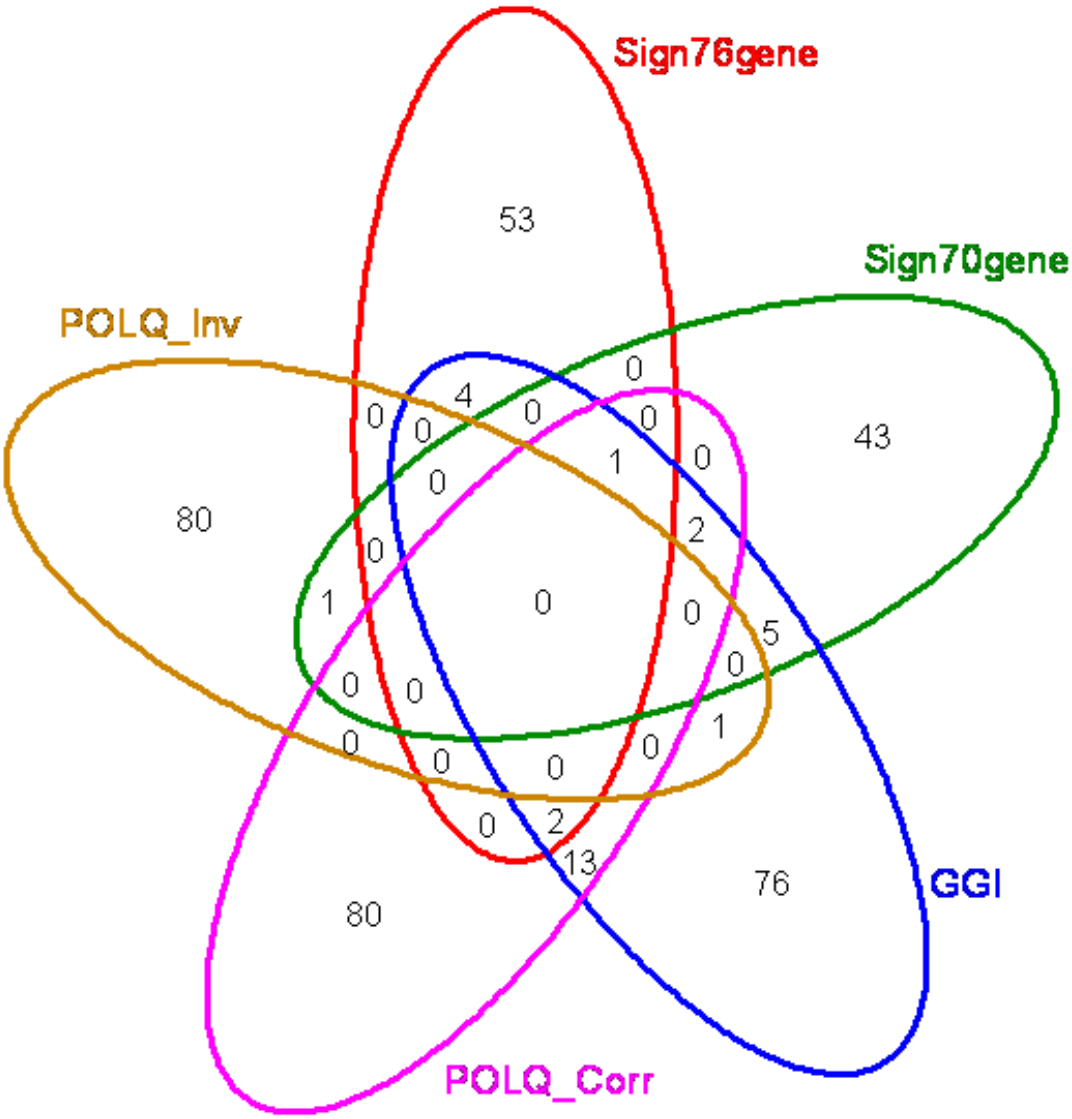

Figure 5.7. Venn diagram showing the overlap of genes whose expression is co-(POLQ_Corr) and inversely (POLQ_Inv) associated with expression of *POLQ* with the Gene expression Grade Index Signature (GGI) (315), the 76-gene signature (Sign76gene) (193), and the 70-genes signature (Sign70genes) (310). Eighteen genes found to be co-expressed with *POLQ* were found to be components of the GGI expression signature.

Symbol	GGI grade[s]	Accession Number	Gene ID	Full name/description
Transcripts co-expressed with POLQ				
AURKA	G_3	NM_003158	6790	aurora kinase A
CCNB2	G_3	NM_004701	9133	cyclin B2
CCNE2	G_3	NM_004702	9134	cyclin E2
CDKN3	G_3	AF213033	1033	cyclin-dependent kinase inhibitor 3 (CDK2-associated dual specificity phosphatase)
CEP55	G_3	NM_018131	55165	centrosomal protein 55kDa
ESPL1	G_3	NM_012291	9700	extra spindle pole bodies homolog 1 (S. cerevisiae)
ESPL1	G_3	D79987	9700	extra spindle pole bodies homolog 1 (S. cerevisiae)
GTSE1	G_3	NM_016426	51512	G-2 and S-phase expressed 1
KIFC1	G_3	BC000712	3833	kinesin family member C1
LMNB1	G_3	NM_005573	4001	lamin B1
MCM2	G_3	NM_004526	4171	MCM2 minichromosome maintenance deficient 2, mitotin (S. cerevisiae)
MELK	G_3	NM_014791	9833	maternal embryonic leucine zipper kinase
MYBL2	G_3	NM_002466	4605	v-myb myeloblastosis viral oncogene homolog (avian)-like 2
NA	G_3	BE966236	NA	NA
NCAPG	G_3	NM_022346	64151	non-SMC condensin I complex, subunit G
POLQ	G_3	NM_006596	10721	polymerase (DNA directed), theta
PRC1	G_3	NM_003981	9055	protein regulator of cytokinesis 1
RRM2	G_3	BC001886	6241	ribonucleotide reductase M2 polypeptide
TIMELESS	G_3	NM_003920	8914	timeless homolog (Drosophila)
TRIP13	G_3	NM_004237	9319	thyroid hormone receptor interactor 13
Transcripts whose expression is inversely associated with POLQ expression				
CX3CR	G_1	U20350	1524	chemokine (C-X3-C motif) receptor 1

[s] G_1 and G_3 are the sets of genes with increased expression in histologic grade 1 and 3 tumours, respectively.

Table 5.1. Overlap between the Genomic Grade Index (GGI) signature (315) and transcripts co- or inversely associated with POLQ in seed-clustering of 1015 breast cancer samples.

***POLQ* overexpresssion confers a poor prognosis that is independent of published prognostic signatures.** As *POLQ* has several genes in common with the GGI signature, and is itself part of the GGI and '76 gene' signatures, it was assessed whether *POLQ* expression remained an independent predictor of relapse when these signatures were included in a multivariate analysis. It was decided to perform these multivariate analyses with the data from Series 1, since these patients had not received adjuvant chemotherapy. This meant that the data was not subject to confounding alterations in prognosis due to the effects of systemic treatment. It was found that *POLQ* expression remained a strong, independent predictor of disease relapse after statistical consideration of these validated expression profiles. The results of the multivariate analysis are shown in the Appendix (Supplementary Table 7) and summarised as a Forest plot in Figure 5.8. When the multivariate analysis included the '76 gene' signature and the '70 gene' signature, the effect of *POLQ* remained strongly significant (HR 4.46; 95% CI 1.40 to 14.22; p=0.012 and HR 5.80; 95% CI 1.32 to 25.53; p=0.002 respectively). When the GGI signature was included in the multivariate analysis, the effect of *POLQ* did not quite reach significance (HR 3.28; 95% CI 0.95 to 11.26; p=0.059). It is possible that the significant overlap between the genes co-expressed with *POLQ* overexpression and those contained within the GGI signature, meant that when the GGI was included in the multivariate analysis, *POLQ* was no longer independently associated with a poor outcome. This is reinforced by the finding that in the multivariate analysis which included both *POLQ* expression and the GGI, the GGI was also no longer independently predictive of poor outcome (HR 1.28; 95% CI 0.98 to 1.68; p=0.0733). The data is summarised in the Forest plot in Figure 5.8.

The poor prognosis associated with *POLQ* expression is independent of Cyclin E expression. *CCNE2* (cyclin E) is the only gene that is a component of all three expression signatures and which is also co-expressed with *POLQ*. As cyclin E overexpression has been identified as being independently associated with an adverse outcome in breast cancer patients (317), it was considered whether the adverse prognosis associated with *POLQ* expression may simply be due to the observation that *CCNE2* is often co-expressed with *POLQ*. A multivariate analysis that included *CCNE2* expression was performed on the data from Series 1. It was found that *POLQ* (HR 4.50; 95% CI 1.14 to 17.74; p=0.031) and *CCNE2* (HR 5.48; 95% CI 1.29 to 23.38; p=0.021) were both independently associated with an increase in RFS. The analysis is summarised in a Forest plot in Figure 5.8.

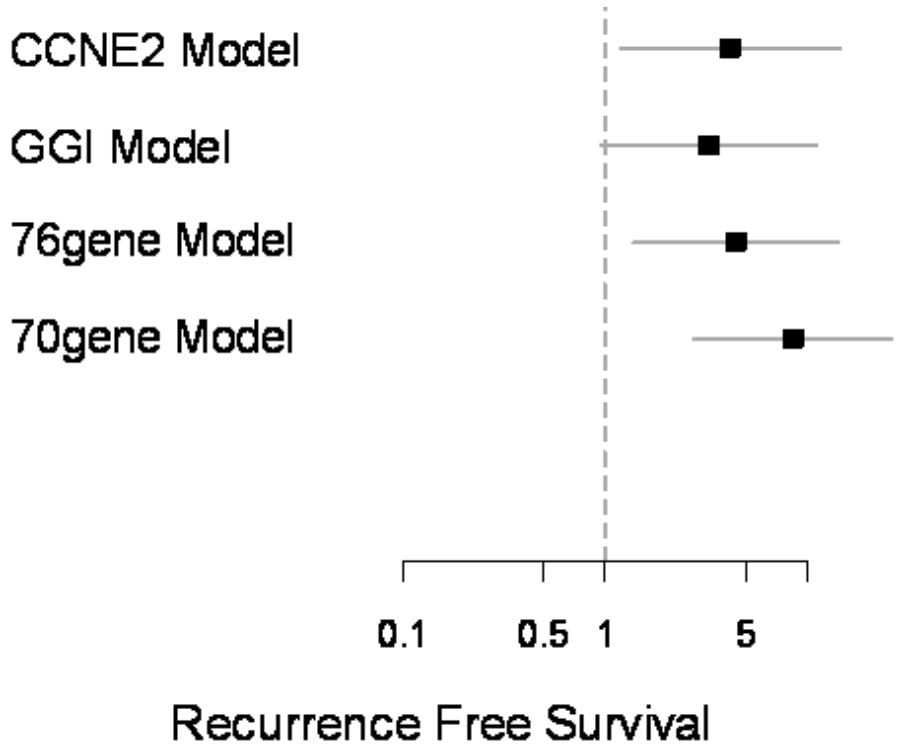

Figure 5.8. Forest plot of *POLQ* Hazard Ratios for Recurrence Free Survival in multivariate analysis of Series 1. Dots represent Hazard Ratios and grey bars the 95% confidence intervals. In each analysis, a multivariate model including *POLQ* expression, all significant clinical variables, and published signature scores (GGI, 76-gene or 70-gene signature) is derived. The expression of *POLQ*, signature scores and *CCNE2* are entered in these models as continuous ranked variables, normalised between 0 (lowest rank) and 1 (highest rank).

In view of this finding that *POLQ* and *CCNE2* confer a poor prognosis independently of each other, the outcomes of patients were assessed on the basis of the expression of both of these genes. The Kaplan-Meier curve in Figure 5.9 shows that those tumours that do not overexpress either gene are associated with a good prognosis, and those that overexpress only one of the genes are associated with an intermediate prognosis. It is striking that tumours that overexpress both *POLQ* and *CCNE2* confer an extremely poor prognosis relative to the average of the other groups (HR 3.26; 95% CI 1.88 to 5.66; p<0.001).

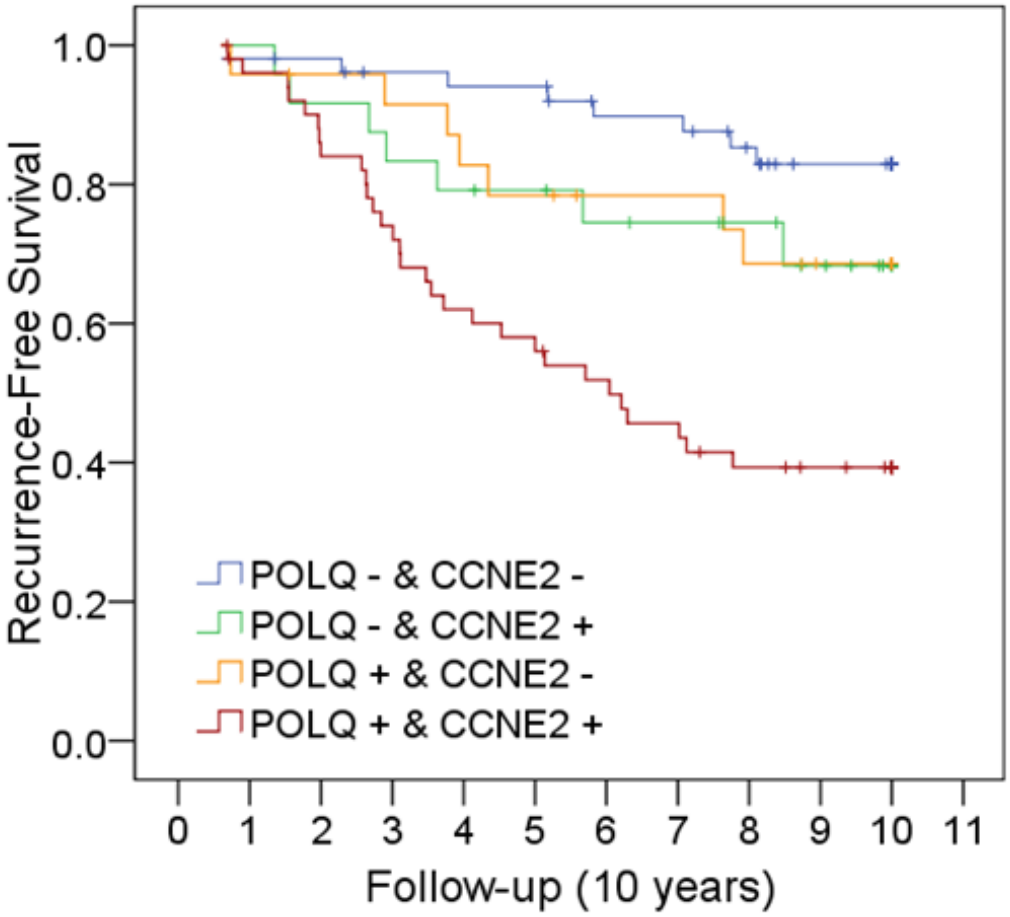

Figure 5.9. Kaplan-Meier plots of Series 1 data. *POLQ* and *CCNE2* expression divided by median value (- indicates below median, + above median). A Helmert contrasts analysis demonstrated that tumours overexpressing both *POLQ* and *CCNE2* were associated with worse outcomes than the average of the other groups (HR 3.26; 95% CI 1.88 to 5.66; p<0.001).

This data suggests that the biological mechanisms by which *POLQ* and *CCNE2* confer a poor prognosis might be independent of each other. These findings could not be confirmed in the other datasets considered, where *POLQ* lost significance after inclusion of *CCNE2*. However it should be noted that in the other series, patients received systemic chemotherapy which could potentially distort prognostically important factors.

5.4 Discussion

The data presented in Chapters 3 and 4, demonstrated that tumour cells depleted of POLQ are rendered more sensitive to radiotherapy and chemotherapy, and that its limited expression in normal tissues make POLQ a potentially exploitable clinical target. In this chapter it has been demonstrated that *POLQ* is frequently upregulated in breast cancers. Although *POLQ* overexpression has previously been demonstrated in lung, gastric and colorectal cancers (215), this is the first time this has been shown in breast cancer.

The clinical significance of tumour expression levels of *POLQ* has not previously been examined in detail. The study by Kawamura *et al* suggested that POLQ overexpression was associated with an adverse prognosis in patients with colorectal cancer (215). However, the significance of this study is limited since it was based on a cohort of only 26 patients, of whom only 8 had tumours that overexpressed POLQ.

A recent study assessed the clinical implications of SNPs using tumour samples obtained from 700 patients with lung cancer. Approximately 25% of these patients had small cell lung cancer and 75% had non-small cell lung cancer. The study

identified a SNP in the central domain of *POLQ* that resulted in an amino acid change from threonine to arginine (rs3218649) and which appeared to be of prognostic significance (318). Patients who were homozygous for this SNP (n=80) had a significantly better prognosis that other patients (HR= 0.67; 95% CI: 0.48–0.94; p=0.021; median survival time 23.4 months compared with 17.3 months). Their data also suggested that this SNP was of even greater significance when they looked at a subgroup of patients treated with platinum based chemotherapy (318). The authors do not give details of the anticipated effects of the SNP on POLQ function. In part this reflects the fact that little is known about the central domain of POLQ, in which the SNP resides. There is no suggestion that individuals with this SNP have a greater chance of developing lung cancer. However, the finding that this SNP is associated with a better prognosis may, if the SNP induces loss of function of POLQ, concur with our findings that POLQ activity is associated with a poor prognosis.

In this current study, a strong correlation has been demonstrated between *POLQ* expression and the presence of other individual factors such as tumour grade and ER negative disease which are known to confer an adverse prognosis (300, 301, 309). It has also been demonstrated that *POLQ* overexpression is associated with markedly increased rates of disease relapse, and using multivariate analysis, that these increased failure rates are independent of its association with poor prognostic features like tumour grade and ER status.

The mechanisms by which *POLQ* overexpression causes these adverse outcomes are not presently clear. It is likely that *POLQ* overexpression confers resistance to

adjuvant chemotherapy and radiotherapy treatment, increasing the likelihood of disease recurrence. However, it is unlikely that this is the sole mechanism by which *POLQ* confers an adverse prognosis. In this chapter, it has been shown in several retrospective series of patients, that *POLQ* is associated with a very poor prognosis. In one of these series ('Series 1') most of the patients received adjuvant radiotherapy although none of them received adjuvant chemotherapy treatment. Although adjuvant radiotherapy treatment plays an important role in reducing the risk of breast cancer recurrence (319), it seems implausible that the effects of *POLQ* expression on radiation resistance could account for the large increases in relapse free survival seen in Series 1 in patients with *POLQ* overexpression. Further work is required to assess whether *POLQ* expression increases tumour cell resistance to endocrine treatments used in the adjuvant treatment of breast cancer patients (320) but even if POLQ does confer resistance to hormone therapies, it would still be difficult to explain the magnitude of differences in survival described here.

The finding that the co-expression of *POLQ* with genes linked to pathways associated with tumour progression, as well as several genes that are contained within the gene expression grade index, suggests that *POLQ* overexpression promotes a more aggressive phenotype, increasing the likelihood of disease recurrence.

A study published very recently, correlated the expression levels of genes involved in DNA replication with clinical outcomes in 74 patients with colorectal cancer (321). Although *POLQ* was not independently associated with adverse outcome, its co-overexpression with at least three other genes involved in DNA replication 'firing'

(from among *CDC45, CDC6, CDT1, SLD5, MCM2*, and *MCM7*) was associated with a worse overall survival. The overall significance of *POLQ* on this finding is not clear since *MCM7* overexpression was shown to be independently associated with adverse survival rates (321). This group suggested that the expression of these genes could produce a more aggressive tumour phenotype by contributing to 'replication stress'. As POLQ is known to repair DNA damage in an error-prone fashion (213, 214), it would seem likely that the poor prognosis that we have described in this study is partially due to POLQ contributing to increased replication stress and genomic instability.

In recent years, attempts have been made to identify gene expression signatures that are capable of predicting patient outcomes with greater accuracy than is currently achievable in routine clinical practice. It is possible that specific gene expression profiles could identify the likelihood of response to individual therapies, enabling clinicians to refine the adjuvant therapy offered to individual patients. The GGI signature (315) identified 97 genes with differential expression between low and high grade breast carcinomas. This signature enabled a more accurate and refined assessment of the risk of disease recurrence in patients with intermediate grade disease (186, 316). A separate '76 gene' expression profile has been created to more accurately identify patients at risk of developing metastatic disease (193) and was shown to predict both distant failure as well as overall survival. Further studies have reinforced the prognostic accuracy of this gene signature (313, 314). A third gene expression profile utilising a '70 gene' signature has also been shown to predict clinical outcome (310) and has also been subsequently validated (311). The prognostic effect of *POLQ* expression on its own has not previously been assessed,

but it is notable that *POLQ* is a component of both the GGI and the '76 gene' expression profiles. Given the large differences that we have shown in relapse rates on the basis of *POLQ* expression, and that these differences are maintained on multivariate analyses that include these signatures, it is possible that *POLQ* may be amongst the most important determinants within these signatures.

Pathway analysis identified several genes, including Cyclin E, that were frequently co-expressed with *POLQ*. Cyclin E overexpression has been identified as being associated with an adverse outcome in breast cancer patients (317). It is the only gene that is a component of all three gene expression signatures and which is also frequently co-expressed with *POLQ*. Cyclin E binds to cyclin-dependent kinase-2 (cdk-2), permitting the transition from G1 to S-phase (322). Increased cyclin E induces enhanced cdk-2 activity, accelerating G1/S transition (323). There is substantial evidence to suggest that *CCNE* overexpression confers a poor prognosis in breast cancer. A recent meta-analysis of 12 independent studies involving 2,534 patients, demonstrated that the combined HR estimate for overall survival and breast cancer specific survival was 2.98 (95% CI, 1.85–4.78) and 2.86 (95% CI, 1.85–4.41) in univariate and multivariate analysis, respectively (324). Although there is ongoing debate as to which fragments of cyclin E are important in predicting outcome (302), the evidence supporting its use in routine clinical assessment have led to calls for large scale clinical trials to investigate this in more detail (324). In this study we have again confirmed that cyclin E overexpression is associated with a poor clinical prognosis on multivariate analysis. In addition we have shown that tumours expressing both *POLQ* and *CCNE2* are associated with an extremely poor outcome. This suggests that these genes confer a poor prognosis through separate

mechanisms. Larger studies are required to investigate whether the risk of relapse from tumours overexpressing cyclin E could be better assessed if further stratified by *POLQ* expression levels.

Independently of its association with other known poor pathological features, *POLQ* overexpression is associated with increased relapse rates. This is the first study to demonstrate that *POLQ* overexpression is associated with an extremely poor outcome in breast cancer on both univariate and multivariate analysis.

Shortly after the work contained within this chapter was published (325), a separate paper by Lemée et al showed very similar findings (326). Using French and Scottish cohorts of patients with early breast cancer, they found that *POLQ* was significantly overexpressed in breast cancer, and that *POLQ* expression was associated with adverse clinical features such as ER negative disease, high tumour grade and large tumour size. They performed a multivariate analysis (which included cyclin E and nodal status, but no other clinical variables) and showed that *POLQ* was associated with a significantly increased risk of death (HR 3.10; 95% CI 1.37 to 6.97; p=0.006). Additionally this group showed that *POLQ* and *Cyclin E* were independently associated with poor outcomes and that patients whose tumours overexpress both of these genes have a particularly poor prognosis (326). These results reinforce our own findings regarding the poor prognosis associated with *POLQ* overexpression. Their work also included some interesting *in vitro* findings. They stably overexpressed POLQ in MRC5-SV cells and found that POLQ overexpression caused cells to accumulate in S phase. It is possible that these findings occur only with supraphysiological expression of POLQ, since the work presented in Chapters 3

and 4 found that depletion of POLQ has no effect on the cell cycle either in the presence or absence of DNA damage (Fig. 3.16 and 4.5).

In addition they found that these cells showed increased γH2AX foci (in cells unexposed to exogenous DNA damage). It is possible that the change in γH2AX foci that they observe with POLQ overexpression may reflect the increased number of cells in S phase (225) rather than an induction of the DNA damage response as suggested by the authors (326). In unirradiated cells depleted of POLQ we did not observe any change in the number of γH2AX foci present (Fig. 3.12). Nevertheless this study produced extremely interesting results which warrant further investigation.

Adjuvant chemotherapy and radiotherapy treatments are very important in the management of patients with early breast cancer (319, 320). The finding that tumour cells depleted of POLQ are rendered more sensitive to both radiotherapy and DNA damaging chemotherapies, could suggest that the poor prognosis associated with *POLQ* overexpression in early breast cancer patients may be partly due to tumour cell resistance to adjuvant therapy. Prospective clinical studies are required to confirm whether tumour overexpression of *POLQ* is predictive of a poor response to DNA damaging chemotherapies such as anthracyclines. If proven, the expression levels of *POLQ* may be useful in identifying those patients unlikely to benefit from chemotherapies that cause damage that is repaired by HR, and who might therefore be better treated with alternative agents. However, as anthracyclines are a proven and effective component of therapy for breast cancer, and topoisomerase II inhibitors are active in a range of tumour types, development of POLQ inhibitors would offer

the opportunity of synergy with such drugs and potentially little normal tissue toxicity, as POLQ is not expressed in most normal tissues.

The poor prognosis associated with *POLQ* expression, the known radio- and chemosensitisation induced by its depletion, and its highly limited normal tissue expression all support the opinion that POLQ is a very appealing target for clinical exploitation.

Chapter 6

GENERAL DISCUSSION

6.1 Assessment of the siRNA radiosensitivity screen

The work presented in Chapter 1 described a siRNA screen of 200 genes involved in DNA damage repair aimed at identifying novel determinants of tumour cell radiosensitivity. This screen successfully identified POLQ as a suitable candidate to investigate further. Subsequent analysis demonstrated that POLQ depletion appeared to cause tumour specific radiosensitisation. The screen was based on the presence of residual γH2AX foci 24h after exposure to 4Gy. The speed and ease with which γH2AX foci can be quantified, means that in principle, it is an ideal endpoint to use for high throughput screening to assess changes in radiosensitivity. Given that this screen succeeded in identifying a novel gene, as well as correctly identifying several genes known to be important in intrinsic radiosensitivity, it is possible that screening larger siRNA libraries using this assay endpoint could successfully identify novel determinants of tumour cell radiosensitivity.

However, using γH2AX foci as a marker for IR induced damage is not entirely straightforward. Previous studies have produced conflicting results regarding the correlation between cell radiosensitivity and the presence of γH2AX foci after IR. Some studies have found that radiosensitive cells show slower rates of γH2AX resolution (169-171), whilst other studies have been unable to do so (172-174). Another potential difficulty arises from the finding that γH2AX foci do not appear only at sites of damaged DNA, but also appear at sites of stalled replication forks in S-phase (225).

The results obtained in Chapter 3 highlight some of the difficulties with using γH2AX foci as an endpoint. It was found that depletion of genes known to induce profound radiosensitisation, showed only modest changes in the mean number of γH2AX foci per cell. Changes in radiosensitivity were therefore assessed by measuring the percentage of irradiated cells that contained more than 7 γH2AX foci per cell. Although this was successful in identifying changes in radiosensitivity caused by depletion of genes directly involved in DNA repair, it is unclear whether this endpoint would be sufficiently sensitive to detect smaller changes arising from depletion of genes that cause radioresistance by a more indirect mechanism (115).

Although this screen was successful in identifying a novel determinant of tumour cell radiosensitivity, it also identified several genes (*INCENP, RAD21, XAB2*) whose depletion was shown in subsequent experiments to induce widespread cell death in the absence of IR. In addition it identified a gene (*APEX2*) which was later found to radiosensitise both normal tissue and tumour cells. Investigating these false positive results is very costly, both in terms of reagent expenses, and in investigator time, and therefore future screens should aim to minimise such 'hits'. Individually excluding the false positive candidates identified by a small screen of only 200 genes is relatively straightforward. However, if a siRNA screen of a 'druggable genome' library (which typically contains approximately 8000 genes) identified false positives at the same rate as seen in our screen it would involve investigating over 160 genes that did not induce tumour specific radiosensitisation. In particular, future screens should try to minimise the identification of genes whose depletion cause cell death in unirradiated cells. One possible way in which this could be done would be to perform

a secondary screen of shortlisted candidate genes with the aim of testing whether siRNA transfection altered cell viability in the absence of irradiation. Several days after transfection, a cell viability assay could be used to identify, and therefore exclude those genes whose depletion caused cell death in the absence of IR.

These difficulties regarding the use of γH2AX foci as an assay endpoint has led our laboratory to investigate suitable alternatives. The gold standard measure of intrinsic radiosensitivity is the clonogenic survival assay (149). We had previously discounted using this assay for high-throughput screening because of our concerns that it is both labour intensive and time consuming. However, we have recently developed a method of performing a clonogenic survival assay in 96 well plates using automated liquid handling to plate cells at different densities into radiation plates and unirradiated control plates. By comparing the number of surviving colonies in the irradiated and unirradiated control plates, the surviving fraction of irradiated cells can be easily calculated. The optimisation of robotic equipment to perform the siRNA transfections and the clonogenic assays has enabled us to screen larger siRNA libraries. Currently our group are in the process of screening an 800 gene 'kinome' library of siRNAs and aim to screen a 'druggable genome' siRNA library thereafter.

Performing 96 well plate clonogenic assays has many advantages over the use of surrogate markers for clonogenic survival such as cell viability assays (147, 148) or the detection of γH2AX foci. It gives a direct measure of clonogenic survival, and prevents the investigation of numerous false positives, since genes which cause cell

death in the absence of radiation will be readily identified by low colony numbers in the unirradiated control plates.

Previous siRNA screens have used cells that contain specific mutations to identify synthetic lethal interactions that occur only in the context of these mutations. A recent siRNA screen demonstrated that cells with mutant *KRAS* show significant sensitivity to suppression of the serine/threonine kinase STK33, whereas STK33 is not required by KRAS independent cells (140). It is probable that other oncogenes also have similar, specific synthetic lethal interactions. This finding highlights the fact that tumour cells with different mutations may have very specific mechanisms for surviving radiation exposure. Activation of some oncogenic pathways such as the EGFR-PI3K-Akt pathway are already well recognised as causing radioresistance (115). Identifying clinically exploitable targets to radiosensitise tumour cells may require siRNA screens to be conducted with several different tumour cells each carrying a different common oncogenic mutation.

6.2 The role of POLQ in DNA repair

POLQ has previously been shown to be overexpressed in lung, gastric and colorectal cancers whilst having limited expression in normal tissues (215, 321). This thesis contains *in vitro* work showing that POLQ is overexpressed in tumour cell lines of different histology and origin. It has also been shown that the tumour cell radio and chemosensitisation that occurs as a result of POLQ depletion arises from a reduction in homologous recombination efficiency rather than a reduction in BER or NHEJ. In Chapter 4, an analysis of the time course of resolution of γH2AX foci

provided indirect evidence that POLQ is not involved in NHEJ. More complicated NHEJ assays have previously been described and could be used in the future to confirm that POLQ does not play a significant role in NHEJ (327). The recent finding that the *Drosophila* homologue of POLQ, *mus308,* is involved in MMEJ warrants further investigation (292, 293). Initial research that we have undertaken in this area suggests that human POLQ depletion does not cause alterations in MMEJ, but more work is required to confirm this.

Further studies investigating the function of POLQ would benefit from the development of an effective POLQ antibody and a *POLQ* expression vector suitable for use in human cells. Attempts to develop these reagents are ongoing. An effective POLQ antibody could, for example, be used to show co-localisation between POLQ, RAD51 and γH2AX foci. This would support the existing data showing that POLQ is involved in HR. The development of a *POLQ* vector would make it possible to assess which parts of the POLQ structure are important in mediating HR efficiency. The effects of inducing specific changes by site-directed mutagenesis could be analysed, providing information as to which components of POLQ should be targeted in the development of pharmacological inhibitors.

6.3 Clinical significance of tumour overexpression of POLQ

The radio and chemosensitisation of tumour cells depleted of POLQ implies that tumours which overexpress POLQ may render tumours resistant to treatments such as chemotherapy and radiotherapy, resulting in patients having poor clinical outcomes. In order to investigate this in more detail, the impact of tumour

overexpression of *POLQ* was examined in retrospective series of patients with early breast cancer. It was found that *POLQ* expression was correlated with clinical factors such as high tumour grade, and ER negative disease which are known to be associated with poor clinical outcomes. Independently of these clinical features, overexpression of *POLQ* is associated with an extremely poor outcome in these patients. The adverse prognosis associated with *POLQ* overexpression appears to be of a striking magnitude, and is at least comparable to the poor outcomes associated with HER2 overexpression prior to the use of trastuzumab (298, 299).

The mechanism by which POLQ causes this adverse outcome is not clear. It is possible that since POLQ is an error prone polymerase (213, 214), the poor prognosis associated with its overexpression is related to POLQ causing an increase in genomic instability, therefore promoting a more aggressive phenotype. In addition the poor prognosis associated with POLQ expression may arise from POLQ conferring resistance to adjuvant radio and chemotherapy treatments that are commonly used in this setting.

The extent to which POLQ induced resistance to adjuvant treatment may alter prognosis is impossible to assess on the basis of the currently available information, since POLQ has not yet been shown to act as a predictive marker (328) of response to either radio or chemotherapy. Prospective clinical studies would be required in order to confirm whether tumour overexpression of *POLQ* is predictive of a poor response to DNA damaging treatments such as radiotherapy or anthracycline chemotherapy. If proven, the expression levels of *POLQ* may be useful in identifying

those patients unlikely to benefit from chemotherapies that cause damage that is repaired by HR, and who might be better treated with alternative agents. If an inhibitor to POLQ could be successfully developed, it is possible that it could be used in conjunction with treatments such as radiotherapy and chemotherapy to improve tumour response to treatment.

6.4 Summary

Radiotherapy treatment could be significantly improved if tumour cells could be rendered more sensitive to ionising radiation. However, the molecular mechanisms that determine tumour cell radiosensitivity are poorly understood.

In summary, the work contained within this thesis was aimed at identifying novel determinants of tumour cell radiosensitivity. A siRNA screen was performed with a library of two hundred genes involved in DNA damage repair. This screen suggested that depletion of POLQ may sensitise tumour cells to radiation. Subsequent work confirmed that POLQ knockdown radiosensitised tumour cells, whilst having little or no effect on normal tissues. In addition it was found that tumour cells depleted of POLQ are rendered significantly more sensitive to several different chemotherapy agents such as cisplatin, mitomycin C, etoposide and doxorubicin. The radio and chemosensitisation caused by depletion of POLQ appears to arise from a reduction in homologous recombination efficiency.

An important implication of these findings is that tumours which overexpress POLQ may be resistant to treatments such as chemotherapy and radiotherapy, resulting in patients having poor clinical outcomes. Accordingly, the prognostic relevance of *POLQ* overexpression was examined in patients with early breast cancer, in whom it was found to confer an extremely poor prognosis.

The limited expression of POLQ suggests that it may be a suitable target for therapeutic exploitation. Inhibition of POLQ may render tumour cells more sensitive to radio and chemotherapy, and reverse the poor prognosis associated with its overexpression.

BIBLIOGRAPHY

1. Saunders M, Dische S, Barrett A, Harvey A, Griffiths G, Palmar M. Continuous, hyperfractionated, accelerated radiotherapy (CHART) versus conventional radiotherapy in non-small cell lung cancer: mature data from the randomised multicentre trial. CHART Steering committee. Radiother Oncol. 1999;52:137-48.

2. Green JA, Kirwan JM, Tierney JF, Symonds P, Fresco L, Collingwood M, et al. Survival and recurrence after concomitant chemotherapy and radiotherapy for cancer of the uterine cervix: a systematic review and meta-analysis. Lancet. 2001;358:781-6.

3. Bonner JA, Harari PM, Giralt J, Azarnia N, Shin DM, Cohen RB, et al. Radiotherapy plus cetuximab for squamous-cell carcinoma of the head and neck. N Engl J Med. 2006;354:567-78.

4. Bonner JA, Harari PM, Giralt J, Cohen RB, Jones CU, Sur RK, et al. Radiotherapy plus cetuximab for locoregionally advanced head and neck cancer: 5-year survival data from a phase 3 randomised trial, and relation between cetuximab-induced rash and survival. Lancet Oncol. 2010;11:21-8.

5. Bentzen SM, Agrawal RK, Aird EG, Barrett JM, Barrett-Lee PJ, Bliss JM, et al. The UK Standardisation of Breast Radiotherapy (START) Trial B of radiotherapy hypofractionation for treatment of early breast cancer: a randomised trial. Lancet. 2008;371:1098-107.

6. Meeuse JJ, van der Linden YM, van Tienhoven G, Gans RO, Leer JW, Reyners AK. Efficacy of radiotherapy for painful bone metastases during the last 12 weeks of life: results from the Dutch Bone Metastasis Study. Cancer. 2010;116:2716-25.

7. Videtic GM, Gaspar LE, Aref AM, Germano IM, Goldsmith BJ, Imperato JP, et al. American College of Radiology appropriateness criteria on multiple brain metastases. Int J Radiat Oncol Biol Phys. 2009;75:961-5.

8. Hall E, editor. Radiobiology For the Radiologist. 6 ed. Philadelphia: Lippincott Williams & Wilkins; 2006.

9. Steel GG, editor. Basic Clinical Radiobiology. 3rd ed. London: Oxford University Press; 2002.

10. Frankenberg-Schwager M. Review of repair kinetics for DNA damage induced in eukaryotic cells in vitro by ionizing radiation. Radiother Oncol. 1989;14:307-20.

11. Coquerelle TM, Weibezahn KF, Lucke-Huhle C. Rejoining of double strand breaks in normal human and ataxia-telangiectasia fibroblasts after exposure to 60Co gamma-rays, 241Am alpha-particles or bleomycin. Int J Radiat Biol Relat Stud Phys Chem Med. 1987;51:209-18.

12. Dikomey E. Effect of hyperthermia at 42 and 45 degrees C on repair of radiation-induced DNA strand breaks in CHO cells. Int J Radiat Biol Relat Stud Phys Chem Med. 1982;41:603-14.

13. Helleday T, Lo J, van Gent DC, Engelward BP. DNA double-strand break repair: from mechanistic understanding to cancer treatment. DNA Repair (Amst). 2007;6:923-35.

14. Gottlieb TM, Jackson SP. The DNA-dependent protein kinase: requirement for DNA ends and association with Ku antigen. Cell. 1993;72:131-42.

15. Yoo S, Dynan WS. Geometry of a complex formed by double strand break repair proteins at a single DNA end: recruitment of DNA-PKcs induces inward translocation of Ku protein. Nucleic Acids Res. 1999;27:4679-86.

16. Yaneva M, Kowalewski T, Lieber MR. Interaction of DNA-dependent protein kinase with DNA and with Ku: biochemical and atomic-force microscopy studies. EMBO J. 1997;16:5098-112.

17. DeFazio LG, Stansel RM, Griffith JD, Chu G. Synapsis of DNA ends by DNA-dependent protein kinase. EMBO J. 2002;21:3192-200.

18. Ma Y, Pannicke U, Schwarz K, Lieber MR. Hairpin opening and overhang processing by an Artemis/DNA-dependent protein kinase complex in nonhomologous end joining and V(D)J recombination. Cell. 2002;108:781-94.

19. Wang J, Pluth JM, Cooper PK, Cowan MJ, Chen DJ, Yannone SM. Artemis deficiency confers a DNA double-strand break repair defect and Artemis phosphorylation status is altered by DNA damage and cell cycle progression. DNA Repair (Amst). 2005;4:556-70.

20. Nick McElhinny SA, Ramsden DA. Sibling rivalry: competition between Pol X family members in V(D)J recombination and general double strand break repair. Immunol Rev. 2004;200:156-64.

21. Grawunder U, Wilm M, Wu X, Kulesza P, Wilson TE, Mann M, et al. Activity of DNA ligase IV stimulated by complex formation with XRCC4 protein in mammalian cells. Nature. 1997;388:492-5.

22. Ahnesorg P, Smith P, Jackson SP. XLF interacts with the XRCC4-DNA ligase IV complex to promote DNA nonhomologous end-joining. Cell. 2006;124:301-13.

23. Lee JH, Paull TT. Direct activation of the ATM protein kinase by the Mre11/Rad50/Nbs1 complex. Science. 2004;304:93-6.

24. Lee JH, Paull TT. ATM activation by DNA double-strand breaks through the Mre11-Rad50-Nbs1 complex. Science. 2005;308:551-4.

25. Matsuoka S, Ballif BA, Smogorzewska A, McDonald ER, 3rd, Hurov KE, Luo J, et al. ATM and ATR substrate analysis reveals extensive protein networks responsive to DNA damage. Science. 2007;316:1160-6.

26. Nimonkar AV, Ozsoy AZ, Genschel J, Modrich P, Kowalczykowski SC. Human exonuclease 1 and BLM helicase interact to resect DNA and initiate DNA repair. Proc Natl Acad Sci U S A. 2008;105:16906-11.

27. Wold MS. Replication protein A: a heterotrimeric, single-stranded DNA-binding protein required for eukaryotic DNA metabolism. Annu Rev Biochem. 1997;66:61-92.

28. Wong AK, Pero R, Ormonde PA, Tavtigian SV, Bartel PL. RAD51 interacts with the evolutionarily conserved BRC motifs in the human breast cancer susceptibility gene brca2. J Biol Chem. 1997;272:31941-4.

29. Sy SM, Huen MS, Chen J. PALB2 is an integral component of the BRCA complex required for homologous recombination repair. Proc Natl Acad Sci U S A. 2009;106:7155-60.

30. Zhang F, Ma J, Wu J, Ye L, Cai H, Xia B, et al. PALB2 links BRCA1 and BRCA2 in the DNA-damage response. Curr Biol. 2009;19:524-9.

31. Sharan SK, Morimatsu M, Albrecht U, Lim DS, Regel E, Dinh C, et al. Embryonic lethality and radiation hypersensitivity mediated by Rad51 in mice lacking Brca2. Nature. 1997;386:804-10.

32. Pellegrini L, Yu DS, Lo T, Anand S, Lee M, Blundell TL, et al. Insights into DNA recombination from the structure of a RAD51-BRCA2 complex. Nature. 2002;420:287-93.

33. Wesoly J, Agarwal S, Sigurdsson S, Bussen W, Van Komen S, Qin J, et al. Differential contributions of mammalian Rad54 paralogs to recombination, DNA damage repair, and meiosis. Mol Cell Biol. 2006;26:976-89.

34. McIlwraith MJ, Vaisman A, Liu Y, Fanning E, Woodgate R, West SC. Human DNA polymerase eta promotes DNA synthesis from strand invasion intermediates of homologous recombination. Mol Cell. 2005;20:783-92.

35. Chen JM, Cooper DN, Chuzhanova N, Ferec C, Patrinos GP. Gene conversion: mechanisms, evolution and human disease. Nat Rev Genet. 2007;8:762-75.

36. Heyer WD, Kanaar R. Recombination mechanisms; fortieth anniversary meeting of the Holliday model. Mol Cell. 2004;16:1-9.

37. McIlwraith MJ, West SC. DNA repair synthesis facilitates RAD52-mediated second-end capture during DSB repair. Mol Cell. 2008;29:510-6.

38. Shi I, Hallwyl SC, Seong C, Mortensen U, Rothstein R, Sung P. Role of the Rad52 amino-terminal DNA binding activity in DNA strand capture in homologous recombination. J Biol Chem. 2009;284:33275-84.

39. Chen XB, Melchionna R, Denis CM, Gaillard PH, Blasina A, Van de Weyer I, et al. Human Mus81-associated endonuclease cleaves Holliday junctions in vitro. Mol Cell. 2001;8:1117-27.

40. Constantinou A, Chen XB, McGowan CH, West SC. Holliday junction resolution in human cells: two junction endonucleases with distinct substrate specificities. EMBO J. 2002;21:5577-85.

41. Johnson RD, Jasin M. Sister chromatid gene conversion is a prominent double-strand break repair pathway in mammalian cells. EMBO J. 2000;19:3398-407.

42. Wu L, Hickson ID. The Bloom's syndrome helicase suppresses crossing over during homologous recombination. Nature. 2003;426:870-4.

43. Ip SC, Rass U, Blanco MG, Flynn HR, Skehel JM, West SC. Identification of Holliday junction resolvases from humans and yeast. Nature. 2008;456:357-61.

44. Bugreev DV, Mazina OM, Mazin AV. Rad54 protein promotes branch migration of Holliday junctions. Nature. 2006;442:590-3.

45. Moynahan ME, Jasin M. Mitotic homologous recombination maintains genomic stability and suppresses tumorigenesis. Nat Rev Mol Cell Biol. 2010;11:196-207.

46. D'Amico AV, McKenna WG. Apoptosis and a re-investigation of the biologic basis for cancer therapy. Radiother Oncol. 1994;33:3-10.

47. Dubray B, Breton C, Delic J, Klijanienko J, Maciorowski Z, Vielh P, et al. In vitro radiation-induced apoptosis and early response to low-dose radiotherapy in non-Hodgkin's lymphomas. Radiother Oncol. 1998;46:185-91.

48. Dewey WC, Ling CC, Meyn RE. Radiation-induced apoptosis: relevance to radiotherapy. Int J Radiat Oncol Biol Phys. 1995;33:781-96.

49. Castedo M, Perfettini JL, Roumier T, Andreau K, Medema R, Kroemer G. Cell death by mitotic catastrophe: a molecular definition. Oncogene. 2004;23:2825-37.

50. Jonathan EC, Bernhard EJ, McKenna WG. How does radiation kill cells? Curr Opin Chem Biol. 1999;3:77-83.

51. Emami B, Lyman J, Brown A, Coia L, Goitein M, Munzenrider JE, et al. Tolerance of normal tissue to therapeutic irradiation. Int J Radiat Oncol Biol Phys. 1991;21:109-22.

52. Sharma RA, Vallis KA, McKenna WG. Abeloff's Clinical Oncology. In: Abeloff MD, Armitage JO, Niederhuber JE, Kastan MB, McKenna WG, editors. 4th ed: Churchill Livingstone; 2008. p. 434.

53. Milano MT, Constine LS, Okunieff P. Normal tissue tolerance dose metrics for radiation therapy of major organs. Semin Radiat Oncol. 2007;17:131-40.

54. Withers HR. The four R's of radiotherapy. Advances in Radiation Biology. 1975;5:241-71.

55. Little JB, Hahn GM, Frindel E, Tubiana M. Repair of potentially lethal radiation damage in vitro and in vivo. Radiology. 1973;106:689-94.

56. Elkind MM, Sutton H. Radiation response of mammalian cells grown in culture. 1. Repair of X-ray damage in surviving Chinese hamster cells. Radiat Res. 1960;13:556-93.

57. Steel GG, Deacon JM, Duchesne GM, Horwich A, Kelland LR, Peacock JH. The dose-rate effect in human tumour cells. Radiother Oncol. 1987;9:299-310.

58. Sinclair WK. Cyclic x-ray responses in mammalian cells in vitro. Radiat Res. 1968;33:620-43.

59. Sinclair WK, Morton RA. X-Ray and Ultraviolet Sensitivity of Synchronized Chinese Hamster Cells at Various Stages of the Cell Cycle. Biophys J. 1965;5:1-25.

60. Esser E, Schumann J, Wannenmacher M. Irradiation treatment of inoperable squamous cell carcinomas of the oral cavity and oropharynx after partial synchronisation. J Maxillofac Surg. 1976;4:26-33.

61. Withers HR, Taylor JM, Maciejewski B. The hazard of accelerated tumor clonogen repopulation during radiotherapy. Acta Oncol. 1988;27:131-46.

62. Horiot JC, Bontemps P, van den Bogaert W, Le Fur R, van den Weijngaert D, Bolla M, et al. Accelerated fractionation (AF) compared to conventional fractionation (CF) improves loco-regional

control in the radiotherapy of advanced head and neck cancers: results of the EORTC 22851 randomized trial. Radiother Oncol. 1997;44:111-21.

63. Saunders M, Dische S, Barrett A, Harvey A, Gibson D, Parmar M. Continuous hyperfractionated accelerated radiotherapy (CHART) versus conventional radiotherapy in non-small-cell lung cancer: a randomised multicentre trial. CHART Steering Committee. Lancet. 1997;350:161-5.

64. Gray LH, Conger AD, Ebert M, Hornsey S, Scott OC. The concentration of oxygen dissolved in tissues at the time of irradiation as a factor in radiotherapy. Br J Radiol. 1953;26:638-48.

65. Wright EA, Howard-Flanders P. The influence of oxygen on the radiosensitivity of mammalian tissues. Acta radiol. 1957;48:26-32.

66. Palcic B, Brosing JW, Skarsgard LD. Survival measurements at low doses: oxygen enhancement ratio. Br J Cancer. 1982;46:980-4.

67. Alper T, Howard-Flanders P. Role of oxygen in modifying the radiosensitivity of E. coli B. Nature. 1956;178:978-9.

68. Held KD, Harrop HA, Michael BD. Effects of oxygen and sulphydryl-containing compounds on irradiated transforming DNA. II. Glutathione, cysteine and cysteamine. Int J Radiat Biol Relat Stud Phys Chem Med. 1984;45:615-26.

69. Hutchinson F. Sulfhydryl groups and the oxygen effect on irradiated dilute solutions of enzymes and nucleic acids. Radiat Res. 1961;14:721-31.

70. Chapman JD, Reuvers AP, Borsa J, Greenstock CL. Chemical radioprotection and radiosensitization of mammalian cells growing in vitro. Radiat Res. 1973;56:291-306.

71. Brizel DM, Sibley GS, Prosnitz LR, Scher RL, Dewhirst MW. Tumor hypoxia adversely affects the prognosis of carcinoma of the head and neck. Int J Radiat Oncol Biol Phys. 1997;38:285-9.

72. Bennett M, Feldmeier J, Smee R, Milross C. Hyperbaric oxygenation for tumour sensitisation to radiotherapy. Cochrane Database Syst Rev. 2005:CD005007.

73. Gordon MS. Managing anemia in the cancer patient: old problems, future solutions. Oncologist. 2002;7:331-41.

74. Warde P, O'Sullivan B, Bristow RG, Panzarella T, Keane TJ, Gullane PJ, et al. T1/T2 glottic cancer managed by external beam radiotherapy: the influence of pretreatment hemoglobin on local control. Int J Radiat Oncol Biol Phys. 1998;41:347-53.

75. Varlotto J, Stevenson MA. Anemia, tumor hypoxemia, and the cancer patient. Int J Radiat Oncol Biol Phys. 2005;63:25-36.

76. Henke M, Laszig R, Rube C, Schafer U, Haase KD, Schilcher B, et al. Erythropoietin to treat head and neck cancer patients with anaemia undergoing radiotherapy: randomised, double-blind, placebo-controlled trial. Lancet. 2003;362:1255-60.

77. Henke M, Mattern D, Pepe M, Bezay C, Weissenberger C, Werner M, et al. Do erythropoietin receptors on cancer cells explain unexpected clinical findings? J Clin Oncol. 2006;24:4708-13.

78. Adams GE, Cooke MS. Electron-affinic sensitization. I. A structural basis for chemical radiosensitizers in bacteria. Int J Radiat Biol Relat Stud Phys Chem Med. 1969;15:457-71.

79. Asquith JC, Watts ME, Patel K, Smithen CE, Adams GE. Electron affinic sensitization. V. Radiosensitization of hypoxic bacteria and mammalian cells in vitro by some nitroimidazoles and nitropyrazoles. Radiat Res. 1974;60:108-18.

80. Urtasun R, Band P, Chapman JD, Feldstein ML, Mielke B, Fryer C. Radiation and high-dose metronidazole in supratentorial glioblastomas. N Engl J Med. 1976;294:1364-7.

81. Mantyla MJ, Nordman EM, Ruotsalainen PJ, Kylmamaa TT. Misonidazole and radiotherapy in lung cancer: a randomized double-blind trial. Int J Radiat Oncol Biol Phys. 1982;8:1719-20.

82. Bleehen NM, Wiltshire CR, Plowman PN, Watson JV, Gleave JR, Holmes AE, et al. A randomized study of misonidazole and radiotherapy for grade 3 and 4 cerebral astrocytoma. Br J Cancer. 1981;43:436-42.

83. Overgaard J, Bentzen SM, Kolstad P, Kjoerstad K, Davy M, Bertelsen K, et al. Misonidazole combined with radiotherapy in the treatment of carcinoma of the uterine cervix. Int J Radiat Oncol Biol Phys. 1989;16:1069-72.

84. Papavasiliou C, Yiogarakis D, Davillas N, Seretakis L, Pappas J, Licourinas M, et al. Treatment of bladder carcinoma with irradiation combined with misonidazole. Int J Radiat Oncol Biol Phys. 1983;9:1631-3.

85. Overgaard J, Hansen HS, Andersen AP, Hjelm-Hansen M, Jorgensen K, Sandberg E, et al. Misonidazole combined with split-course radiotherapy in the treatment of invasive carcinoma of larynx and pharynx: report from the DAHANCA 2 study. Int J Radiat Oncol Biol Phys. 1989;16:1065-8.

86. Melgaard B, Kohler O, Sand Hansen H, Overgaard J, Munck-Hansen J, Paulson OB. Misonidazole neuropathy. A prospective study. J Neurooncol. 1988;6:227-30.

87. Overgaard J, Hansen HS, Overgaard M, Bastholt L, Berthelsen A, Specht L, et al. A randomized double-blind phase III study of nimorazole as a hypoxic radiosensitizer of primary radiotherapy in supraglottic larynx and pharynx carcinoma. Results of the Danish Head and Neck Cancer Study (DAHANCA) Protocol 5-85. Radiother Oncol. 1998;46:135-46.

88. Wardman P. Chemical radiosensitizers for use in radiotherapy. Clin Oncol (R Coll Radiol). 2007;19:397-417.

89. Horsman MR. Nicotinamide and other benzamide analogs as agents for overcoming hypoxic cell radiation resistance in tumours. A review. Acta Oncol. 1995;34:571-87.

90. Kaanders JH, Pop LA, Marres HA, Bruaset I, van den Hoogen FJ, Merkx MA, et al. ARCON: experience in 215 patients with advanced head-and-neck cancer. Int J Radiat Oncol Biol Phys. 2002;52:769-78.

91. Hoskin P, Rojas A, Saunders M. Accelerated radiotherapy, carbogen, and nicotinamide (ARCON) in the treatment of advanced bladder cancer: mature results of a Phase II nonrandomized study. Int J Radiat Oncol Biol Phys. 2009;73:1425-31.

92. Steel GG, McMillan TJ, Peacock JH. The 5Rs of radiobiology. Int J Radiat Biol. 1989;56:1045-8.

93. Fertil B, Malaise EP. Inherent cellular radiosensitivity as a basic concept for human tumor radiotherapy. Int J Radiat Oncol Biol Phys. 1981;7:621-9.

94. Deacon J, Peckham MJ, Steel GG. The radioresponsiveness of human tumours and the initial slope of the cell survival curve. Radiother Oncol. 1984;2:317-23.

95. Bjork-Eriksson T, West C, Karlsson E, Mercke C. Tumor radiosensitivity (SF2) is a prognostic factor for local control in head and neck cancers. Int J Radiat Oncol Biol Phys. 2000;46:13-9.

96. West CM, Davidson SE, Roberts SA, Hunter RD. The independence of intrinsic radiosensitivity as a prognostic factor for patient response to radiotherapy of carcinoma of the cervix. Br J Cancer. 1997;76:1184-90.

97. Girinsky T, Bernheim A, Lubin R, Tavakoli-Razavi T, Baker F, Janot F, et al. In vitro parameters and treatment outcome in head and neck cancers treated with surgery and/or radiation: cell characterization and correlations with local control and overall survival. Int J Radiat Oncol Biol Phys. 1994;30:789-94.

98. Eastman A, Barry MA. Interaction of trans-diamminedichloroplatinum(II) with DNA: formation of monofunctional adducts and their reaction with glutathione. Biochemistry. 1987;26:3303-7.

99. Richmond RC, Khokhar AR, Teicher BA, Douple EB. Toxic variability and radiation sensitization by Pt(II) analogs in Salmonella typhimurium cells. Radiat Res. 1984;99:609-26.

100. Amorino GP, Freeman ML, Carbone DP, Lebwohl DE, Choy H. Radiopotentiation by the oral platinum agent, JM216: role of repair inhibition. Int J Radiat Oncol Biol Phys. 1999;44:399-405.

101. Marino P, Preatoni A, Cantoni A. Randomized trials of radiotherapy alone versus combined chemotherapy and radiotherapy in stages IIIa and IIIb nonsmall cell lung cancer. A meta-analysis. Cancer. 1995;76:593-601.

102. Rose PG, Bundy BN, Watkins EB, Thigpen JT, Deppe G, Maiman MA, et al. Concurrent cisplatin-based radiotherapy and chemotherapy for locally advanced cervical cancer. N Engl J Med. 1999;340:1144-53.

103. Bernier J, Domenge C, Ozsahin M, Matuszewska K, Lefebvre JL, Greiner RH, et al. Postoperative irradiation with or without concomitant chemotherapy for locally advanced head and neck cancer. N Engl J Med. 2004;350:1945-52.

104. Pignon JP, le Maitre A, Maillard E, Bourhis J. Meta-analysis of chemotherapy in head and neck cancer (MACH-NC): an update on 93 randomised trials and 17,346 patients. Radiother Oncol. 2009;92:4-14.

105. Grem JL. 5-Fluorouracil: forty-plus and still ticking. A review of its preclinical and clinical development. Invest New Drugs. 2000;18:299-313.

106. Lawrence TS, Davis MA, Chang EY, Canman CE, Maybaum J, Radany EH. Lack of dependence of 5-fluorodeoxyuridine-mediated radiosensitization on cytotoxicity. Radiat Res. 1995;143:281-5.

107. Cooper JS, Guo MD, Herskovic A, Macdonald JS, Martenson JA, Jr., Al-Sarraf M, et al. Chemoradiotherapy of locally advanced esophageal cancer: long-term follow-up of a prospective randomized trial (RTOG 85-01). Radiation Therapy Oncology Group. JAMA. 1999;281:1623-7.

108. Morris M, Eifel PJ, Lu J, Grigsby PW, Levenback C, Stevens RE, et al. Pelvic radiation with concurrent chemotherapy compared with pelvic and para-aortic radiation for high-risk cervical cancer. N Engl J Med. 1999;340:1137-43.

109. Bartelink H, Roelofsen F, Eschwege F, Rougier P, Bosset JF, Gonzalez DG, et al. Concomitant radiotherapy and chemotherapy is superior to radiotherapy alone in the treatment of locally advanced anal cancer: results of a phase III randomized trial of the European Organization for Research and Treatment of Cancer Radiotherapy and Gastrointestinal Cooperative Groups. J Clin Oncol. 1997;15:2040-9.

110. Jeremic B, Shibamoto Y, Milicic B, Nikolic N, Dagovic A, Aleksandrovic J, et al. Hyperfractionated radiation therapy with or without concurrent low-dose daily cisplatin in locally advanced squamous cell carcinoma of the head and neck: a prospective randomized trial. J Clin Oncol. 2000;18:1458-64.

111. Rubin Grandis J, Melhem MF, Gooding WE, Day R, Holst VA, Wagener MM, et al. Levels of TGF-alpha and EGFR protein in head and neck squamous cell carcinoma and patient survival. J Natl Cancer Inst. 1998;90:824-32.

112. Gupta AK, McKenna WG, Weber CN, Feldman MD, Goldsmith JD, Mick R, et al. Local recurrence in head and neck cancer: relationship to radiation resistance and signal transduction. Clin Cancer Res. 2002;8:885-92.

113. Sheridan MT, O'Dwyer T, Seymour CB, Mothersill CE. Potential indicators of radiosensitivity in squamous cell carcinoma of the head and neck. Radiat Oncol Investig. 1997;5:180-6.

114. Ang KK, Berkey BA, Tu X, Zhang HZ, Katz R, Hammond EH, et al. Impact of epidermal growth factor receptor expression on survival and pattern of relapse in patients with advanced head and neck carcinoma. Cancer Res. 2002;62:7350-6.

115. Kim IA, Bae SS, Fernandes A, Wu J, Muschel RJ, McKenna WG, et al. Selective inhibition of Ras, phosphoinositide 3 kinase, and Akt isoforms increases the radiosensitivity of human carcinoma cell lines. Cancer Res. 2005;65:7902-10.

116. Harari PM, Huang SM. Head and neck cancer as a clinical model for molecular targeting of therapy: combining EGFR blockade with radiation. Int J Radiat Oncol Biol Phys. 2001;49:427-33.

117. Thomas M. Cetuximab: adverse event profile and recommendations for toxicity management. Clin J Oncol Nurs. 2005;9:332-8.

118. Fire A, Xu S, Montgomery MK, Kostas SA, Driver SE, Mello CC. Potent and specific genetic interference by double-stranded RNA in Caenorhabditis elegans. Nature. 1998;391:806-11.

119. Elbashir SM, Harborth J, Lendeckel W, Yalcin A, Weber K, Tuschl T. Duplexes of 21-nucleotide RNAs mediate RNA interference in cultured mammalian cells. Nature. 2001;411:494-8.

120. Siomi H, Siomi MC. On the road to reading the RNA-interference code. Nature. 2009;457:396-404.

121. Bernstein E, Caudy AA, Hammond SM, Hannon GJ. Role for a bidentate ribonuclease in the initiation step of RNA interference. Nature. 2001;409:363-6.

122. Liu X, Jiang F, Kalidas S, Smith D, Liu Q. Dicer-2 and R2D2 coordinately bind siRNA to promote assembly of the siRISC complexes. RNA. 2006;12:1514-20.

123. Khvorova A, Reynolds A, Jayasena SD. Functional siRNAs and miRNAs exhibit strand bias. Cell. 2003;115:209-16.

124. Schwarz DS, Hutvagner G, Du T, Xu Z, Aronin N, Zamore PD. Asymmetry in the assembly of the RNAi enzyme complex. Cell. 2003;115:199-208.

125. Leuschner PJ, Ameres SL, Kueng S, Martinez J. Cleavage of the siRNA passenger strand during RISC assembly in human cells. EMBO Rep. 2006;7:314-20.

126. Liu J, Carmell MA, Rivas FV, Marsden CG, Thomson JM, Song JJ, et al. Argonaute2 is the catalytic engine of mammalian RNAi. Science. 2004;305:1437-41.

127. Zamore PD, Aronin N. siRNAs knock down hepatitis. Nat Med. 2003;9:266-7.

128. Whitehurst AW, Bodemann BO, Cardenas J, Ferguson D, Girard L, Peyton M, et al. Synthetic lethal screen identification of chemosensitizer loci in cancer cells. Nature. 2007;446:815-9.

129. Bridge AJ, Pebernard S, Ducraux A, Nicoulaz AL, Iggo R. Induction of an interferon response by RNAi vectors in mammalian cells. Nat Genet. 2003;34:263-4.

130. Sledz CA, Holko M, de Veer MJ, Silverman RH, Williams BR. Activation of the interferon system by short-interfering RNAs. Nat Cell Biol. 2003;5:834-9.

131. Reynolds A, Anderson EM, Vermeulen A, Fedorov Y, Robinson K, Leake D, et al. Induction of the interferon response by siRNA is cell type- and duplex length-dependent. RNA. 2006;12:988-93.

132. Jackson AL, Bartz SR, Schelter J, Kobayashi SV, Burchard J, Mao M, et al. Expression profiling reveals off-target gene regulation by RNAi. Nat Biotechnol. 2003;21:635-7.

133. Semizarov D, Frost L, Sarthy A, Kroeger P, Halbert DN, Fesik SW. Specificity of short interfering RNA determined through gene expression signatures. Proc Natl Acad Sci U S A. 2003;100:6347-52.

134. Jackson AL, Burchard J, Leake D, Reynolds A, Schelter J, Guo J, et al. Position-specific chemical modification of siRNAs reduces "off-target" transcript silencing. RNA. 2006;12:1197-205.

135. Birmingham A, Anderson EM, Reynolds A, Ilsley-Tyree D, Leake D, Fedorov Y, et al. 3' UTR seed matches, but not overall identity, are associated with RNAi off-targets. Nat Methods. 2006;3:199-204.

136. Lin X, Ruan X, Anderson MG, McDowell JA, Kroeger PE, Fesik SW, et al. siRNA-mediated off-target gene silencing triggered by a 7 nt complementation. Nucleic Acids Res. 2005;33:4527-35.

137. Lewis BP, Shih IH, Jones-Rhoades MW, Bartel DP, Burge CB. Prediction of mammalian microRNA targets. Cell. 2003;115:787-98.

138. Kolas NK, Chapman JR, Nakada S, Ylanko J, Chahwan R, Sweeney FD, et al. Orchestration of the DNA-damage response by the RNF8 ubiquitin ligase. Science. 2007;318:1637-40.

139. Doil C, Mailand N, Bekker-Jensen S, Menard P, Larsen DH, Pepperkok R, et al. RNF168 binds and amplifies ubiquitin conjugates on damaged chromosomes to allow accumulation of repair proteins. Cell. 2009;136:435-46.

140. Scholl C, Frohling S, Dunn IF, Schinzel AC, Barbie DA, Kim SY, et al. Synthetic lethal interaction between oncogenic KRAS dependency and STK33 suppression in human cancer cells. Cell. 2009;137:821-34.

141. Turner NC, Lord CJ, Iorns E, Brough R, Swift S, Elliott R, et al. A synthetic lethal siRNA screen identifying genes mediating sensitivity to a PARP inhibitor. EMBO J. 2008;27:1368-77.

142. Iorns E, Turner NC, Elliott R, Syed N, Garrone O, Gasco M, et al. Identification of CDK10 as an important determinant of resistance to endocrine therapy for breast cancer. Cancer Cell. 2008;13:91-104.

143. Woods CM, Zhu J, McQueney PA, Bollag D, Lazarides E. Taxol-induced mitotic block triggers rapid onset of a p53-independent apoptotic pathway. Mol Med. 1995;1:506-26.

144. Mandlekar S, Kong AN. Mechanisms of tamoxifen-induced apoptosis. Apoptosis. 2001;6:469-77.

145. Heddle JA, Carrano AV. The DNA content of micronuclei induced in mouse bone marrow by gamma-irradiation: evidence that micronuclei arise from acentric chromosomal fragments. Mutat Res. 1977;44:63-9.

146. Erenpreisa J, Cragg MS. Mitotic death: a mechanism of survival? A review. Cancer Cell Int. 2001;1:1.

147. Zheng M, Morgan-Lappe SE, Yang J, Bockbrader KM, Pamarthy D, Thomas D, et al. Growth inhibition and radiosensitization of glioblastoma and lung cancer cells by small interfering RNA silencing of tumor necrosis factor receptor-associated factor 2. Cancer Res. 2008;68:7570-8.

148. Sudo H, Tsuji AB, Sugyo A, Imai T, Saga T, Harada YN. A loss of function screen identifies nine new radiation susceptibility genes. Biochem Biophys Res Commun. 2007;364:695-701.

149. Franken NA, Rodermond HM, Stap J, Haveman J, van Bree C. Clonogenic assay of cells in vitro. Nat Protoc. 2006;1:2315-9.

150. Muller WU, Nusse M, Miller BM, Slavotinek A, Viaggi S, Streffer C. Micronuclei: a biological indicator of radiation damage. Mutat Res. 1996;366:163-9.

151. Fenech M. The cytokinesis-block micronucleus technique and its application to genotoxicity studies in human populations. Environ Health Perspect. 1993;101 Suppl 3:101-7.

152. Carrano AV, Natarajan AT. International Commission for Protection Against Environmental Mutagens and Carcinogens. ICPEMC publication no. 14. Considerations for population monitoring using cytogenetic techniques. Mutat Res. 1988;204:379-406.

153. Fenech M. Cytokinesis-block micronucleus assay evolves into a "cytome" assay of chromosomal instability, mitotic dysfunction and cell death. Mutat Res. 2006;600:58-66.

154. Guo GZ, Sasai K, Oya N, Shibata T, Shibuya K, Hiraoka M. A significant correlation between clonogenic radiosensitivity and the simultaneous assessment of micronucleus and apoptotic cell frequencies. Int J Radiat Biol. 1999;75:857-64.

155. Liu ZZ, Huang WY, Li XS, Lin JS, Cai XK, Lian KH, et al. Prediction value of radiosensitivity of hepatocarcinoma cells for apoptosis and micronucleus assay. World J Gastroenterol. 2005;11:7036-9.

156. Bergqvist AS, Brattstrom D, Bergqvist M, Brodin O, Wagenius G, Zetterberg LA. The frequency of micronuclei in lung cancer cell lines and their correlation to intrinsic radiation sensitivity. Anticancer Res. 2001;21:3853-6.

157. Bush C, McMillan TJ. Micronucleus formation in human tumour cells: lack of correlation with radiosensitivity. Br J Cancer. 1993;67:102-6.

158. Fenech M. Cytokinesis-block micronucleus cytome assay. Nat Protoc. 2007;2:1084-104.

159. Vakifahmetoglu H, Olsson M, Zhivotovsky B. Death through a tragedy: mitotic catastrophe. Cell Death Differ. 2008;15:1153-62.

160. Bhattathiri NV, Bharathykkutty C, Prathapan R, Chirayathmanjiyil DA, Nair KM. Prediction of radiosensitivity of oral cancers by serial cytological assay of nuclear changes. Radiother Oncol. 1998;49:61-5.

161. Frankenberg-Schwager M, Frankenberg D, Blocher D, Adamczyk C. Effect of dose rate on the induction of DNA double-strand breaks in eucaryotic cells. Radiat Res. 1981;87:710-7.

162. Bedford JS. Sublethal damage, potentially lethal damage, and chromosomal aberrations in mammalian cells exposed to ionizing radiations. Int J Radiat Oncol Biol Phys. 1991;21:1457-69.

163. Rogakou EP, Pilch DR, Orr AH, Ivanova VS, Bonner WM. DNA double-stranded breaks induce histone H2AX phosphorylation on serine 139. J Biol Chem. 1998;273:5858-68.

164. Furuta T, Takemura H, Liao ZY, Aune GJ, Redon C, Sedelnikova OA, et al. Phosphorylation of histone H2AX and activation of Mre11, Rad50, and Nbs1 in response to replication-dependent DNA double-strand breaks induced by mammalian DNA topoisomerase I cleavage complexes. J Biol Chem. 2003;278:20303-12.

165. Burma S, Chen BP, Murphy M, Kurimasa A, Chen DJ. ATM phosphorylates histone H2AX in response to DNA double-strand breaks. J Biol Chem. 2001;276:42462-7.

166. Shiloh Y. ATM and related protein kinases: safeguarding genome integrity. Nat Rev Cancer. 2003;3:155-68.

167. Sedelnikova OA, Rogakou EP, Panyutin IG, Bonner WM. Quantitative detection of (125)IdU-induced DNA double-strand breaks with gamma-H2AX antibody. Radiat Res. 2002;158:486-92.

168. Riballo E, Kuhne M, Rief N, Doherty A, Smith GC, Recio MJ, et al. A pathway of double-strand break rejoining dependent upon ATM, Artemis, and proteins locating to gamma-H2AX foci. Mol Cell. 2004;16:715-24.

169. Banath JP, Macphail SH, Olive PL. Radiation sensitivity, H2AX phosphorylation, and kinetics of repair of DNA strand breaks in irradiated cervical cancer cell lines. Cancer Res. 2004;64:7144-9.

170. Taneja N, Davis M, Choy JS, Beckett MA, Singh R, Kron SJ, et al. Histone H2AX phosphorylation as a predictor of radiosensitivity and target for radiotherapy. J Biol Chem. 2004;279:2273-80.

171. Klokov D, MacPhail SM, Banath JP, Byrne JP, Olive PL. Phosphorylated histone H2AX in relation to cell survival in tumor cells and xenografts exposed to single and fractionated doses of X-rays. Radiother Oncol. 2006;80:223-9.

172. Joubert A, Zimmerman KM, Bencokova Z, Gastaldo J, Chavaudra N, Favaudon V, et al. DNA double-strand break repair defects in syndromes associated with acute radiation response: at least two different assays to predict intrinsic radiosensitivity? Int J Radiat Biol. 2008;84:107-25.

173. Markova E, Schultz N, Belyaev IY. Kinetics and dose-response of residual 53BP1/gamma-H2AX foci: co-localization, relationship with DSB repair and clonogenic survival. Int J Radiat Biol. 2007;83:319-29.

174. Mahrhofer H, Burger S, Oppitz U, Flentje M, Djuzenova CS. Radiation induced DNA damage and damage repair in human tumor and fibroblast cell lines assessed by histone H2AX phosphorylation. Int J Radiat Oncol Biol Phys. 2006;64:573-80.

175. Pilch DR, Sedelnikova OA, Redon C, Celeste A, Nussenzweig A, Bonner WM. Characteristics of gamma-H2AX foci at DNA double-strand breaks sites. Biochem Cell Biol. 2003;81:123-9.

176. Pollard JM, Gatti RA. Clinical radiation sensitivity with DNA repair disorders: an overview. Int J Radiat Oncol Biol Phys. 2009;74:1323-31.

177. Kasid U, Pfeifer A, Weichselbaum RR, Dritschilo A, Mark GE. The raf oncogene is associated with a radiation-resistant human laryngeal cancer. Science. 1987;237:1039-41.

178. Zhao Y, Thomas HD, Batey MA, Cowell IG, Richardson CJ, Griffin RJ, et al. Preclinical evaluation of a potent novel DNA-dependent protein kinase inhibitor NU7441. Cancer Res. 2006;66:5354-62.

179. Kapuscinski J. DAPI: a DNA-specific fluorescent probe. Biotech Histochem. 1995;70:220-33.

180. Boutros M, Bras LP, Huber W. Analysis of cell-based RNAi screens. Genome Biol. 2006;7:R66.

181. Puck TT, Marcus PI. Action of x-rays on mammalian cells. J Exp Med. 1956;103:653-66.

182. Wouters A, Pauwels B, Lambrechts HA, Pattyn GG, Ides J, Baay M, et al. Counting clonogenic assays from normoxic and anoxic irradiation experiments manually or by using densitometric software. Phys Med Biol. 2010;55:N167-78.

183. Barber PR, Vojnovic B, Kelly J, Mayes CR, Boulton P, Woodcock M, et al. Automated counting of mammalian cell colonies. Phys Med Biol. 2001;46:63-76.

184. Dale RG. The application of the linear-quadratic dose-effect equation to fractionated and protracted radiotherapy. Br J Radiol. 1985;58:515-28.

185. Pierce AJ, Johnson RD, Thompson LH, Jasin M. XRCC3 promotes homology-directed repair of DNA damage in mammalian cells. Genes Dev. 1999;13:2633-8.

186. Loi S, Haibe-Kains B, Desmedt C, Lallemand F, Tutt AM, Gillet C, et al. Definition of clinically distinct molecular subtypes in estrogen receptor-positive breast carcinomas through genomic grade. J Clin Oncol. 2007;25:1239-46.

187. Loi S, Haibe-Kains B, Desmedt C, Wirapati P, Lallemand F, Tutt AM, et al. Predicting prognosis using molecular profiling in estrogen receptor-positive breast cancer treated with tamoxifen. BMC Genomics. 2008;9:239.

188. Camps C, Buffa FM, Colella S, Moore J, Sotiriou C, Sheldon H, et al. hsa-miR-210 Is induced by hypoxia and is an independent prognostic factor in breast cancer. Clin Cancer Res. 2008;14:1340-8.

189. Wu Z IR, Gentleman R, Martinez-Murillo F, Spencer F. A Model-Based Background Adjustment for Oligonucleotide Expression Arrays. Journal of the American Statistical Association 2004;99:909–17.

190. Bioconductor Open Source Software For Bioinformatics. http://wwwbioconductor.org/

191. National Centre for Biotechnology Information Gene Expression Omnibus. http://www.ncbi.nlm.nih.gov/geo/

192. Miller LD, Smeds J, George J, Vega VB, Vergara L, Ploner A, et al. An expression signature for p53 status in human breast cancer predicts mutation status, transcriptional effects, and patient survival. Proc Natl Acad Sci U S A. 2005;102:13550-5.

193. Wang Y, Klijn JG, Zhang Y, Sieuwerts AM, Look MP, Yang F, et al. Gene-expression profiles to predict distant metastasis of lymph-node-negative primary breast cancer. Lancet. 2005;365:671-9.

194. Carroll JS, Meyer CA, Song J, Li W, Geistlinger TR, Eeckhoute J, et al. Genome-wide analysis of estrogen receptor binding sites. Nat Genet. 2006;38:1289-97.

195. Buffa FM, Harris AL, West CM, Miller CJ. Large meta-analysis of multiple cancers reveals a common, compact and highly prognostic hypoxia metagene. Br J Cancer. 2010;102:428-35.

196. Nogales-Cadenas R, Carmona-Saez P, Vazquez M, Vicente C, Yang X, Tirado F, et al. GeneCodis: interpreting gene lists through enrichment analysis and integration of diverse biological information. Nucleic Acids Res. 2009;37:W317-22.

197. Hudis CA, Barlow WE, Costantino JP, Gray RJ, Pritchard KI, Chapman JA, et al. Proposal for standardized definitions for efficacy end points in adjuvant breast cancer trials: the STEEP system. J Clin Oncol. 2007;25:2127-32.

198. Prevo R, Deutsch E, Sampson O, Diplexcito J, Cengel K, Harper J, et al. Class I PI3 kinase inhibition by the pyridinylfuranopyrimidine inhibitor PI-103 enhances tumor radiosensitivity. Cancer Res. 2008;68:5915-23.

199. Zhou C, Smith JL, Liu J. Role of BRCA1 in cellular resistance to paclitaxel and ionizing radiation in an ovarian cancer cell line carrying a defective BRCA1. Oncogene. 2003;22:2396-404.

200. Abbott DW, Freeman ML, Holt JT. Double-strand break repair deficiency and radiation sensitivity in BRCA2 mutant cancer cells. J Natl Cancer Inst. 1998;90:978-85.

201. Yun MH, Hiom K. CtIP-BRCA1 modulates the choice of DNA double-strand-break repair pathway throughout the cell cycle. Nature. 2009;459:460-3.

202. Adachi N, Ishino T, Ishii Y, Takeda S, Koyama H. DNA ligase IV-deficient cells are more resistant to ionizing radiation in the absence of Ku70: Implications for DNA double-strand break repair. Proc Natl Acad Sci U S A. 2001;98:12109-13.

203. Finnie NJ, Gottlieb TM, Blunt T, Jeggo PA, Jackson SP. DNA-dependent protein kinase activity is absent in xrs-6 cells: implications for site-specific recombination and DNA double-strand break repair. Proc Natl Acad Sci U S A. 1995;92:320-4.

204. Kurimasa A, Ouyang H, Dong LJ, Wang S, Li X, Cordon-Cardo C, et al. Catalytic subunit of DNA-dependent protein kinase: impact on lymphocyte development and tumorigenesis. Proc Natl Acad Sci U S A. 1999;96:1403-8.

205. Kao GD, McKenna WG, Guenther MG, Muschel RJ, Lazar MA, Yen TJ. Histone deacetylase 4 interacts with 53BP1 to mediate the DNA damage response. J Cell Biol. 2003;160:1017-27.

206. Chou DM, Elledge SJ. Tipin and Timeless form a mutually protective complex required for genotoxic stress resistance and checkpoint function. Proc Natl Acad Sci U S A. 2006;103:18143-7.

207. Burkovics P, Hajdu I, Szukacsov V, Unk I, Haracska L. Role of PCNA-dependent stimulation of 3'-phosphodiesterase and 3'-5' exonuclease activities of human Ape2 in repair of oxidative DNA damage. Nucleic Acids Res. 2009;37:4247-55.

208. Burkovics P, Szukacsov V, Unk I, Haracska L. Human Ape2 protein has a 3'-5' exonuclease activity that acts preferentially on mismatched base pairs. Nucleic Acids Res. 2006;34:2508-15.

209. Nakatsu Y, Asahina H, Citterio E, Rademakers S, Vermeulen W, Kamiuchi S, et al. XAB2, a novel tetratricopeptide repeat protein involved in transcription-coupled DNA repair and transcription. J Biol Chem. 2000;275:34931-7.

210. Lord CJ, McDonald S, Swift S, Turner NC, Ashworth A. A high-throughput RNA interference screen for DNA repair determinants of PARP inhibitor sensitivity. DNA Repair (Amst). 2008;7:2010-9.

211. Yamamoto G, Irie T, Aida T, Nagoshi Y, Tsuchiya R, Tachikawa T. Correlation of invasion and metastasis of cancer cells, and expression of the RAD21 gene in oral squamous cell carcinoma. Virchows Arch. 2006;448:435-41.

212. Atienza JM, Roth RB, Rosette C, Smylie KJ, Kammerer S, Rehbock J, et al. Suppression of RAD21 gene expression decreases cell growth and enhances cytotoxicity of etoposide and bleomycin in human breast cancer cells. Mol Cancer Ther. 2005;4:361-8.

213. Arana ME, Seki M, Wood RD, Rogozin IB, Kunkel TA. Low-fidelity DNA synthesis by human DNA polymerase theta. Nucleic Acids Res. 2008;36:3847-56.

214. Seki M, Masutani C, Yang LW, Schuffert A, Iwai S, Bahar I, et al. High-efficiency bypass of DNA damage by human DNA polymerase Q. EMBO J. 2004;23:4484-94.

215. Kawamura K, Bahar R, Seimiya M, Chiyo M, Wada A, Okada S, et al. DNA polymerase theta is preferentially expressed in lymphoid tissues and upregulated in human cancers. Int J Cancer. 2004;109:9-16.

216. Martomo SA, Saribasak H, Yokoi M, Hanaoka F, Gearhart PJ. Reevaluation of the role of DNA polymerase theta in somatic hypermutation of immunoglobulin genes. DNA Repair (Amst). 2008;7:1603-8.

217. Chen S, Blank JL, Peters T, Liu XJ, Rappoli DM, Pickard MD, et al. Genome-wide siRNA screen for modulators of cell death induced by proteasome inhibitor bortezomib. Cancer Res. 2010;70:4318-26.

218. Ang F, Wong AP, Ng MM, Chu JJ. Small interference RNA profiling reveals the essential role of human membrane trafficking genes in mediating the infectious entry of dengue virus. Virol J. 2010;7:24.

219. Harrington H. The effect of x irradiation on the progress of strain U-12 fibroblasts through the mitotic cycle. Ann N Y Acad Sci. 1961;95:901-10.

220. Stupp R, Mason WP, van den Bent MJ, Weller M, Fisher B, Taphoorn MJ, et al. Radiotherapy plus concomitant and adjuvant temozolomide for glioblastoma. N Engl J Med. 2005;352:987-96.

221. Trivedi RN, Almeida KH, Fornsaglio JL, Schamus S, Sobol RW. The role of base excision repair in the sensitivity and resistance to temozolomide-mediated cell death. Cancer Res. 2005;65:6394-400.

222. Yoshimura M, Kohzaki M, Nakamura J, Asagoshi K, Sonoda E, Hou E, et al. Vertebrate POLQ and POLbeta cooperate in base excision repair of oxidative DNA damage. Mol Cell. 2006;24:115-25.

223. Prasad R, Longley MJ, Sharief FS, Hou EW, Copeland WC, Wilson SH. Human DNA polymerase theta possesses 5'-dRP lyase activity and functions in single-nucleotide base excision repair in vitro. Nucleic Acids Res. 2009;37:1868-77.

224. Brunner TB, Geiger M, Grabenbauer GG, Lang-Welzenbach M, Mantoni TS, Cavallaro A, et al. Phase I trial of the human immunodeficiency virus protease inhibitor nelfinavir and chemoradiation for locally advanced pancreatic cancer. J Clin Oncol. 2008;26:2699-706.

225. Bencokova Z, Kaufmann MR, Pires IM, Lecane PS, Giaccia AJ, Hammond EM. ATM activation and signaling under hypoxic conditions. Mol Cell Biol. 2009;29:526-37.

226. Gotoff SP, Amirmokri E, Liebner EJ. Ataxia telangiectasia. Neoplasia, untoward response to x-irradiation, and tuberous sclerosis. Am J Dis Child. 1967;114:617-25.

227. Morgan JL, Holcomb TM, Morrissey RW. Radiation reaction in ataxia telangiectasia. Am J Dis Child. 1968;116:557-8.

228. McManus KJ, Hendzel MJ. ATM-dependent DNA damage-independent mitotic phosphorylation of H2AX in normally growing mammalian cells. Mol Biol Cell. 2005;16:5013-25.

229. Hadi MZ, Wilson DM, 3rd. Second human protein with homology to the Escherichia coli abasic endonuclease exonuclease III. Environ Mol Mutagen. 2000;36:312-24.

230. Ide Y, Tsuchimoto D, Tominaga Y, Nakashima M, Watanabe T, Sakumi K, et al. Growth retardation and dyslymphopoiesis accompanied by G2/M arrest in APEX2-null mice. Blood. 2004;104:4097-103.

231. Yonemasu R, Minami M, Nakatsu Y, Takeuchi M, Kuraoka I, Matsuda Y, et al. Disruption of mouse XAB2 gene involved in pre-mRNA splicing, transcription and transcription-coupled DNA repair results in preimplantation lethality. DNA Repair (Amst). 2005;4:479-91.

232. Hoque MT, Ishikawa F. Human chromatid cohesin component hRad21 is phosphorylated in M phase and associated with metaphase centromeres. J Biol Chem. 2001;276:5059-67.

233. Birkenbihl RP, Subramani S. Cloning and characterization of rad21 an essential gene of Schizosaccharomyces pombe involved in DNA double-strand-break repair. Nucleic Acids Res. 1992;20:6605-11.

234. Sehl ME, Langer LR, Papp JC, Kwan L, Seldon JL, Arellano G, et al. Associations between single nucleotide polymorphisms in double-stranded DNA repair pathway genes and familial breast cancer. Clin Cancer Res. 2009;15:2192-203.

235. Severin DM, Leong T, Cassidy B, Elsaleh H, Peters L, Venter D, et al. Novel DNA sequence variants in the hHR21 DNA repair gene in radiosensitive cancer patients. Int J Radiat Oncol Biol Phys. 2001;50:1323-31.

236. Azria D, Ozsahin M, Kramar A, Peters S, Atencio DP, Crompton NE, et al. Single nucleotide polymorphisms, apoptosis, and the development of severe late adverse effects after radiotherapy. Clin Cancer Res. 2008;14:6284-8.

237. Zan H, Shima N, Xu Z, Al-Qahtani A, Evinger Iii AJ, Zhong Y, et al. The translesion DNA polymerase theta plays a dominant role in immunoglobulin gene somatic hypermutation. EMBO J. 2005;24:3757-69.

238. Masuda K, Ouchida R, Hikida M, Nakayama M, Ohara O, Kurosaki T, et al. Absence of DNA polymerase theta results in decreased somatic hypermutation frequency and altered mutation patterns in Ig genes. DNA Repair (Amst). 2006;5:1384-91.

239. Harris PV, Mazina OM, Leonhardt EA, Case RB, Boyd JB, Burtis KC. Molecular cloning of Drosophila mus308, a gene involved in DNA cross-link repair with homology to prokaryotic DNA polymerase I genes. Mol Cell Biol. 1996;16:5764-71.

240. Boyd JB, Sakaguchi K, Harris PV. mus308 mutants of Drosophila exhibit hypersensitivity to DNA cross-linking agents and are defective in a deoxyribonuclease. Genetics. 1990;125:813-9.

241. Justice MJ, Noveroske JK, Weber JS, Zheng B, Bradley A. Mouse ENU mutagenesis. Hum Mol Genet. 1999;8:1955-63.

242. Shima N, Hartford SA, Duffy T, Wilson LA, Schimenti KJ, Schimenti JC. Phenotype-based identification of mouse chromosome instability mutants. Genetics. 2003;163:1031-40.

243. Shima N, Munroe RJ, Schimenti JC. The mouse genomic instability mutation chaos1 is an allele of Polq that exhibits genetic interaction with Atm. Mol Cell Biol. 2004;24:10381-9.

244. Sharief FS, Vojta PJ, Ropp PA, Copeland WC. Cloning and chromosomal mapping of the human DNA polymerase theta (POLQ), the eighth human DNA polymerase. Genomics. 1999;59:90-6.

245. Maga G, Shevelev I, Ramadan K, Spadari S, Hubscher U. DNA polymerase theta purified from human cells is a high-fidelity enzyme. J Mol Biol. 2002;319:359-69.

246. Seki M, Marini F, Wood RD. POLQ (Pol theta), a DNA polymerase and DNA-dependent ATPase in human cells. Nucleic Acids Res. 2003;31:6117-26.

247. Marini F, Wood RD. A human DNA helicase homologous to the DNA cross-link sensitivity protein Mus308. J Biol Chem. 2002;277:8716-23.

248. Marini F, Kim N, Schuffert A, Wood RD. POLN, a nuclear PolA family DNA polymerase homologous to the DNA cross-link sensitivity protein Mus308. J Biol Chem. 2003;278:32014-9.

249. Muzzini DM, Plevani P, Boulton SJ, Cassata G, Marini F. Caenorhabditis elegans POLQ-1 and HEL-308 function in two distinct DNA interstrand cross-link repair pathways. DNA Repair (Amst). 2008;7:941-50.

250. Takata K, Arana ME, Seki M, Kunkel TA, Wood RD. Evolutionary conservation of residues in vertebrate DNA polymerase N conferring low fidelity and bypass activity. Nucleic Acids Res. 2010;38:3233-44.

251. Lindahl T, Nyberg B. Rate of depurination of native deoxyribonucleic acid. Biochemistry. 1972;11:3610-8.

252. Nakamura J, Walker VE, Upton PB, Chiang SY, Kow YW, Swenberg JA. Highly sensitive apurinic/apyrimidinic site assay can detect spontaneous and chemically induced depurination under physiological conditions. Cancer Res. 1998;58:222-5.

253. Loeb LA. Apurinic sites as mutagenic intermediates. Cell. 1985;40:483-4.

254. Guillet M, Boiteux S. Endogenous DNA abasic sites cause cell death in the absence of Apn1, Apn2 and Rad1/Rad10 in Saccharomyces cerevisiae. EMBO J. 2002;21:2833-41.

255. Kusumoto R, Masutani C, Iwai S, Hanaoka F. Translesion synthesis by human DNA polymerase eta across thymine glycol lesions. Biochemistry. 2002;41:6090-9.

256. Johnson RE, Washington MT, Haracska L, Prakash S, Prakash L. Eukaryotic polymerases iota and zeta act sequentially to bypass DNA lesions. Nature. 2000;406:1015-9.

257. Seki M, Wood RD. DNA polymerase theta (POLQ) can extend from mismatches and from bases opposite a (6-4) photoproduct. DNA Repair (Amst). 2008;7:119-27.

258. Rajewsky K, Forster I, Cumano A. Evolutionary and somatic selection of the antibody repertoire in the mouse. Science. 1987;238:1088-94.

259. Muramatsu M, Sankaranand VS, Anant S, Sugai M, Kinoshita K, Davidson NO, et al. Specific expression of activation-induced cytidine deaminase (AID), a novel member of the RNA-editing deaminase family in germinal center B cells. J Biol Chem. 1999;274:18470-6.

260. Di Noia J, Neuberger MS. Altering the pathway of immunoglobulin hypermutation by inhibiting uracil-DNA glycosylase. Nature. 2002;419:43-8.

261. Zeng X, Winter DB, Kasmer C, Kraemer KH, Lehmann AR, Gearhart PJ. DNA polymerase eta is an A-T mutator in somatic hypermutation of immunoglobulin variable genes. Nat Immunol. 2001;2:537-41.

262. Masuda K, Ouchida R, Takeuchi A, Saito T, Koseki H, Kawamura K, et al. DNA polymerase theta contributes to the generation of C/G mutations during somatic hypermutation of Ig genes. Proc Natl Acad Sci U S A. 2005;102:13986-91.

263. Masuda K, Ouchida R, Hikida M, Kurosaki T, Yokoi M, Masutani C, et al. DNA polymerases eta and theta function in the same genetic pathway to generate mutations at A/T during somatic hypermutation of Ig genes. J Biol Chem. 2007;282:17387-94.

264. Kohzaki M, Nishihara K, Hirota K, Sonoda E, Yoshimura M, Ekino S, et al. DNA polymerases nu and theta are required for efficient immunoglobulin V gene diversification in chicken. J Cell Biol. 2010;189:1117-27.

265. Barnes DE, Lindahl T, Sedgwick B. DNA repair. Curr Opin Cell Biol. 1993;5:424-33.

266. Demple B, Herman T, Chen DS. Cloning and expression of APE, the cDNA encoding the major human apurinic endonuclease: definition of a family of DNA repair enzymes. Proc Natl Acad Sci U S A. 1991;88:11450-4.

267. Sobol RW, Prasad R, Evenski A, Baker A, Yang XP, Horton JK, et al. The lyase activity of the DNA repair protein beta-polymerase protects from DNA-damage-induced cytotoxicity. Nature. 2000;405:807-10.

268. Allinson SL, Dianova, II, Dianov GL. DNA polymerase beta is the major dRP lyase involved in repair of oxidative base lesions in DNA by mammalian cell extracts. EMBO J. 2001;20:6919-26.

269. Sleeth KM, Robson RL, Dianov GL. Exchangeability of mammalian DNA ligases between base excision repair pathways. Biochemistry. 2004;43:12924-30.

270. Podlutsky AJ, Dianova, II, Podust VN, Bohr VA, Dianov GL. Human DNA polymerase beta initiates DNA synthesis during long-patch repair of reduced AP sites in DNA. EMBO J. 2001;20:1477-82.

271. Zharkov DO. Base excision DNA repair. Cell Mol Life Sci. 2008;65:1544-65.

272. Kim K, Biade S, Matsumoto Y. Involvement of flap endonuclease 1 in base excision DNA repair. J Biol Chem. 1998;273:8842-8.

273. Friedrich-Heineken E, Toueille M, Tannler B, Burki C, Ferrari E, Hottiger MO, et al. The two DNA clamps Rad9/Rad1/Hus1 complex and proliferating cell nuclear antigen differentially regulate flap endonuclease 1 activity. J Mol Biol. 2005;353:980-9.

274. David SS, O'Shea VL, Kundu S. Base-excision repair of oxidative DNA damage. Nature. 2007;447:941-50.

275. Wijeratne SS, Cuppett SL, Schlegel V. Hydrogen peroxide induced oxidative stress damage and antioxidant enzyme response in Caco-2 human colon cells. J Agric Food Chem. 2005;53:8768-74.

276. Goff JP, Shields DS, Seki M, Choi S, Epperly MW, Dixon T, et al. Lack of DNA Polymerase theta (POLQ) Radiosensitizes Bone Marrow Stromal Cells In Vitro and Increases Reticulocyte Micronuclei after Total-Body Irradiation. Radiat Res. 2009;172:165-74.

277. Wang X, Szabo C, Qian C, Amadio PG, Thibodeau SN, Cerhan JR, et al. Mutational analysis of thirty-two double-strand DNA break repair genes in breast and pancreatic cancers. Cancer Res. 2008;68:971-5.

278. Sinha BK, Haim N, Dusre L, Kerrigan D, Pommier Y. DNA strand breaks produced by etoposide (VP-16,213) in sensitive and resistant human breast tumor cells: implications for the mechanism of action. Cancer Res. 1988;48:5096-100.

279. Tewey KM, Rowe TC, Yang L, Halligan BD, Liu LF. Adriamycin-induced DNA damage mediated by mammalian DNA topoisomerase II. Science. 1984;226:466-8.

280. Swift LP, Rephaeli A, Nudelman A, Phillips DR, Cutts SM. Doxorubicin-DNA adducts induce a non-topoisomerase II-mediated form of cell death. Cancer Res. 2006;66:4863-71.

281. Eisenhauer EA, Vermorken JB. The taxoids. Comparative clinical pharmacology and therapeutic potential. Drugs. 1998;55:5-30.

282. Goldenberg GJ, Wang H, Blair GW. Resistance to adriamycin: relationship of cytotoxicity to drug uptake and DNA single- and double-strand breakage in cloned cell lines of adriamycin-sensitive and -resistant P388 leukemia. Cancer Res. 1986;46:2978-83.

283. Mao Z, Bozzella M, Seluanov A, Gorbunova V. Comparison of nonhomologous end joining and homologous recombination in human cells. DNA Repair (Amst). 2008;7:1765-71.

284. Kuhne M, Riballo E, Rief N, Rothkamm K, Jeggo PA, Lobrich M. A double-strand break repair defect in ATM-deficient cells contributes to radiosensitivity. Cancer Res. 2004;64:500-8.

285. Lobrich M, Shibata A, Beucher A, Fisher A, Ensminger M, Goodarzi AA, et al. gammaH2AX foci analysis for monitoring DNA double-strand break repair: strengths, limitations and optimization. Cell Cycle. 2010;9:662-9.

286. Sonoda E, Sasaki MS, Buerstedde JM, Bezzubova O, Shinohara A, Ogawa H, et al. Rad51-deficient vertebrate cells accumulate chromosomal breaks prior to cell death. EMBO J. 1998;17:598-608.

287. Bindra RS, Schaffer PJ, Meng A, Woo J, Maseide K, Roth ME, et al. Down-regulation of Rad51 and decreased homologous recombination in hypoxic cancer cells. Mol Cell Biol. 2004;24:8504-18.

288. Higgins GS, Prevo R, Lee YF, Helleday T, Muschel RJ, Taylor S, et al. A small interfering RNA screen of genes involved in DNA repair identifies tumor-specific radiosensitization by POLQ knockdown. Cancer Res. 2010;70:2984-93.

289. Hartlerode AJ, Scully R. Mechanisms of double-strand break repair in somatic mammalian cells. Biochem J. 2009;423:157-68.

290. Helleday T. Homologous recombination in cancer development, treatment and development of drug resistance. Carcinogenesis. 2010;31:955-60.

291. McVey M, Lee SE. MMEJ repair of double-strand breaks (director's cut): deleted sequences and alternative endings. Trends Genet. 2008;24:529-38.

292. Chan SH, Yu AM, McVey M. Dual roles for DNA polymerase theta in alternative end-joining repair of double-strand breaks in Drosophila. PLoS Genet. 2010;6:e1001005.

293. Yu AM, McVey M. Synthesis-dependent microhomology-mediated end joining accounts for multiple types of repair junctions. Nucleic Acids Res. 2010.

294. Ukai A, Maruyama T, Mochizuki S, Ouchida R, Masuda K, Kawamura K, et al. Role of DNA polymerase theta in tolerance of endogenous and exogenous DNA damage in mouse B cells. Genes Cells. 2006;11:111-21.

295. Galea MH, Blamey RW, Elston CE, Ellis IO. The Nottingham Prognostic Index in primary breast cancer. Breast Cancer Res Treat. 1992;22:207-19.

296. Williams C, Brunskill S, Altman D, Briggs A, Campbell H, Clarke M, et al. Cost-effectiveness of using prognostic information to select women with breast cancer for adjuvant systemic therapy. Health Technol Assess. 2006;10:iii-iv, ix-xi, 1-204.

297. Piccart-Gebhart MJ, Procter M, Leyland-Jones B, Goldhirsch A, Untch M, Smith I, et al. Trastuzumab after adjuvant chemotherapy in HER2-positive breast cancer. N Engl J Med. 2005;353:1659-72.

298. Andrulis IL, Bull SB, Blackstein ME, Sutherland D, Mak C, Sidlofsky S, et al. neu/erbB-2 amplification identifies a poor-prognosis group of women with node-negative breast cancer. Toronto Breast Cancer Study Group. J Clin Oncol. 1998;16:1340-9.

299. Seshadri R, Firgaira FA, Horsfall DJ, McCaul K, Setlur V, Kitchen P. Clinical significance of HER-2/neu oncogene amplification in primary breast cancer. The South Australian Breast Cancer Study Group. J Clin Oncol. 1993;11:1936-42.

300. Parl FF, Schmidt BP, Dupont WD, Wagner RK. Prognostic significance of estrogen receptor status in breast cancer in relation to tumor stage, axillary node metastasis, and histopathologic grading. Cancer. 1984;54:2237-42.

301. Kinne DW, Butler JA, Kimmel M, Flehinger BJ, Menendez-Botet C, Schwartz M. Estrogen receptor protein of breast cancer in patients with positive nodes. High recurrence rates in the postmenopausal estrogen receptor-negative group. Arch Surg. 1987;122:1303-6.

302. Harris L, Fritsche H, Mennel R, Norton L, Ravdin P, Taube S, et al. American Society of Clinical Oncology 2007 update of recommendations for the use of tumor markers in breast cancer. J Clin Oncol. 2007;25:5287-312.

303. Chen HY, Yu SL, Chen CH, Chang GC, Chen CY, Yuan A, et al. A five-gene signature and clinical outcome in non-small-cell lung cancer. N Engl J Med. 2007;356:11-20.

304. Pramana J, Van den Brekel MW, van Velthuysen ML, Wessels LF, Nuyten DS, Hofland I, et al. Gene expression profiling to predict outcome after chemoradiation in head and neck cancer. Int J Radiat Oncol Biol Phys. 2007;69:1544-52.

305. de Jong MC, Pramana J, Knegjens JL, Balm AJ, van den Brekel MW, Hauptmann M, et al. HPV and high-risk gene expression profiles predict response to chemoradiotherapy in head and neck cancer, independent of clinical factors. Radiother Oncol. 2010;95:365-70.

306. Clark-Langone KM, Wu JY, Sangli C, Chen A, Snable JL, Nguyen A, et al. Biomarker discovery for colon cancer using a 761 gene RT-PCR assay. BMC Genomics. 2007;8:279.

307. Eschrich SA, Pramana J, Zhang H, Zhao H, Boulware D, Lee JH, et al. A gene expression model of intrinsic tumor radiosensitivity: prediction of response and prognosis after chemoradiation. Int J Radiat Oncol Biol Phys. 2009;75:489-96.

308. Winter SC, Buffa FM, Silva P, Miller C, Valentine HR, Turley H, et al. Relation of a hypoxia metagene derived from head and neck cancer to prognosis of multiple cancers. Cancer Res. 2007;67:3441-9.

309. Elston CW, Ellis IO. Pathological prognostic factors in breast cancer. I. The value of histological grade in breast cancer: experience from a large study with long-term follow-up. Histopathology. 1991;19:403-10.

310. van 't Veer LJ, Dai H, van de Vijver MJ, He YD, Hart AA, Mao M, et al. Gene expression profiling predicts clinical outcome of breast cancer. Nature. 2002;415:530-6.

311. van de Vijver MJ, He YD, van't Veer LJ, Dai H, Hart AA, Voskuil DW, et al. A gene-expression signature as a predictor of survival in breast cancer. N Engl J Med. 2002;347:1999-2009.

312. Knauer M, Mook S, Rutgers EJ, Bender RA, Hauptmann M, van de Vijver MJ, et al. The predictive value of the 70-gene signature for adjuvant chemotherapy in early breast cancer. Breast Cancer Res Treat. 2010;120:655-61.

313. Foekens JA, Atkins D, Zhang Y, Sweep FC, Harbeck N, Paradiso A, et al. Multicenter validation of a gene expression-based prognostic signature in lymph node-negative primary breast cancer. J Clin Oncol. 2006;24:1665-71.

314. Desmedt C, Piette F, Loi S, Wang Y, Lallemand F, Haibe-Kains B, et al. Strong time dependence of the 76-gene prognostic signature for node-negative breast cancer patients in the TRANSBIG multicenter independent validation series. Clin Cancer Res. 2007;13:3207-14.

315. Sotiriou C, Wirapati P, Loi S, Harris A, Fox S, Smeds J, et al. Gene expression profiling in breast cancer: understanding the molecular basis of histologic grade to improve prognosis. J Natl Cancer Inst. 2006;98:262-72.

316. Desmedt C, Giobbie-Hurder A, Neven P, Paridaens R, Christiaens MR, Smeets A, et al. The Gene expression Grade Index: a potential predictor of relapse for endocrine-treated breast cancer patients in the BIG 1-98 trial. BMC Med Genomics. 2009;2:40.

317. Nielsen NH, Arnerlov C, Emdin SO, Landberg G. Cyclin E overexpression, a negative prognostic factor in breast cancer with strong correlation to oestrogen receptor status. Br J Cancer. 1996;74:874-80.

318. Matakidou A, el Galta R, Webb EL, Rudd MF, Bridle H, Eisen T, et al. Genetic variation in the DNA repair genes is predictive of outcome in lung cancer. Hum Mol Genet. 2007;16:2333-40.

319. Clarke M, Collins R, Darby S, Davies C, Elphinstone P, Evans E, et al. Effects of radiotherapy and of differences in the extent of surgery for early breast cancer on local recurrence and 15-year survival: an overview of the randomised trials. Lancet. 2005;366:2087-106.

320. Effects of chemotherapy and hormonal therapy for early breast cancer on recurrence and 15-year survival: an overview of the randomised trials. Lancet. 2005;365:1687-717.

321. Pillaire MJ, Selves J, Gordien K, Gourraud PA, Gentil C, Danjoux M, et al. A 'DNA replication' signature of progression and negative outcome in colorectal cancer. Oncogene. 2010;29:876-87.

322. Koff A, Giordano A, Desai D, Yamashita K, Harper JW, Elledge S, et al. Formation and activation of a cyclin E-cdk2 complex during the G1 phase of the human cell cycle. Science. 1992;257:1689-94.

323. Resnitzky D, Gossen M, Bujard H, Reed SI. Acceleration of the G1/S phase transition by expression of cyclins D1 and E with an inducible system. Mol Cell Biol. 1994;14:1669-79.

324. Wang L, Shao ZM. Cyclin e expression and prognosis in breast cancer patients: a meta-analysis of published studies. Cancer Invest. 2006;24:581-7.

325. Higgins GS, Harris AL, Prevo R, Helleday T, McKenna WG, Buffa FM. Overexpression Of POLQ Confers a Poor Prognosis In Early Breast Cancer Patients. Oncotarget. 2010;1:175-84.

326. Lemee F, Bergoglio V, Fernandez-Vidal A, Machado-Silva A, Pillaire MJ, Bieth A, et al. DNA polymerase {theta} up-regulation is associated with poor survival in breast cancer, perturbs DNA replication, and promotes genetic instability. Proc Natl Acad Sci U S A. 2010;107:13390-5.

327. Pastwa E, Somiari RI, Malinowski M, Somiari SB, Winters TA. In vitro non-homologous DNA end joining assays--the 20th anniversary. Int J Biochem Cell Biol. 2009;41:1254-60.

328. Cianfrocca M, Goldstein LJ. Prognostic and predictive factors in early-stage breast cancer. Oncologist. 2004;9:606-16.

APPENDIX

Supplementary Table 1. The radiosensitivity screen was conducted on a custom designed siRNA library of 200 genes involved in DNA repair comprising the genes listed above.

AKT1	CDK6	ERCC6	IRS1	NEIL1	POLM	RECQL	TOP1
AKT2	CETN2	EXO1	KIAA1596	NEIL2	POLN	RECQL4	TOP2A
APEX1	CFDP1	FANCA	LGP2	NEIL3	POLQ	RECQL5	TOP3A
APEX2	CHEK1	FANCB	LIG3	NEK2	POT1	REV1L	TOP3B
ATM	CHEK2	FANCC	LIG4	NTHL1	PP3856	REV3L	TOPBP1
ATR	CHTF18	FANCD2	MAD2L2	NUDT1	PRDX2	RFC1	TP53BP1
BLM	CKN1	FANCE	MAP2K2	PARP1	PRKDC	RNF40	TP73
BRCA1	CLSPN	FANCF	MAPK1	PARP2	PTCH	RPA1	TREX1
BRCA2	CUL4A	FANCG	MDC1	PHB	PTEN	RUVBL2	TREX1
BRIP1	CUL4B	FANCL	MEN1	PIR51	PTTG1	SHPRH	TREX2
C17orf41	DCLRE1A	FBXO18	MGC5178	PLK2	RAD1	SIRT1	UBE2A
C9ORF76	DCLRE1B	FEN1	MGC5528	PLK3	RAD17	SIRT6	UBE2B
CCNA1	DCLRE1C	FLJ10719	MGMT	PMS1	RAD18	SMARCA1	UBE2I
CCNA2	DDB1	FLJ12610	MLH1	PMS2	RAD21	SMARCA2	UBE2N
CCNB1	DDB2	FLJ21816	MMS19L	PNKP	RAD23A	SMARCA3	UBE2V2
CCNB2	DEPC-1	FLJ35220	MNAT1	POLB	RAD23B	SMARCA4	UNG
CCNB3	DNMT1	G22P1	MPG	POLD1	RAD50	SMC5L1	WDHD1
CCND1	DUT	GTF2H2	MRC1	POLE	RAD51C	SMUG1	WRN
CCND2	EGFR	H2AFX	MRE11A	POLE3	RAD51L1	SOD1	XAB2
CCND3	EME1	HUS1	MSH2	POLE4	RAD51L3	STK11	XPC
CCNE1	EME2	IGF1	MSH3	POLG	RAD52	TDG	XRCC1
CCNE2	ERCC1	IGF1R	MSH6	POLH	RAD54B	TDP1	XRCC2
CDC2	ERCC2	IGF2	MUS81	POLI	RAD54L	TERF2IP	XRCC3
CDK2	ERCC4	INCENP	MUTYH	POLK	RAD9A	TIMELESS	XRCC4
CDK4	ERCC5	INSR	NBS1	POLL	RBBP8	TNKS2	XRCC5

Supplementary Table 2A. Patient details. The demographics, clinical-pathological characteristics, and treatment for Series 1 (N=152).

Series 1						
Continous/Ordinal Covariates	*Mean*	*Median*	*St.Dev.*	*Minimum*	*Maximum*	*Missing*
Age at operation (yrs)	59.3	61	11	32	86	0
Tumour size (cm)	2.5	2.1	1.3	0.2	9.0	0
Number of nodes involved	0.8	0	2.4	0	16	1
Categorical Covariates	*Value*	*Frequency*	*Percent*	*Missing*		
ER status	Negative	26	17	4		
	Positive	122	80			
Tumour Grade	1	23	15	23		
	2	74	49			
	3	32	21			
Histology	Ductal	122	80	0		
	Lobular	22	15			
	Mixed	5	3			
	Others	3	2			
Treatment						
Tamoxifen	No	61	40			
	Yes	91	60			
Radiotherapy	No	26	17			
	Yes	126	83			
Chemotherapy (CMF)	No	152	100			
	Yes	0	0			

Supplementary Table 2B. Patient details. The demographics, clinical-pathological characteristics, and treatment for Series 2 (N=127).

Series 2						
Continous/Ordinal Covariates	*Mean*	*Median*	*St.Dev.*	*Minimum*	*Maximum*	*Missing*
Age at operation (yrs)	53.3	54	10.4	26	73	0
Tumour size (cm)	2.7	2.5	1.4	0.0	7.0	0
Number of nodes involved	2.1	1	3.1	0	15	1
Categorical Covariates	*Value*	*Frequency*	*Percent*	*Missing*		
ER status	Negative	50	39	0		
	Positive	77	61			
Tumour Grade	1	28	22	16		
	2	48	38			
	3	35	28			
Histology	Ductal	92	72	0		
	Lobular	15	12			
	Mixed	13	10			
	Others	7	6			
Treatment						
Tamoxifen	No	51	40			
	Yes	76	60			
Radiotherapy	No	21	17			
	Yes	106	83			
Chemotherapy (CMF)	No	74	58			
	Yes	53	42			

Supplementary Table 3. Two probesets matched to *POLQ* gene ID 10721 on the Affymetrix U133A gene array; one matched on Illumina Human RefSeq-8 v1 arrays.

Probe Set ID	Gene Symbol	Transcript ID	RefSeq Protein ID	Target Sequence
219510_at	POLQ	AF052573 /// AY032677 /// AY338826 /// ENST00000264233 /// ENST00000393672 /// NM_199420 /// uc003eed.1 /// uc003eee.1	NP_955452	tagcactttggttccacatctgtctgg gtaaaccatgaagaaaatgaagctg ctgcctcaatcgacccagacagcagc cataggcagataaagatttggtttcac cctggtggtggtaggcatcgtgtgtga ctttttttcctctaatatcaattttacag tacggaaatagtattttaaaatagtat tggctaataaattatgaattctataaa gtagtaagacttggtatggttggagtg taggaatgaatattcatgaaatgtttc ttattgcttttccttccctaattcataca atgaatgtatttggaatacttacatat tataaaataaactatacctcttcaaga ggtatcctgttctgtaagatcagatgt ttttattgcaggtcaatataatactgc cagagacagaaaataccccttatca gtcccttagtgcctctttctgtttgtgg catggtgagaaaacccatgctgaaa agattgtactttgtgatcccaatcaga
207746_at	POLQ	AF090919	NP_955452	aaagcaggtttcaccggtcatctatca tggccttaaaaataagtcatttattat acagtggctaagattgtgggctctag gatcagactgccttagttcaacttttg gcctcatcacttagtaatcatataacc ttgggtaagtatttaacctctcttacga ttccatttcctcatttgtaaaatggag ataataatacccacctcagggctgat agtctttgatgaatgtttggtatctga ataaatgtttaataacatctattatttc tagtaaattctcccataaacattatgt aagtcatttgccaaattacctaactac tcctactcctgttccctctctaaaacgt gaagactgttggcagtgttagtatgct gaatgcttgtggttagtggtcttgtata cttctctcaccattcgagttgtatgccc ttcaagagttagttgtgttcccaaactt gttcatgtcagtt
ILMN_6520504	POLQ	NM_006596	NP_955452	taatactgccagagacagaaaatacc cccttatcagtcccttagtgcctc

Supplementary Table 4. Datasets used for the seed-clustering data-mining.

Name	Size	Site	Reference
GSE6532Oxf	149	Breast	[1]
GSE6532KI	178	Breast	[1]
GSE6532GUY	87	Breast	[1]
GSE2034	286	Breast	[2]
GSE3494	315	Breast	[3]

References

1. Loi S, Haibe-Kains B, Desmedt C, Wirapati P, Lallemand F, Tutt AM, Gillet C, Ellis P, Ryder K, Reid JF, Daidone MG, Pierotti MA, Berns EM, Jansen MP, Foekens JA, Delorenzi M, Bontempi G, Piccart MJ, Sotiriou C (2008) Predicting prognosis using molecular profiling in estrogen receptor-positive breast cancer treated with tamoxifen. *BMC Genomics* **9:** 239

2. Carroll JS, Meyer CA, Song J, Li W, Geistlinger TR, Eeckhoute J, Brodsky AS, Keeton EK, Fertuck KC, Hall GF, Wang Q, Bekiranov S, Sementchenko V, Fox EA, Silver PA, Gingeras TR, Liu XS, Brown M (2006) Genome-wide analysis of estrogen receptor binding sites. *Nat Genet* **38:** 1289-97

3. Miller LD, Smeds J, George J, Vega VB, Vergara L, Ploner A, Pawitan Y, Hall P, Klaar S, Liu ET, Bergh J (2005) An expression signature for p53 status in human breast cancer predicts mutation status, transcriptional effects, and patient survival. *Proc Natl Acad Sci U S A* **102:** 13550-5

Supplementary Table 5. Results of the multivariate analyses performed on each data series. Data summarised in Figure 5.5.

Series 1: 152 breast cancer cases on Affymetrix arrays

Multivariate analysis:

					95.0% CI for HR	
	B	SE	p	Hazard Ratio	Lower	Upper
POLQ2 score	2.090	0.633	0.001	8.086	2.340	27.948
Age	0.008	0.017	0.625	1.009	0.975	1.043
Grade	0.028	0.266	0.916	0.972	0.577	1.638
Tumour Size	0.243	0.103	0.018	1.275	1.042	1.561
ER status	-0.622	0.580	0.284	0.537	0.172	1.673
Tamoxifen	0.218	0.505	0.666	1.244	0.462	3.349
Nodal status	-0.029	0.077	0.711	0.972	0.836	1.130

Backward Likelihood Reduced model :

					95.0% CI for HR	
	B	SE	P	Hazard Ratio	Lower	Upper
Tumour Size	0.227	0.085	0.007	1.255	1.063	1.482
POLQ2 score	2.132	0.576	0.000	8.435	2.727	26.089

Series 2: 127 breast cancer cases on Illumina arrays

Multivariate analysis.

					95.0% CI for Haxard Ratio	
Variables	B	SE	Sig.	Hazard Ratio	Lower	Upper
Age (Decade)	0.487	0.171	0.004	1.628	1.165	2.275
Tumor Size (cm)	0.129	0.118	0.274	1.138	0.903	1.435
Nodes Involved	0.266	0.045	0.000	1.304	1.194	1.426
ER status	-0.236	0.359	0.510	0.790	0.391	1.596
Tamoxifen	-0.145	0.358	0.686	0.865	0.429	1.747
Grade	0.122	0.289	0.672	1.130	0.642	1.990
POLQ	1.627	0.700	0.020	5.087	1.290	20.064

Backward Likelihood Reduced model:

Age (Decade)	0.454	0.163	0.005	1.574	1.143	2.169
Nodes Involved	0.268	0.043	0.000	1.307	1.202	1.423
POLQ	1.939	0.611	0.002	6.952	2.099	23.028

GSE2034 dataset: 286 breast cancer cases on Affymetrix U133A arrays

Relapse-Free Survival

Multivariate analysis:

					95.0% CI for HR	
	B	SE	P	Hazard Ratio	Lower	Upper
POLQ2 score	0.737	0.355	0.038	2.090	1.042	4.192
ER Status	0.113	0.229	0.622	1.119	0.715	1.754

Backward Likelihood Reduced model:

					95.0% CI for HR	
	B	SE	P	Hazard Ratio	Lower	Upper
POLQ2 score	0.6949	0.3451	0.0441	2.0034	1.0186	3.9402

GSE3494 dataset: 251 breast cancer cases on Affymetrix U133A arrays

Disease specific survival (Gene expression as continuous variable : samples are ranked from low to high expression, and the ranks are normalised between 0 and 1)

					95.0% CI for HR	
	B	SE	p	Hazard Ratio	Lower	Upper
POLQ2 Score	0.806	0.478	0.092	2.239	0.877	5.712

Supplementary Table 6. Seed-clustering with bootstrap resampling identified 97 genes co-expressed with *POLQ.* Probes with a Connectivity Normalised Rank greater than 0.5 are shown; this corresponds to probes that are significantly co-expressed with both *POLQ* seeds in at least 2 datasets.

Gene Symbol	RefSeq	Unigene	Name	Connectivity Normalised Rank (0=lowest, 1=highest)
PRB3	NM_006249	Hs.73031	proline-rich protein BstNI subfamily 3	0.995104
LLGL1	D50550	Hs.513983	lethal giant larvae homolog 1 (Drosophila)	0.991976
GSK3A	NM_019884	Hs.466828	glycogen synthase kinase 3 alpha	0.991949
ESPL1	D79987	Hs.153479	extra spindle poles like 1 (S. cerevisiae)	0.988352
POLA2	NM_002689	Hs.201897	polymerase (DNA directed), alpha 2 (70kD subunit)	0.986047
MINK1	AB041926	Hs.443417	misshapen-like kinase 1 (zebrafish)	0.984246
MTRF1L	AU145135	Hs.225836	mitochondrial translational release factor 1-like	0.969734
FLJ10719	W74442	Hs.513126	NA	0.968868
MYBL2	NM_002466	Hs.179718	v-myb myeloblastosis viral oncogene homolog (avian)-like 2	0.968597
BYSL	NM_004053	Hs.106880	bystin-like	0.963122
hCAP-H2	BC001298	Hs.180903	NA	0.960984
BMP7	BC004248	Hs.473163	bone morphogenetic protein 7 (osteogenic protein 1)	0.959162
MYST3	NM_006766	Hs.491577	MYST histone acetyltransferase (monocytic leukemia) 3	0.958289
PPP2R5B	NM_006244	Hs.75199	protein phosphatase 2, regulatory subunit B (B56), beta isoform	0.946218
ZFX	R51161	Hs.370424	zinc finger protein, X-linked	0.941965
SIL	NM_003035	Hs.525198	TAL1 (SCL) interrupting locus	0.940061
DDX11	NM_030653	Hs.443960	DEAD/H (Asp-Glu-Ala-Asp/His) box polypeptide 11 (CHL1-like helicase homolog, S. cerevisiae)	0.936715

TOP2A	AU159942	Hs.156346	topoisomerase (DNA) II alpha 170kDa	0.935946
GTSE1	BC006325	Hs.386189	G-2 and S-phase expressed 1	0.93441
HCAP-G	NM_022346	Hs.446201	NA	0.929025
D21S2056E	NM_003683	Hs.110757	NA	0.927897
NPAL2	NM_024759	Hs.309489	NIPA-like domain containing 2	0.92778
STK6	NM_003158	Hs.250822	serine/threonine kinase 6	0.924998
MRPL2	NM_015950	Hs.55041	mitochondrial ribosomal protein L2	0.914122
KRT8L2	AI357616	Hs.101651	keratin 8-like 2	0.905579
ZBTB7A	AF097916	Hs.465623	zinc finger and BTB domain containing 7A	0.896152
METAP2	NM_006838	Hs.444986	methionyl aminopeptidase 2	0.887015
LOC155060	AU151157	Hs.490512	NA	0.882748
LIME1	NM_017806	Hs.233220	Lck interacting transmembrane adaptor 1	0.863774
GFER	NM_005262	Hs.27184	growth factor, augmenter of liver regeneration (ERV1 homolog, S. cerevisiae)	0.861185
RBM21	NM_022830	Hs.256184	RNA binding motif protein 21	0.849952
DNAJC4	NM_005528	Hs.172847	DnaJ (Hsp40) homolog, subfamily C, member 4	0.84681
LAT2	BC006080	Hs.56607	linker for activation of T cells family, member 2	0.846083
KIAA0101	NM_014736	Hs.81892	KIAA0101	0.84319
C20orf172	NM_024918	Hs.266273	chromosome 20 open reading frame 172	0.839673
ST3GAL4	NM_006278	Hs.504251	ST3 beta-galactoside alpha-2,3-sialyltransferase 4	0.830919
ZNHIT4	NM_031288	Hs.410786	zinc finger, HIT type 4	0.826217
PLEKHG5	AI275938	Hs.284232	pleckstrin homology domain containing, family G (with RhoGef domain) member 5	0.818154
PELP1	BC002875	Hs.513883	NA	0.81699

HLRC1	NM_031304	Hs.515064	HEAT-like (PBS lyase) repeat containing 1	0.806763
TIMELESS	NM_003920	Hs.118631	timeless homolog (Drosophila)	0.793701
MYH14	NM_024729	Hs.467142	myosin, heavy polypeptide 14	0.792221
FAM3A	BC002934	Hs.289108	family with sequence similarity 3, member A	0.78676
LOC127406	AL353681	Hs.112622	NA	0.779367
GIPC1	NM_005716	Hs.6454	GIPC PDZ domain containing family, member 1	0.76827
LRP6	NM_002336	Hs.210343	low density lipoprotein receptor-related protein 6	0.765471
SEC22L2	NM_012430	Hs.477361	SEC22 vesicle trafficking protein-like 2 (S. cerevisiae)	0.741914
ARL6IP2	AW301806	Hs.190440	ADP-ribosylation factor-like 6 interacting protein 2	0.722053
KIFC1	BC000712	Hs.436912	kinesin family member C1	0.71913
PLEKHM2	AB020649	Hs.145049	pleckstrin homology domain containing, family M (with RUN domain) member 2	0.715511
KIAA1217	AK022045	Hs.445885	KIAA1217	0.711276
MXD3	NM_031300	Hs.442993	MAX dimerization protein 3	0.701903
C20orf67	AL162458	Hs.472856	chromosome 20 open reading frame 67	0.69726
KIAA0894	NM_014896	Hs.38621	NA	0.691729
C14orf172	AI679213	Hs.525610	chromosome 14 open reading frame 172	0.673026
PHF20L1	AK022280	Hs.304362	PHD finger protein 20-like 1	0.670319
GRK6	NM_002082	Hs.235116	G protein-coupled receptor kinase 6	0.652819
ALDH3B1	BC002553	Hs.523841	aldehyde dehydrogenase 3 family, member B1	0.648404
SUV39H1	NM_003173	Hs.522639	suppressor of variegation 3-9 homolog 1 (Drosophila)	0.646578
POLH	NM_006502	Hs.439153	polymerase (DNA directed), eta	0.645134

BRCA1	NM_007295	Hs.194143	breast cancer 1, early onset	0.639475
TSC22D4	NM_030935	Hs.469798	TSC22 domain family, member 4	0.633456
CDKN3	AF213033	Hs.84113	cyclin-dependent kinase inhibitor 3 (CDK2-associated dual specificity phosphatase)	0.625792
DC12	AI937543	Hs.458320	NA	0.625254
WBSCR20B	AI768378	Hs.549260	NA	0.619754
P2RY6	NM_004154	Hs.16362	pyrimidinergic receptor P2Y, G-protein coupled, 6	0.619286
ZNF85	NM_003429	Hs.37138	zinc finger protein 85 (HPF4, HTF1)	0.615009
RNGTT	NM_003800	Hs.127219	RNA guanylyltransferase and 5'-phosphatase	0.613018
CABYR	NM_012189	Hs.511983	calcium binding tyrosine-(Y)-phosphorylation regulated (fibrousheathin 2)	0.611607
TBPIP	BE964655	Hs.279032	NA	0.601713
NPR1	NM_000906	Hs.490330	natriuretic peptide receptor A/guanylate cyclase A (atrionatriuretic peptide receptor A)	0.59293
DAPP1	NM_014395	Hs.436271	dual adaptor of phosphotyrosine and 3-phosphoinositides	0.591941
MELK	NM_014791	Hs.184339	maternal embryonic leucine zipper kinase	0.589271
RAD51AP1	BE966146	Hs.504550	RAD51 associated protein 1	0.584931
TRIP13	NM_004237	Hs.436187	thyroid hormone receptor interactor 13	0.582128
CCNE2	NM_004702	Hs.408658	cyclin E2	0.572964
ZNF669	NM_024804	Hs.163754	zinc finger protein 669	0.567312
CHRNB2	NM_000748	Hs.2306	cholinergic receptor, nicotinic, beta polypeptide 2 (neuronal)	0.558279
KNTC1	NM_014708	Hs.300559	kinetochore associated 1	0.556752
IFNAR2	NM_000874	Hs.549042	interferon (alpha, beta and omega) receptor 2	0.542515
LMNB1	NM_005573	Hs.89497	lamin B1	0.539327

TDP1	NM_018319	Hs.209945	tyrosyl-DNA phosphodiesterase 1	0.533353
38596	AA702163	Hs.283743	septin 5	0.530598
MCM2	NM_004526	Hs.477481	MCM2 minichromosome maintenance deficient 2, mitotin (S. cerevisiae)	0.526137
PRC1	NM_003981	Hs.459362	protein regulator of cytokinesis 1	0.525493
PPP2R5D	NM_006245	Hs.533308	protein phosphatase 2, regulatory subunit B (B56), delta isoform	0.524502
TEAD4	NM_003213	Hs.94865	TEA domain family member 4	0.51957
PPARD	NM_006238	Hs.485196	peroxisome proliferative activated receptor, delta	0.519112
ERN2	AI732416	Hs.528301	endoplasmic reticulum to nucleus signalling 2	0.516475
C10orf3	NM_018131	Hs.14559	chromosome 10 open reading frame 3	0.507976
HFE	AF144241	Hs.233325	hemochromatosis	0.507621
RPL23AP13	NM_020217	Hs.534472	NA	0.507549
TACC3	NM_006342	Hs.104019	transforming, acidic coiled-coil containing protein 3	0.506786
RRM2	BE966236	Hs.226390	ribonucleotide reductase M2 polypeptide	0.503332
GMEB2	AL133646	Hs.473286	glucocorticoid modulatory element binding protein 2	0.503213
CCNB2	NM_004701	Hs.194698	cyclin B2	0.502737
LILRA4	AF041261	Hs.406708	leukocyte immunoglobulin-like receptor, subfamily A (with TM domain), member 4	0.501853

Supplementary Table 7. Results of the multivariate analyses performed on the data from Series 1 after inclusion of *CCNE2* and the expression profiles previously described showing that POLQ expression remains prognostically significant. Data summarised in Chapter 5, Fig 4A.

Multivariate analysis including CCNE2:

					95.0% CI for HR	
	B	SE	p	Hazard Ratio	Lower	Upper
POLQ2 score	1.5039	0.7000	0.0317	4.4990	1.1410	17.7392
Age	0.0031	0.0173	0.8570	1.0031	0.9697	1.0377
Grade	-0.1982	0.2871	0.4900	0.8202	0.4672	1.4398
Tumour Size	0.2264	0.1039	0.0293	1.2540	1.0231	1.5372
ER status	-0.5609	0.5985	0.3487	0.5707	0.1766	1.8444
Tamoxifen	0.2888	0.5242	0.5816	1.3349	0.4778	3.7293
Nodal status	0.0038	0.0762	0.9601	1.0038	0.8646	1.1655
CCNE2 score	1.7018	0.7399	0.0214	5.4836	1.2861	23.3803

Backward Likelihood Reduced model :

					95.0% CI for HR	
	B	SE	p	Hazard Ratio	Lower	Upper
Tumour Size	0.2166	0.0897	0.0158	1.2418	1.0416	1.4805
POLQ2 score	1.4203	0.6364	0.0256	4.1383	1.1889	14.4046
CCNE2 score	1.6191	0.6815	0.0175	5.0488	1.3278	19.1974

Multivariate analysis including GGI:

					95.0% CI for HR	
	B	SE	p	Hazard Ratio	Lower	Upper
POLQ2 score	1.2387	0.6309	0.0496	3.4510	1.0021	11.8847
Age	0.0152	0.0159	0.3380	1.0153	0.9842	1.0474
Tumour Size	0.1754	0.0869	0.0435	1.1917	1.0052	1.4129
ER status	-0.1149	0.4885	0.8140	0.8915	0.3422	2.3222
Tamoxifen	-0.1936	0.4016	0.6297	0.8240	0.3751	1.8102
Nodal status	0.0172	0.0634	0.7861	1.0173	0.8985	1.1519
GGI score	0.2418	0.1488	0.1042	1.2736	0.9514	1.7049

Backward Likelihood Reduced model:

					95.0% CI for HR	
	B	SE	p	Hazard Ratio	Lower	Upper
Tumour Size	0.1799	0.0805	0.0254	1.1971	1.0224	1.4017
POLQ2 score	1.1876	0.6296	0.0593	3.2791	0.9547	11.2629
GGI score	0.2482	0.1386	0.0733	1.2817	0.9769	1.6817

Multivariate analysis including 76 gene signature:

					95.0% CI for HR	
	B	SE	p	Hazard Ratio	Lower	Upper
POLQ2 score	1.6378	0.6400	0.0105	5.1439	1.4673	18.0330
Age	0.0009	0.0178	0.9589	1.0009	0.9666	1.0365
Grade	-0.2085	0.2675	0.4356	0.8118	0.4806	1.3712
Tumour Size	0.2199	0.1081	0.0420	1.2460	1.0080	1.5402
ER status	-1.9410	0.7471	0.0094	0.1436	0.0332	0.6208
Tamoxifen	0.2904	0.5109	0.5698	1.3369	0.4912	3.6391
Nodal status	0.0123	0.0816	0.8800	1.0124	0.8628	1.1879
76 gene	2.6936	0.9077	0.0030	14.7851	2.4955	87.5972

Backward Likelihood Reduced model :

					95.0% CI for HR	
	B	SE	p	Hazard Ratio	Lower	Upper
Tumour Size	0.2182	0.0912	0.0167	1.2438	1.0402	1.4872
ER status	-1.5408	0.5678	0.0067	0.2142	0.0704	0.6519
POLQ2 score	1.4943	0.5920	0.0116	4.4562	1.3964	14.2203
76 gene	2.5696	0.8865	0.0038	13.0602	2.2979	74.2299

Multivariate analysis including 70 gene signature:

					95.0% CI for HR	
	B	SE	p	Hazard Ratio	Lower	Upper
POLQ2 score	1.7584	0.7558	0.0200	5.8031	1.3193	25.5260
Age	0.0065	0.0175	0.7090	1.0065	0.9727	1.0416
Grade	-0.0815	0.2752	0.7672	0.9218	0.5375	1.5807
Tumour Size	0.2409	0.1030	0.0194	1.2724	1.0397	1.5572
ER status	-0.5224	0.5990	0.3831	0.5931	0.1833	1.9184
Tamoxifen	0.2063	0.5179	0.6903	1.2292	0.4455	3.3917
Nodal status	-0.0221	0.0752	0.7694	0.9782	0.8441	1.1336
70 gene	0.6413	0.7805	0.4113	1.8989	0.4113	8.7671